Molecular Weight Modulation in Polyhydroxybutyrate Fermentations

By

Benjamin Ragan Waters

B.S. Chemical Engineering
Texas A&M University, College Station, 2002

M.S. Chemical Engineering Practice
Massachusetts Institute of Technology, 2004

SUBMITTED TO THE DEPARTMENT OF CHEMICAL ENGINEERING IN PARTIAL FULFILLMENT OF THE REQUIREMENTS FOR THE DEGREE OF

DOCTOR OF PHILOSOPHY OF CHEMICAL ENGINEERING
AT THE
MASSACHUSETTS INSTITUTE OF TECHNOLOGY

May 2007
[June 2007]

Signature of Author: _____
Department of Chemical Engineering
May 25, 2007

Certified by: _____
Charles L. Cooney
Professor of Chemical and Biochemical Engineering
Thesis Supervisor

Accepted by: _____
William Deen
Professor of Chemical Engineering
Chairman, Committee for Graduate Students

Molecular Weight Formation in Polyhydroxybutyrate Fermentations

by

Benjamin Ragan Waters

Submitted to the Department of Chemical Engineering on September 15, 2004
in Partial Fulfillment of the Requirements for the Degree of
Doctor of Philosophy of Chemical Engineering
Supervisor: Charles L. Cooney

ABSTRACT

Polyhydroxybutyrate (PHB) is a material with significant potential for commercial applications. It has material properties similar to isotactic polypropylene; it can be produced from renewable resources; it is biodegradable. Unfortunately, it is very brittle when compared to polypropylene. The physical property that most significantly affects elastic behavior is molecular weight. In an effort to understand how molecular weight is formed in PHB production, kinetic studies of PHB fermentations have been performed using fermentation conditions which allow biomass growth and PHB production phases to be separated. These data indicate that molecular weight increases very quickly and then remains fairly constant in PHB fermentations. Additional studies have indicated that only slight changes in molecular weight can be caused by changing fermentation process conditions or using mutants of the polymerization enzyme. Additionally, one mutant polymerization enzyme has been shown to excrete moderate levels of PHB monomer, 3-hydroxybutyrate, into the fermentation media. This may have application in achieving synthetic production of PHB.

Thesis Supervisor: Charles L. Cooney
Title: Professor of Chemical and Biochemical Engineering

TABLE OF CONTENTS

LIST OF FIGURES

LIST OF TABLES

1. INTRODUCTION

Polyhydroxyalkanoates (PHA) comprise a class of biodegradable polyesters which can be produced by various microorganisms. Polyhydroxybutyrate (PHB), the most common PHA, has physical properties similar to polypropylene and can be produced from a variety of sources, including sugar, food processing waste, and toxic chemicals. (Maskow, 2000; Wong, 1998) These factors, biodegradability, production from cheap, renewable resources, and polymer strength, make PHB a compelling competitive product for polypropylene, which would have obvious benefits for the environment. Unfortunately, PHB as a homopolymer is brittle when compared to polypropylene. Some co-polymers, such as P(3HB-*co*-4HB), have shown better elastic properties; however, the most efficient and economic production of PHB will probably occur in transgenic plants, which can only produce the homopolymer. (Saito, 1996) Thus it is very important to understand how to control PHB homopolymer mechanical properties, most notably extension-to-break. One of the main factors in extension-to-break performance is molecular weight. At this time, the mechanism for how molecular weight is formed and controlled in PHB production is not well known. This research has been conducted to better understand what factors affect molecular weight by collecting kinetic data on PHB production rates and molecular weight under various process conditions and using multiple enzyme mutations.

2. LITERATURE REVIEW

2.1. PHB History

Lipid-like, sudanophilic inclusions from *Bacillus megaterium* first were identified as PHB in the 1920s. (Sudesh, 2000) At the time, PHB was not considered seriously for wide-spread applications, due to its brittle nature. However, in 1974 Wallen and Rohweder identified other hydroxyalkanoates that could be polymerized, including 3-hydroxyvalerate and 3-hydroxyhexanoate. (Wallen, 1974) The identification of these materials and the fact that co-polymers of 3-hydroxybutyrate and these other hydroxyalkanoates could be produced resulted in further research into the use of PHB. In the 1980s, the genes for PHB production were cloned from *Ralstonia eutropha* and shown to be active when inserted into *Escherichia coli*. (Peoples, 1989) It was found that only three enzymes were required for PHB production, and that the synthase polymerization enzyme was the most important. Since that time, many organisms have been identified that contain synthase enzymes. (Rehm, 1999) Additionally, synthase enzymes have shown the ability to polymerize many other hydroxyalkanoate subunits. (Doi, 1990)

2.2. PHB Mechanical Properties

The mechanical properties of PHB, such as Young's modulus and tensile strength, produced by wild-type bacteria are very similar to isotactic polypropylene, as shown in Table 2.2-1. (Goodfellow, 2005; Sudesh, 2000) However, the extension-to-break for PHB (5%) is much less than that seen in polypropylene (400%). (Sudesh, 2000) This causes the PHB homopolymer to

exhibit brittle properties, which may prevent it from becoming an adequate substitute for polypropylene. High molecular weight PHB has been shown to have better extension-to-break performance (58%); but it still falls far short of that seen in polypropylene. (Kusaka, 1998) So co-polymers have shown even better performance, with one film of P(3HB-*co*-4HB) showing an extension-to-break of 444% at the cost of a small loss of strength. (Saito, 1996)

Table 2.2-1: Polymer Mechanical Properties

	Molecular Weight	Young's Modulus	Tensile Strength	Extension-to-break
Wild Type PHB	3 MDa	3.5 GPa	43 MPa	5%
High Molecular Weight PHB	11 MDa	1.1 GPa	62 MPa	58%
P(3HB-*co*-4HB) 16 mol% 4HB	432 KDa	not reported	26 Mpa	444%
Isotactic Polypropylene	not reported	1.5 GPa	40 MPa	400%

2.3. PHB Synthesis Route and Co-polymers

In *R. eutropha*, PHB is synthesized in three steps from acetyl-CoA, as shown in Figure 2.3-1. Acetyl-CoA is the final metabolite produced in the glycolysis pathway; and in non-PHB-producing organisms, it enters the citric acid cycle, where the carbon is converted into carbon dioxide.

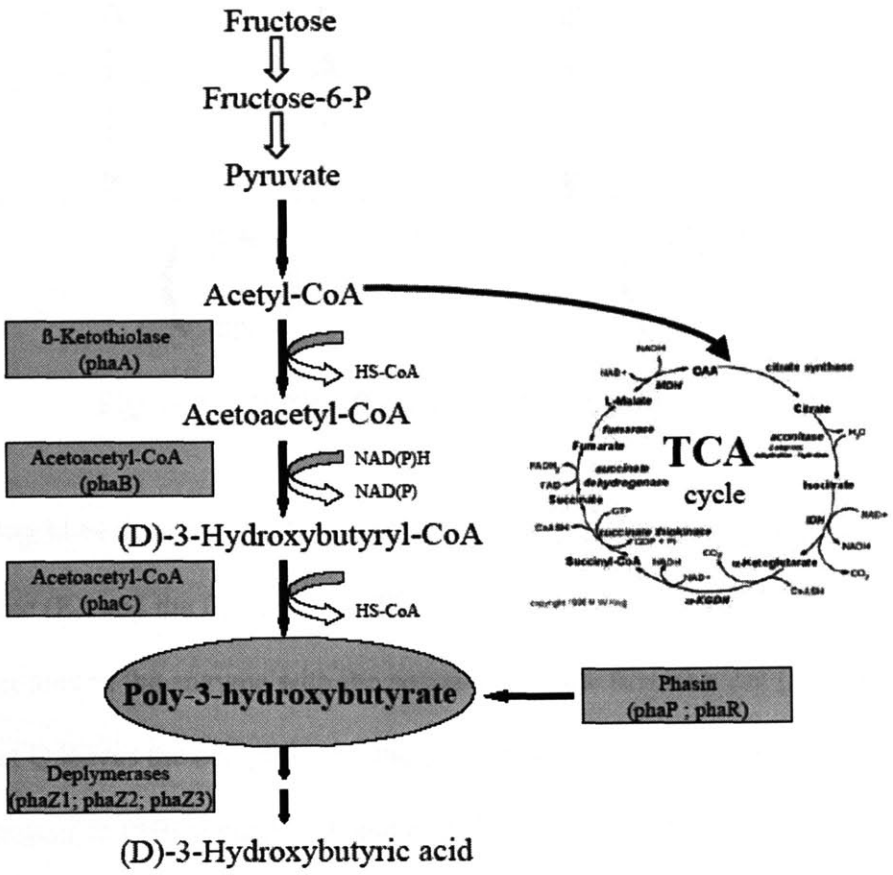

Figure 2.3-1: PHB Synthesis Pathway

In the first synthetic step, two acetyl-CoA (AcCoA) molecules are combined into acetoacetyl-CoA (AcAcCoA) at the thiolase enzyme and release a molecule of CoA (CoASH), as shown in Equation 2.3-1. The thiolase reaction occurs according to a ping-pong Bi-Bi mechanism, as shown in Figure 2.3-2. (Cleland, 1963; Davis, 1987; Leaf, 1998)

$$2\ \text{AcCoA} \rightleftharpoons \text{AcAcCoA} + \text{CoASH} \qquad (2.3\text{-}1)$$

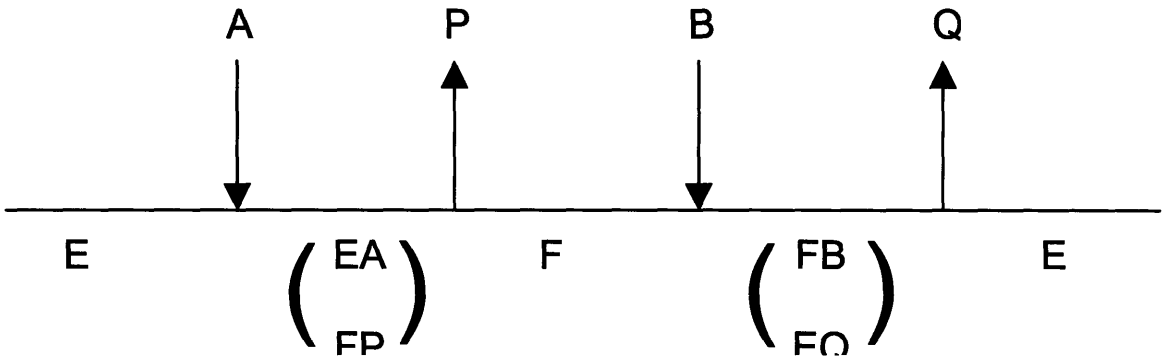

Figure 2.3-2: Ping-Pong Bi-Bi Reaction Mechanism

In the ping-pong bi-bi reaction, the first reactant, represented by A in Figure 2.3-2, combines with the enzyme (E), and the first product (P) leaves the complex. Then the second reactant (B) adds to the complex of the enzyme with the remainder of the first reactant (F). Finally, the second product Q leaves the complex, and the enzyme returns to its original state. In the case of the thiolase enzyme in PHB synthesis, A and B are both AcCoA molecules, P is CoASH, and Q is AcAcCoA. The rate equation for a ping-pong bi-bi reaction is shown in Equation 2.3-2 and the equilibrium constant equation is shown in Equation 2.3-3.

$$v_{Thiolase} = \frac{V_1 V_2 \left(AB - \frac{PQ}{K_{eq}} \right)}{K_b V_2 A + K_a V_2 B + \frac{K_q V_1 P + K_p V_1 Q + V_1 PQ}{K_{eq}} + \frac{K_q V_1 AP}{K_{ia} K_{eq}} + \frac{K_a V_2 BQ}{K_{iq}}} \qquad (2.3\text{-}2)$$

$$K_{eq} = \frac{[AcAcCoA][CoASH]}{[AcCoA]^2} \qquad (2.3\text{-}3)$$

V_1 and V_2 are the maximum forward and reverse rates, respectively. A, B, P, and Q are the same as in the ping-pong bi-bi mechanism shown in Figure 2.3-2; and K_a, K_b, K_q, K_p, K_{ia}, and K_{iq} are kinetic constants akin to Michaelis constants or inhibition constants.

In the second synthetic step, acetoacetyl-CoA is reduced to 3-hydroxybutyric-CoA (3HBCoA) with the conversion of one NADPH molecule to $NADP^+$ at the reductase enzyme, as shown in Equation 2.3-4. Dehydrogenase reactions that involve pyridine-nucleotide cofactors generally occur by ternary-complex mechanisms, and the simplest mechanism for kinetic rate constants is a rapid equilibrium random bi-bi, as shown in Figure 2.3-4. (Cleland, 1963; Laidler, 1973)

$$AcAcCoA + NADPH + H^+ \rightleftharpoons 3HBCoA + NADP \qquad (2.3\text{-}4)$$

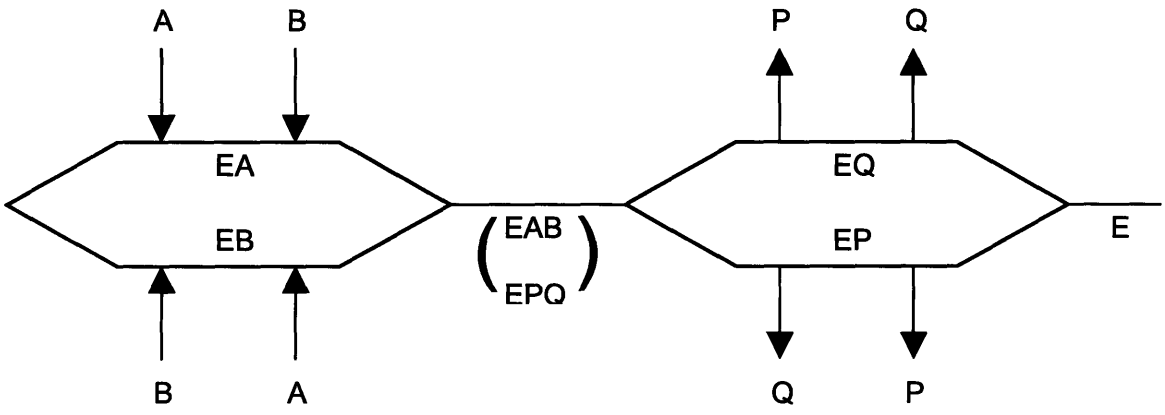

Figure 2.3-4: Rapid Equilibrium Random Bi-Bi Reaction Mechanism

In the rapid equilibrium random bi-bi reaction, both reactants, A and B in Figure 2.3-4, bind to the enzyme before any reaction takes place. It does not matter which reactant binds first. Then the complex of the enzyme and the reactants (EAB) undergoes the reaction, and both products, (P and Q) leave, which returns the enzyme to its original state. In the case of the reductase

enzyme, the reactants (A and B) are AcAcCoA and NADPH; the products (Q and P) are 3HBCoA and $NADP^+$. The rate equation and equilibrium constant expression are shown in Equations 2.3-5 and 2.3-6, respectively; they use notation similar to that used in Equations 2.3-2 and 2.3-3.

$$v_{Reductase} = \frac{V_1 V_2 \left(AB - \frac{PQ}{K_{eq}} \right)}{K_{ia} K_b V_2 + K_b V_2 A + K_a V_2 B + V_2 AB + \frac{K_q V_1 P + K_p V_1 Q + V_1 PQ}{K_{eq}}} \tag{2.3-5}$$

$$K_{eq} = \frac{[3HBCoA][NADP^+]}{[AcAcCoA][NADPH][H^+]} \tag{2.3-6}$$

Units of 3-hydroxybutyric-CoA are then polymerized into PHB at the synthase enzyme, as shown in Equation 2.3-7. Little is known about the PHB synthase mechanism. Two different mechanisms have been proposed. One operates through a single covalent intermediate, as shown in Figure 2.3-5; the other goes through two covalent intermediates, as shown in Figure 2.3-6. (Stubbe, 2005)

$$3HBCoA + \text{enzyme} - S - (3HB)_n \rightleftharpoons CoASH + \text{enzyme} - S - (3HB)_{n+1} \tag{2.3-7}$$

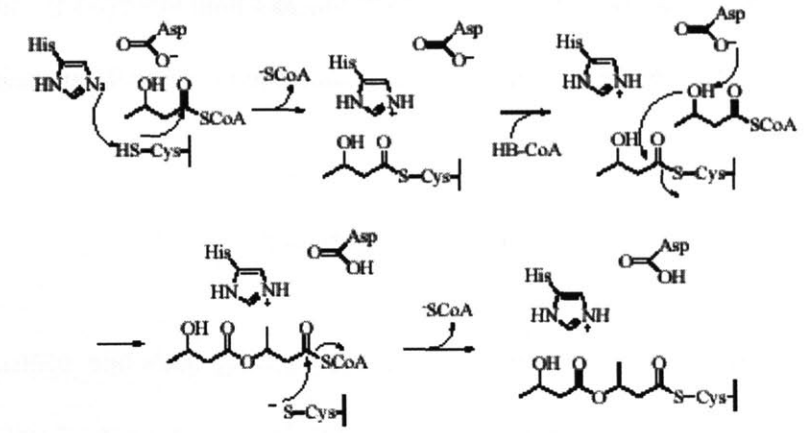

Figure 2.3-5: Synthase Polymerization Mechanism with a Single Covalent Intermediate

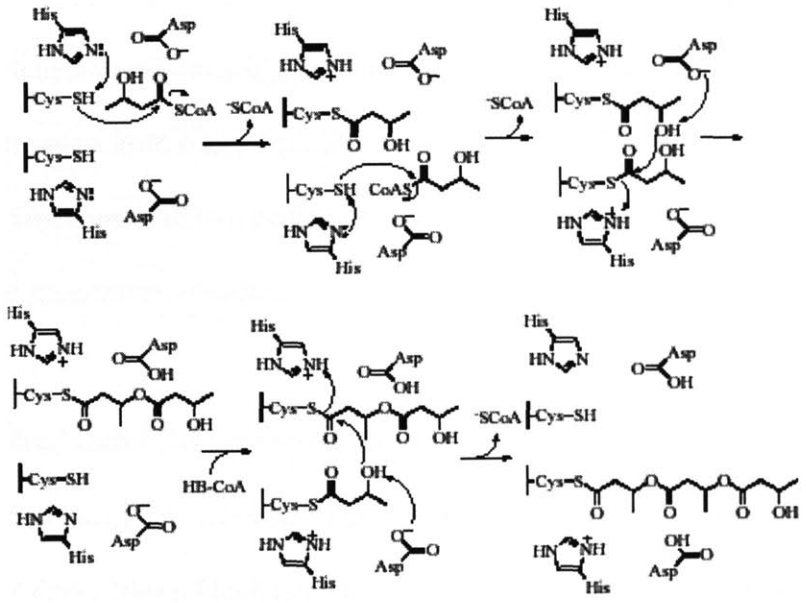

Figure 2.3-5: Synthase Polymerization Mechanism with a Two Covalent Intermediates

Both mechanisms make use of the histidine, aspartic acid, and cysteine amino acids in the active site. In the single covalent intermediate mechanism, 3HB-CoA diffuses into the active site and is added to a covalently attached growing PHB chain. In the two covalent intermediates mechanism, the 3HB-CoA is first covalently bound to an additional cysteine, where it loses the CoA, and then is inserted into a growing chain covalently attached to the cysteine in the active

site. In addition to the covalent intermediate mechanisms, a non-covalent intermediate mechanism that accounts for chain termination has also been proposed. (Lawrence, 2005b)

2.4. PHB Genetics

The thiolase, reductase, and PHB synthase enzymes are encoded in *R. eutropha* by the genes PhaA, PhaB, and PhaC, respectively. These genes are contained on a single operon and are expressed together. (Peoples, 1989) Three types of PHB synthases have been identified from various organisms. Class I synthases, the type which is found in R. eutropha, are active toward short-chain-length hydroxyalkanoate monomers. The class II synthases can polymerize larger monomers, which range from 6 to 14 carbon atoms. The class III synthases, the type which is found in *A. vinosum*, consist of two protein subunits and also polymerize short-chain-length hydroxyalkanoate monomers. (Sudesh, 2000)

Other genes involved with PHB production include PhaP, PhaR, and the PhaZ depolymerases. PhaP encodes for a phasin that helps stabilize the hydrophobic/aqueous interface at the PHB granule surface. (York, 2001) PhaR encodes for a regulatory protein that represses the expression of PhaP. (York, 2002) The PhaR protein can also help stabilize the granule surface. PhaZ1 encodes for an intracellular depolymerase. PhaZ2 and PhaZ3 were identified as homologous to PhaZ1 and are thought to encode for other intracellular depolymerases. (York, 2003) Additionally, an oligmer hydrolase has been identified as operating on PHB. (Sugiyama, 2004)

2.5. PHB Granule Growth

PHB granule growth is largely related to the presence of the phasin encoded by PhaP. (Jurasek, 2004) When PHB is produced in wild type *R. eutropha*, levels of PHB greater than 80% of cell dry weight can be reached. In this process a small number of granules are initiated and then coalesce into fewer granules by the end of the production. (Tian, 2005) When PHB is produced in the absence of PhaP in *R. eutropha*, only a single large granule is seen. (Stubbe, 2005) When PhaP is over expressed, many small granules are seen. (Stubbe, 2005) This is also seen when the genes for PHB production are inserted into *E. coli*. If PhaP is not present, a single large granule is seen. If PhaP is expressed, the normal amount of granules is seen. If PhaEC is inserted into *E. coli*, even without the presence of PhaP, the normal amount of granules is seen. (Lawrence, 2005a) A typical growth pattern is shown in Figure 2.5-1. (Tian, 2005)

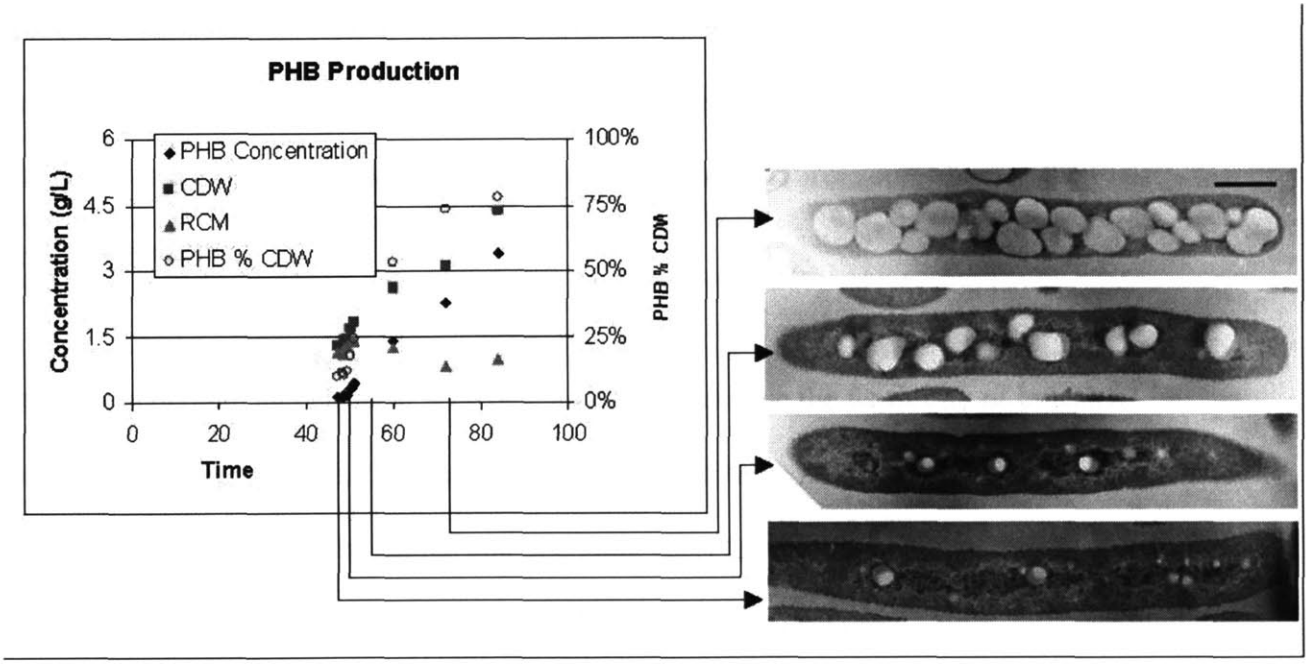

Figure 2.5-1: Typical PHB Granule Growth in *R. eutropha*

2.6. Modeling

Four different types of modeling have been performed on PHB production systems: metabolic, economic, granule growth, and molecular weight. The most extensive of the models is the metabolic model. The metabolic models have focused on the three synthesis enzymes and related metabolites. In one model, complex expressions for the rate equations of each enzyme were developed. (Leaf, 1998) This model showed that using the complex expressions gave significantly different results than models that used simplified Michaelis-Menten expressions for each of the enzymes. Additionally, the model, which utilized data from various published experiments, showed that no single step could obviously be identified as rate limiting. In the second metabolic model, metabolic control analysis was preformed on experimental data. (van Wegen, 2001) This model showed that the PHB production rate depended greatly on the acetyl-CoA/CoA ratio and the total acetyl-CoA + CoA concentration. Additionally, the experimental data on which the model was based showed no accumulation of any of the metabolites. This is likely due to a rate limiting step or some sort of regulatory control somewhere in the PHB synthesis pathway.

Multiple economic models have been developed to determine the feasibility of industrial production of PHB. (Choi, 1997; van Wegen, 1998) In these models, a PHB production and recovery is designed and the capital and operating costs for the plant are determined. The overall cost of producing PHB per unit weight is calculated from these values and compared to the known cost for conventional plastics. Based on previous values, the best estimates of PHB production costs still was high compared to conventional plastics. However, it is believed that at this time the production costs, for a company such as Metabolix, are more competitive.

Granule growth modeling considers the growth of granules inside a single cell during the production of PHB. (Jurasek, 2004) The granule growth model basically takes a number of different initiation sites for PHB synthesis and allows the sites to grow into granules over time and then coalesce into larger granules. It also accounts for the impact of PhaP and other granule stabilizing proteins and closely matches empirical observations. These models accurately account for the growth in size of granules during PHB production. However, the models do not provide information about the internal structure of the granules or the effect of packing on PHB molecular weight.

Additionally, a population balance model for molecular weight has been proposed. (Mantzaris, 2002) This model fits groups PHB chains into to two groups: those that are actively growing and those that have become inactive. The model utilizes some experimental parameters; however, they are difficult to obtain from experimental data due to the rapidity with which the synthase enzyme acts. Additionally, the model does not make any provisions for what causes chain termination; in effect, it is only an empirical representation of how the population of active chains changes over time. Each of the models, metabolic, economic, granule growth, and molecular weight, have a place in the overall PHB production picture. However, the models have not yielded fundamental information, such as a rate determining step, or led to drastically different production methods.

2.7. Features of PHB Synthesis Not Resolved in Literature

A number of issues have not been adequately explored in the PHB literature. Many of these center around the PHB synthase reaction mechanism. Though a catalytic triad for the synthase has been identified, it is unknown whether a non-covalent intermediate, a single covalent intermediate, or two covalent intermediates are involved in the elongation process. Additionally, the mechanism for initiation of the polymer chain, which may require some sort of primer molecular, is not known. Granule growth and structure is also not well understood. It is not clear whether the PHB granules have some internal structure or how the internal state of the granule may affect molecular weight. In addition to these mechanistic issues, the mechanism for PHB chain termination has not been determined. PHB chain termination obviously would have a significant impact on molecular weight, and if it were well understood, control of PHB molecular weight would probably become easier to manipulate. If each of these mechanistic details was understood better, it is likely that many of the issues surrounding commercial production of PHB would be resolved.

3. GOALS AND OBJECTIVES

One of the largest barriers to PHB becoming competitive with polypropylene is its brittleness. If the PHB extension-to-break performance could be improved, the only remaining barrier would be cost, which could be overcome through a number of creative solutions. One of the main factors which has been shown to contribute to extension-to-break performance is molecular weight. Therefore, the following goals have been identified for this research.

1. Obtain a better understanding of how PHB molecular weight evolves over time.

2. Determine what effect process variables have on PHB molecular weight and production rate.

3. Determine what effect mutations to the synthase enzyme have on PHB molecular weight and production rate.

4. MATERIALS AND METHODS

4.1. Strains

All experiments were performed using *Ralstonia eutropha* H16 (ATCC 17699) provided by the Sinskey Laboratory at MIT. Where noted, wild type *R. eutropha* refers to *R. eutropha* H16. In some experiments gene replacement strains of the wild type *R. eutropha* were used. In one of these strains, the gene for the native class I synthase from *R. eutropha* was deleted from the chromosome, and the gene for the class III synthase from *Allochromatium vinosum* was inserted in its place. This procedure of deletion and replacement also was used with nine other synthases than contained point mutations. The various point mutations are listed in Figure 7.1-1.

4.2. Media

Precultures were grown in tryptic soy broth-dextrose free (TSB) medium. Fermentations were carried out in the minimal medium shown in Table 4.2-1. (Peoples, 1989)

Table 4.2-1: Minimal Media

Minimal Medium		
Sodium phosphate monobasic	6.7	mM
Sodium phosphate dibasic	6.5	mM
Potassium sulfate	2.6	mM
Sodium hydroxide	1.0	mM
Magnesium sulfate	0.39	g/L
Calcium chloride	0.062	g/L
Trace Salts	1.0	Ml
Trace Salts in 0.1N HCl		
Cupric sulfate $5H_2O$	4.8	mg/L
Zinc sulfate $7H_2O$	24	mg/L
Manganese sulfate $1H_2O$	24	mg/L
Ferrous sulfate $7H_2O$	150	mg/L

The minimal medium was supplemented with 0.25% fructose, 0.25% citrate, 0.10% ammonium chloride, and 10μg/ml gentamicin, unless otherwise noted. The pH of this mixture is 6.8

4.3. Preculture Methods

A TSB and agar plate with 10 μg/ml gentamicin was grown from frozen stock for 24-48 hours. A second TSB and agar plate with 10 μg/ml gentamicin was then grown for 24 hours from a colony on the first plate. Then a single colony was picked from the second TSB and agar plate and inoculated into 5 ml of TSB and 10 μg/ml gentamicin and grown for 16 hours at 30°C. (Lawrence, 2005c)

4.4. Seed Culture Methods

Seed cultures were grown from 5% inoculums of the saturated preculture in TSB and 10 μg/ml gentamicin for approximately 10 hours in a baffled flask at 30°C with shaking at 140 RPM until an OD_{600} between 0.5 and 2 was reached. Typically, the TSB volume used was 100 ml or 1 L depending on whether the cells would be used in a 500 ml fermentation or a 10 L fermentation. Once the desired OD_{600} was reached, the cells were centrifuged at 3500 rpm for 10 minutes and resuspended in 50 ml sterile media. (Lawrence, 2005c)

4.5. Shake Flask Methods

In the shake flask experiments, baffled 500 mL flasks containing 100 mL of the minimal media described above, or some close variation, were inoculated to an OD_{600} of 0.05. The cultures were grown at 30°C with shaking at 140 RPM.

4.6. Fermentors

Fermentors of 500 ml and 10 L were used in the experiments. The Sixfors 500 ml fermentors were manufactured by Infors and control software was used to both control and collect data on the fermentations. The 10 L fermentor was manufactured by Biolaffitte and Paragon control software was used to control the fermentation and collect process data. Both sets of fermentors were equipped with agitation, temperature, pH, and air flow control; dissolved oxygen concentration could also be measured. In the 500 ml fermentors, which are glass, 2M NaOH and 2M HCl were used to control pH. In the 10 L fermentor, which is stainless steel, 2M NaOH and

20% H_2SO_4 were used to control pH. Both fermentors used parastolic pumps to control the addition of acid or base. The 10 L fermentor has the capability to measure the composition of the overhead gas using a Perkin-Elmer MGA1600 mass spectrometer. (Lawrence, 2005c)

4.7. Fermentation Method

In order to view three phases of PHB production in *R. eutropha* (growth, PHB production, and utilization) separately, the following procedure was used. After inoculation to 0.05 OD_{600}, cells were allowed to grow without pH control until a pH of 8 was reached. The pH was held at 8 until approximately 48 hours after inoculation. During this time, all of the fructose, ammonium, and citrate in the original medium are used up, and most of the PHB produced by the cells is degraded. The pH is adjusted to the production pH, usually 7.0, and the cells are allowed to adjust to the new environmental conditions for two hours. Fructose is then added to the fermentor until a concentration of 7.5 g/L is reached. The cells are allowed to remain in the production phase for 48 hours, during which time all of the fructose is consumed. If it is desired to view the utilization phase, ammonium chloride is added until a concentration of 1 g/L is reached, and the cells are allowed to remain in the utilization phase for 72 hours. pH control in this procedure was accomplished by the following method. For approximately the first 16 hours the pH set point is set at 8 and the base pump is turned off. This effectively keeps the pH from rising above 8, but takes no action to raise the pH. Once pH 8 is reached, the base control is turned on to keep the pH at 8 for the rest of the growth phase. Just prior to the production phase, the pH is set to the production pH and standard pH control is used for the rest of the fermentation.

4.8. Cell Dry Weight Analysis Method

In order to measure cell dry weight, 16 mm X 100 mm glass test tubes were dried for 16 hours at 105°C and a vacuum of 30 mmHg. The tubes were allowed to cool for 30 minutes in a vacuum desiccator and then weighed to within 0.1 mg. Sample volumes between 2 ml and 10 ml were added to the tubes and centrifuged at 3500 rpm. The supernatant was discarded and the cell pellets were dried for 16 hours at 80°C in a vacuum of 30 mmHg. The tubes and samples were allowed to cool for 30 minutes and then weighed. The difference between the dry tube weight and the tube plus sample weight is the cell dry weight (CDW). (Lawrence, 2005c)

4.9. PHB Analysis Method

For PHB analysis, the pellet from the CDW is boiled in 1 ml concentrated sulfuric acid for 30 minutes. The PHB reacts completely to form crotonic acid. The mixture is diluted with 4 ml of 0.01 N sulfuric acid and filtered. 100 ml of the filtered product is then added to 900 ml of 0.01 N sulfuric acid in an HPLC vial. A mobile phase of 0.01 N sulfuric acid, a flow rate of 0.6 L/min, and an organic acid analysis ion exclusion column (Amines HPX-87H, Bio-Rad, Hercules, CA) are used in the HPLC. PHB mass is measured by comparing absorption at 210 nm and at a retention time of 27 minutes to a standard curve produced by using measured weights of PHB in the above procedure instead of cell pellets over a range of 0.1 – 10 mg/ml. Residual cell mass (RCM) was calculated by subtracting the mass of PHB from the CDW. (Lawrence, 2005c)

4.10. Fructose and Citrate Analysis

For fructose analysis, 1 ml of culture was pelleted in a microcentrifuge at 14,000 rpm, and the supernatant was filtered through a 0.2 mm filter directly into an HPLC vial. The same ion exclusion column and mobile phase used in PHB analysis are used for fructose and citrate analysis. Fructose concentration is detected by change in refractive index at a retention time of 10 minutes and compared to a standard curve over the range of 0.1 – 15 g/L. Citrate concentration is measured by absorption at 260 nm and at a retention time of 8 minutes and compared to a standard curve over the range of 0.1 – 10 g/L. (Lawrence, 2005c)

4.11. Ammonium Analysis

Ammonium concentration was measured according to Berthelot's method. 10 µl of filtered sample used for fructose and citrate analysis is diluted in 990 µl of water. 100 µl of the diluted sample is further diluted in 900 µl of water. These dilutions are preformed to get to the linear range of the assay. One drop of 0.003 M $MgSO_4$, 50 µl 1% HClO, and 60 µl 0.1 g/L phenate are added to the 1 ml sample. The formation of indophenol was monitored by absorption at 600 nm and compared to a standard curve over the range of 500 – 10 µg/L. (Lawrence, 2005c)

4.12. Molecular Weight Analysis

Samples for molecular weight analysis were collected in the same way as the samples for CDW and PHB analysis. 5 ml to 50 ml of sample were centrifuged at 3500 rpm (5,000 x g, 10 min), and the supernatant was removed. The samples were stored at -80°C for approximately 1 week.

The samples were lyophilized for 16 hours. The PHB in the lyophilized samples was extracted by refluxing with 5 ml of chloroform at 60°C for 48 hours. Any chloroform that was lost during refluxing was replaced, and the samples were filtered through a 0.2 μm PTFE membrane into 12 mL scintillation vials. The chloroform was evaporated under nitrogen, and the required volume of tetrafluoroethanol (TFE) was added to the sample to bring it to a PHB concentration of 1 mg/ml. The samples were allowed to dissolve into TFE for 24 hours and then 250 μl of sample was filtered through a 0.2 μm PTFE membrane and added to 750 μl TFE in a 2 mL scintillation vial, which resulted in a 25 mg/ml PHB concentration. The sample was injected into the gel permeation chromatography/multiple angle light scattering (GPC MALS) apparatus.

In the GPC MALS apparatus, the sample is pumped through a mixed B (column) gel permeation column using a TFE mobile phase. After coming off the column a laser is passed through the sample in the direction of flow. Two signals from the laser are of interest. The refractive index as the laser passes through the sample gives the mass of the sample. Additionally, the way in which the light from the laser is scattered is detected by 18 detectors spaced around the flow chamber. The readings from these detectors are fit to a curve using Zimm's method and the amount of light scattered forward is calculated. This value gives the molecular weight of the sample. The principle for this is that small particles scatter light in every direction equally. However, larger particles tend to scatter more of the light forward than backward.

The light scattering apparatus is normalized by injecting a sample of 18 kDa polymethylmethacrylate (PMMA). These particles are below the threshold (~20 nm) at which particles scatter light equally in all directions. Each of the multiple detectors, which are facing

the sample at different angles, is then normalized. The apparatus is calibrated with a PMMA sample which contains polymer chains that have molecular weights of 20 – 2000 kDa. (Lawrence, 2005b)

4.13. Gas Chromatography Mass Spectrometry Analysis

A Hewlett-Packard 5890 Series II gas chromatograph coupled to an HP 5971 Mass Selective Detector operated under ionization by electron impact at 70 eV was used for identification of 3-hydroxybutyrate. A DB1701 capillary column was used for the gas chromatography, and 1 µl samples were injected in pulsed splitless mode at a flow rate of 0.74 ml of Helium per minute. The injection port temperature was 270°C, and the interface temperature was held at 300°C. The column was held at 80°C for the first minute of the analysis, and then the temperature was raised 10°C each minute until the column reached 280°C, where it was held for 9 minutes. The mass spectrometer was operated in scan mode and detected masses between 100 and 450 amu at 1.9 scans per second. (Villas-Boas, 2005)

Two samples were analyzed by GCMS: a control sample containing 3-hydroxybutyric acid (Sigma Aldrich 166898) dissolved to a 1% m/v concentration in water and a fermentation media sample obtained by centrifuging fermentation broth at 3500 rpm for 10 minutes and filtering the supernatant through a 0.2 µm filter. Both samples sample was derivatized by drying the samples and redissolving in 50 µL pyridine. 70 µL of MTBSTFA (N-Methyl-N-(tert-butyldimethylsilyl)-trifluoroacetamide) + 1% TBDMCS (N-(tert-butyldimethylsilyl)-N-methyltrifluoroacetamide) was added to the sample and incubated for 30 minutes at 60°C. The sample was then centrifuged

for 5 minutes at 14, 000 rpm and the supernatant was transferred to a GCMS injection vial. (Villas-Boas, 2005)

5. WILD TYPE FERMENTATIONS

5.1. Fermentation Procedure Experiments

Multiple experiments were performed to establish standard fermentation conditions for viewing PHB production rates and molecular weight formation kinetics. In addition to establishing standard conditions, the experiments were designed to separate the growth and PHB production phases in *Ralstonia eutropha* fermentations. These experiments consisted of shake flask and 500 mL fermentations and focused on the effect of different carbon sources and pH control regimens.

5.1.1. Carbon Source Shake Flask Experiments

Carbon source shake flask experiments were performed to find a suitable media for allowing growth to occur without significant production of PHB. Thus, the optimal carbon source mixture would produce a high cell dry weight but low amount of PHB. Pre-cultures for the carbon source shake flask experiments were prepared as described in section 4.3. Seven different carbon source mixtures were used in minimal PHB media that was inoculated to OD_{600}=0.05: including 5 g/L fructose; 5 g/L citrate; 5 g/L succinate; 2.5 g/L fructose and 2.5 g/L citrate; 5 g/L fructose and 5 g/L citrate; 2.5 g/L fructose and 2.5 g/L succinate; 5 g/L fructose and 5 g/L succinate. The cultures were grown at 30°C with shaking at 140 RPM. Samples for PHB and cell dry weight (CDW) analysis were taken after 20 hours and 44 hours. It was found that a mixture of 0.25% citrate and 0.25% fructose met the high growth/low PHB criteria the best, as shown in Figure 5.1.1-1.

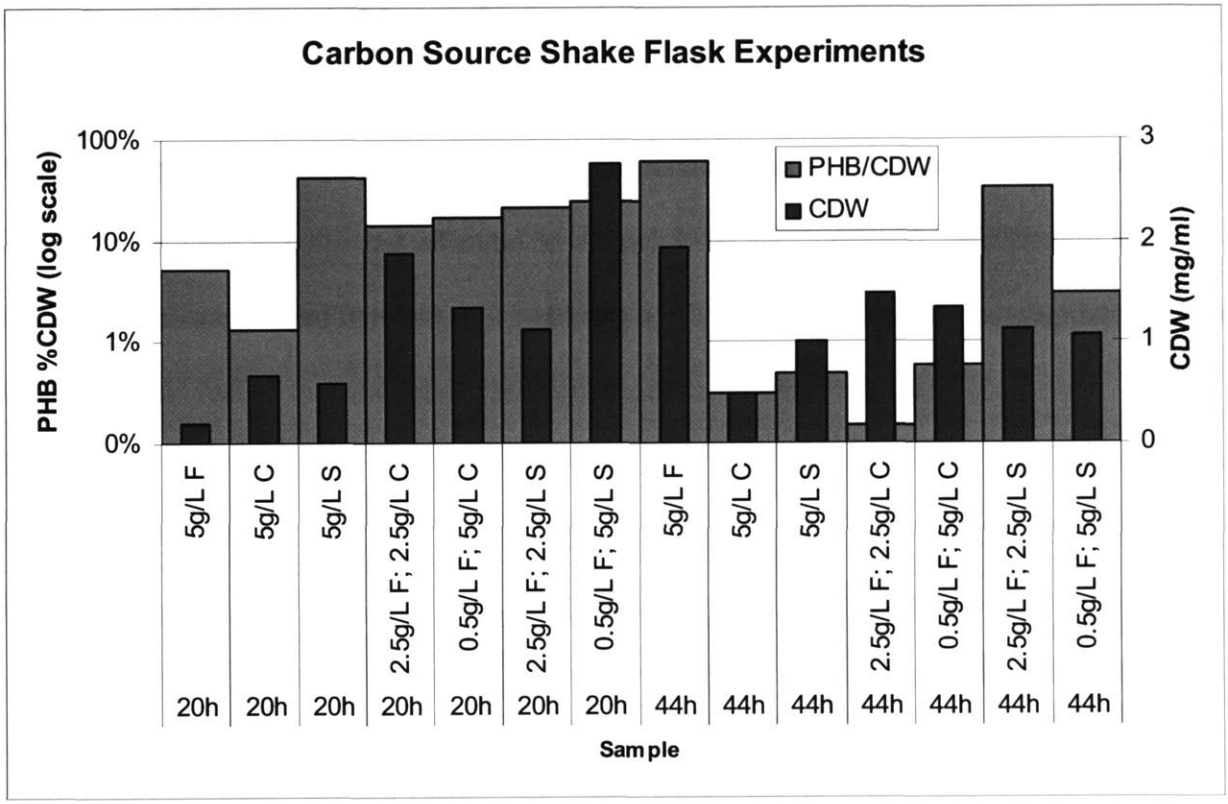

Figure 5.1.1-1: Carbon Sources Shake Flask Experiments

5.1.2. Buffering Shake Flask Experiments

The buffering shake flask experiments were performed to determine whether pH or the reduction state of the nitrogen source had an effect on the amount of PHB produced because it was noted that the pH at the end of the carbon source experiments was quite high. Two carbon sources were used in the experiments: 5 g/L fructose and a mixture of 2.5 g/L fructose and 2.5 g/L citrate. With each of these media, three different experiments were performed. One flask contained a control; one flask contained MOPS to regulate the pH to 7; and one flask replaced

NH_4Cl with $NaNO_3$. The cultures were grown for 46 hours at 30°C and 140 RPM. Samples were taken at 22 hours and 46 hours after inoculation.

The buffering and redox shake flask experiments showed that the redox state of the nitrogen source did not have a significant effect on how much PHB was produced. Additionally, the experiments also indicated that adding a buffering agent to the media would not regulate pH in a way that would reduce the amount of PHB produced, as shown in Figure 5.1.2-1.

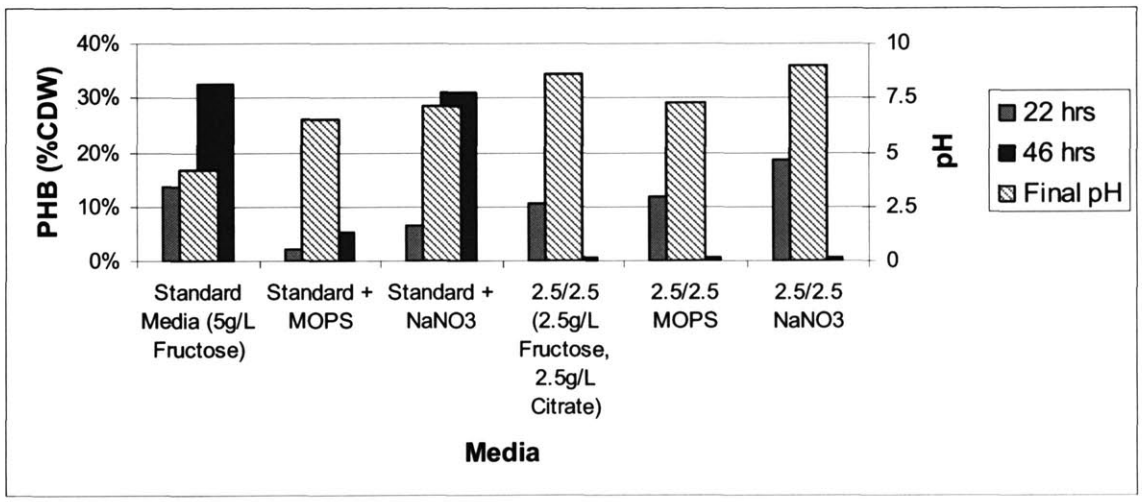

Figure 5.1.2-1: Buffering and Nitrogen Source Redox State Experiments

5.1.3. Carbon Source Fermentations

In order to explore the best carbon source mixture/pH combination, two different carbon source mixtures were used in fermentations that capped pH at three different levels. The two carbon source mixtures used were 2.5 g/L fructose and 2.5 g/L citrate and 1.25 g/L fructose and 2.5 g/L

citrate. The three pHs used were 7.5, 7.75, and 8.0. Samples were taken after 8, 15, and 33 hours.

It was seen that capping the pH at 8 instead of 7.75 seemed to result in a lower PHB level, which may be related to an unpublished observation from Amin He that PhaZ1, a depolymerase found in *R. eutropha*, has a higher activity at pH 8, as shown in Figure 5.1.3-1. Additionally, the mixture of 2.5 g/L fructose and 2.5 g/L citrate produced lower levels of PHB at the pH 7.75 condition than the mixture of 1.25 g/L fructose and 2.5 g/L citrate; therefore it was determined that the future condition set would be a mixture of 2.5 g/L fructose and 2.5 g/L citrate with the pH capped at 8.

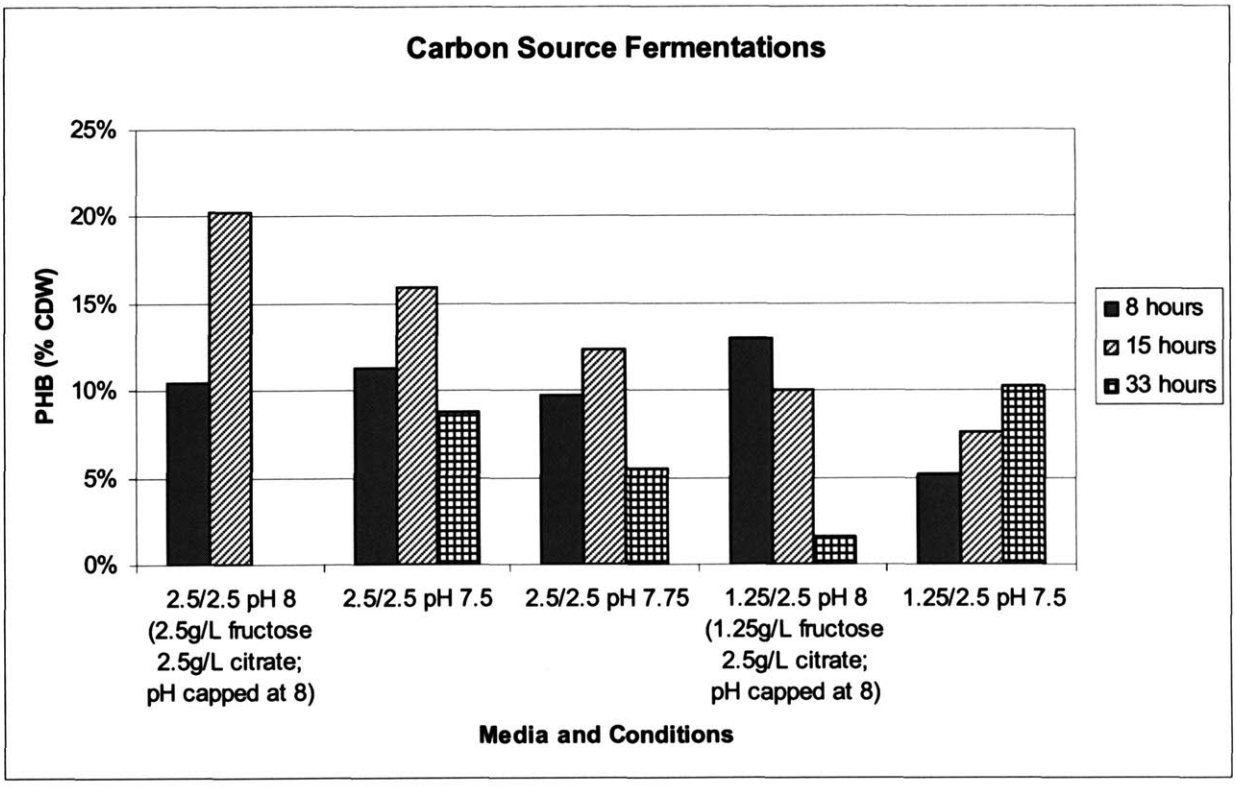

Figure 5.1.3-1: pH and Carbon Source Fermentation Experiments

5.1.4. pH Control Fermentations

An additional fermentation was performed to verify that PHB could be produced to acceptable levels after the high pH growth phase. A fermentation in minimal PHB media was run where pH control was left on manual, which is the same as turning the pH control off, for the first 25 hours; and the pH was allowed to increase to approximately 8.5. The pH was then lowered to 7 for the rest of the fermentation. At 50 hours a fructose bolus, which raised the fructose concentration from zero to approximately 10 g/L was applied. Time course samples were analyzed for CDW, PHB, and fructose, as shown in Figure 5.1.4-1. The fermentation produced the desired results because a PHB level of zero occurred before the fructose bolus at 50 hours. Additionally, the cells, even after being subjected to a pH of 8.5 were able to produce PHB to a level of 60% of CDW.

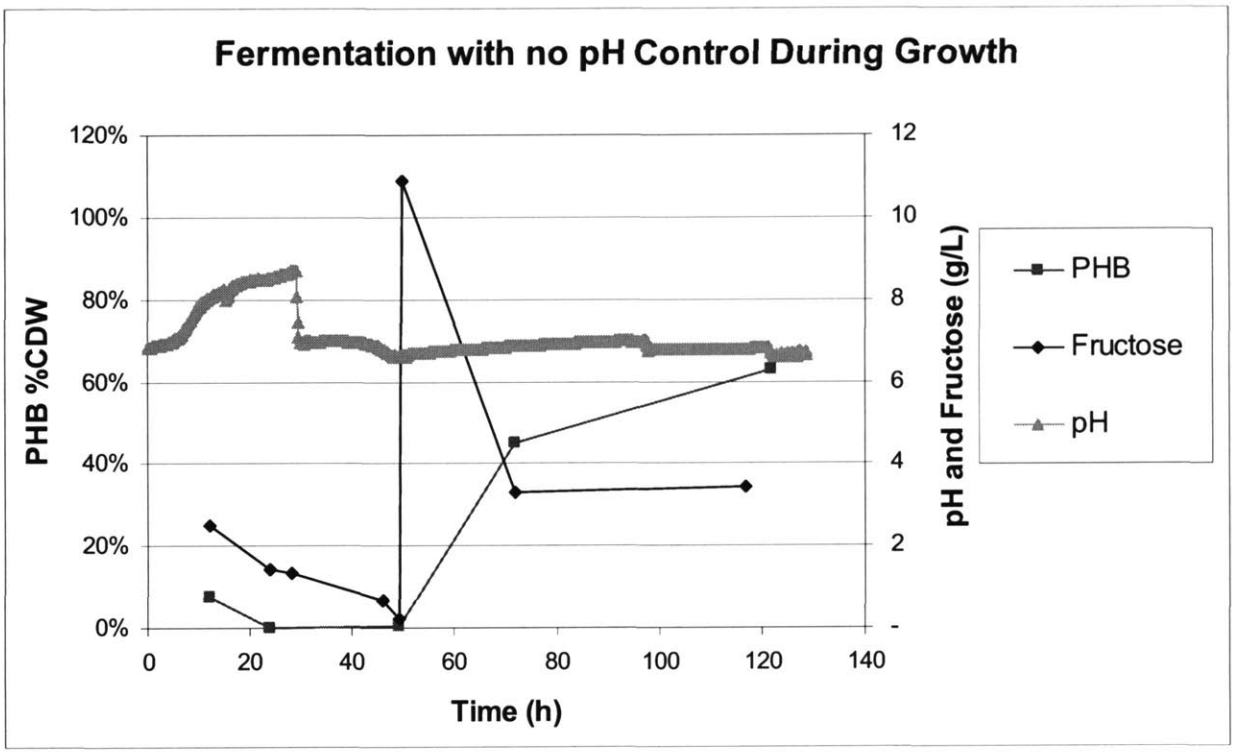

Figure 5.1.4-1: No pH Control during Growth Fermentation

5.1.5. pH Optimization Fermentations

Two additional fermentations were performed to determine whether a lower and less toxic pH could be used during the growth phase. pH settings of 7.75 and 8.0 were used to determine which would allow for growth with the lowest level of PHB. The pH was capped at these levels for the first 48 hours of the fermentation. Then the pH was reduced to 7 for the rest of the fermentation. Time course samples for these fermentations were analyzed for CDW, PHB, fructose, citrate, and ammonia. The media used in these fermentations contained 2.5 g/L fructose and 2.5 g/L citrate. Additionally, a nitrogen bolus was given at the end of the PHB production phase to determine whether the cells could be induced into the utilization phase without changing the whole media. The PHB production and RCM for the pH 8 and pH 7.75

fermentations are shown in Figure 5.1.5-1a and Figure 5.1.5-1b, respectively. The nutrient utilization of the pH 8 and pH 7.75 fermentations are shown in Figure 5.1.5-1c and Figure 5.1.5-1d, respectively. The results indicated that a lower level of PHB could be reached by capping the pH at 8; therefore, this setting was used for the remainder of the experiments.

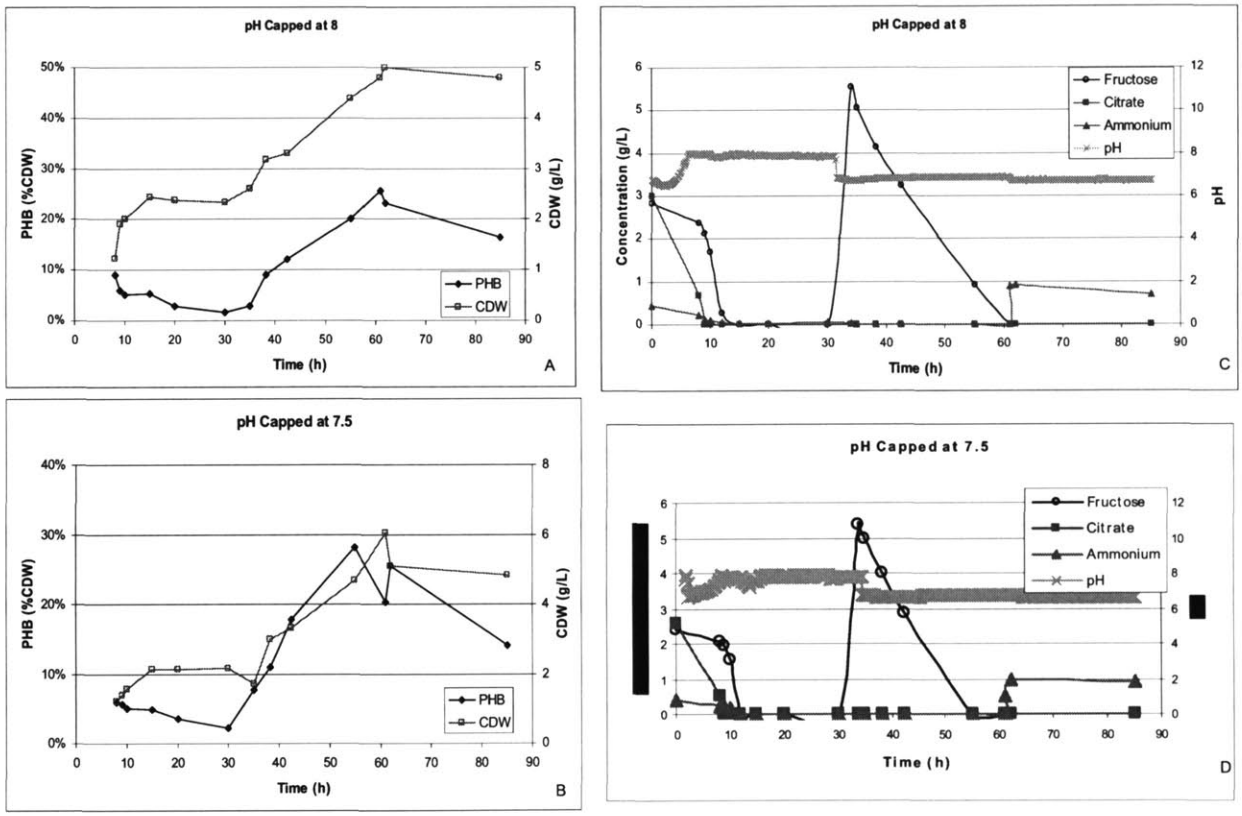

Figure 5.5-1: Production and Nutrient Data at Different pH Caps

5.1.6. Fermentation Procedure Experiments Summary

The fermentation procedure that was used in the rest of the wild type *R. eutropha* fermentations was established from these experiments. The final procedure, as described in section 4.7, separated the growth phase from the production phase through the manipulation of the media

carbon source and the pH control scheme. The final media utilized a mixed carbon source of 2.5 g/L citrate and 2.5 g/L fructose for the growth phase and then was given a fructose bolus to 7.5 g/L to start the production phase after 48 hours. The pH control was capped at 8 for the first 25 hours and then held at eight until 46 hours had elapsed; the pH was then reduced to the production phase pH for the rest of the fermentation. This procedure typically resulted in PHB content, as a percentage of cell dry weight, of less that 2.5% at the end of the growth phase.

5.2. Wild Type Fermentations

Multiple wild type *R. eutropha* fermentations were performed using the procedure established in section 5.1 to observe the kinetics of PHB production and molecular weight formation. Additionally, a carbon balance was performed to determine whether significant byproducts were produced during the fermentations; and the effects of changes in process variables, such as temperature and pH, on the PHB production rate and molecular weight formation kinetics were also observed.

5.2.1. Wild Type Carbon Balance Fermentation

A 10 L fermentation using the wild type *R. eutropha* strain was performed to examine the kinetics of PHB molecular weight formation and determine whether significant carbon-based byproducts were produced during the course of PHB production. The fermentation was performed as described in Section 4.7. Using this procedure, the growth phase and production phases of the fermentation were analyzed separately. Figure 5.2.1-1 shows the details of the fermentation.

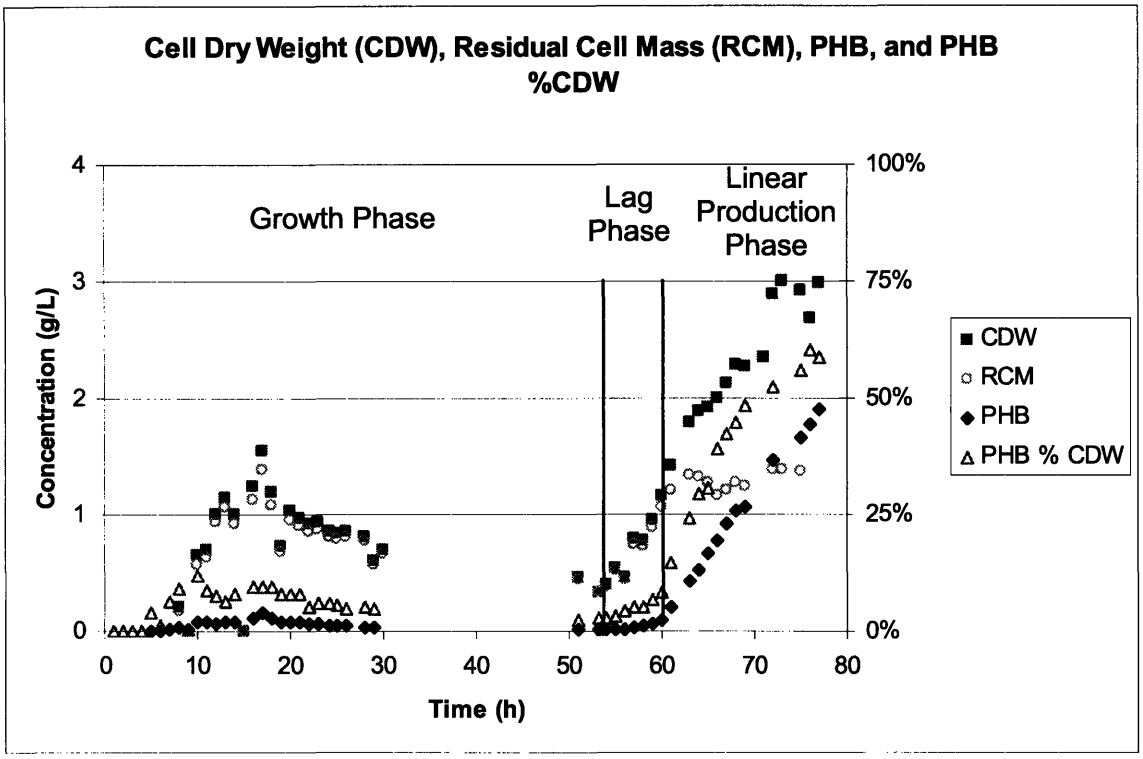

Figure 5.2.1-1: CDW, RCM, PHB, and PHB %CDW vs Time

The cell dry weight and PHB content increased initially during the growth phase of the fermentation, and then fell during prolonged exposure to pH 8. The uncontrolled rise in pH to a value of 8, where it was held for the rest of the growth phase is shown in Figure 5.2.1-2.

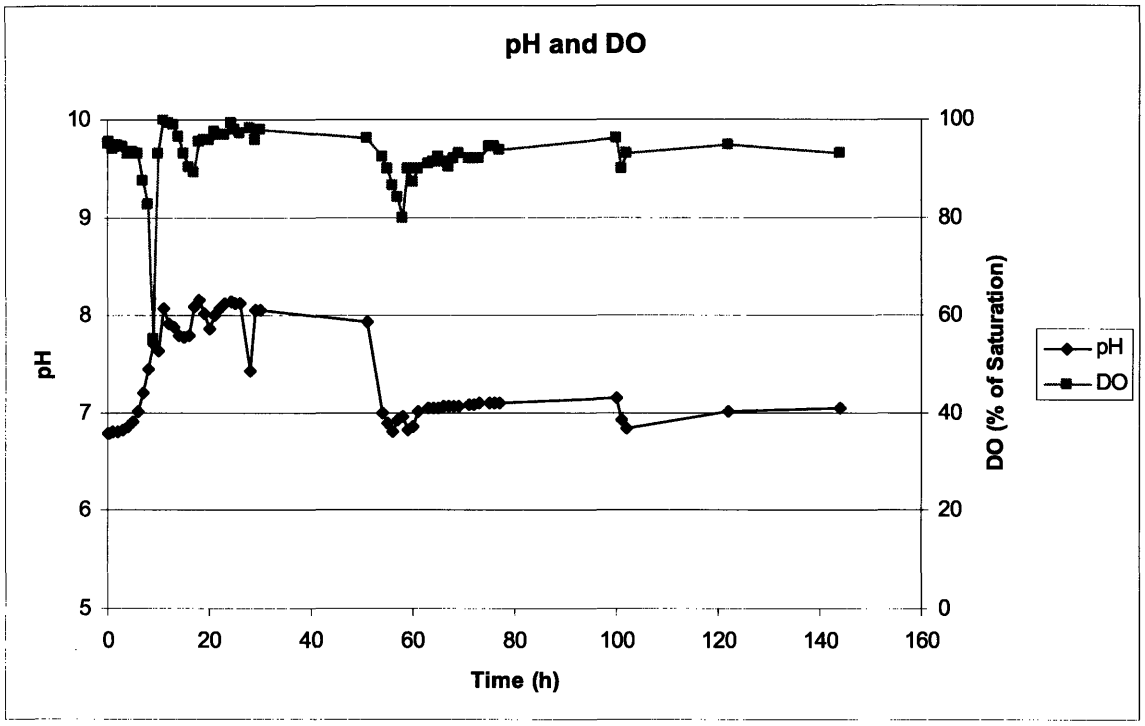

Figure 5.2.1-2: pH and DO vs Time

Other experiments have shown that the increase in pH is due to the presence of citrate in the media. *R. eutropha* fermentations that only contain fructose actually experience a natural decrease in pH. Figure 5.2.1-1 also shows the production phase of the fermentation, where PHB is shown to increase linearly with time after a short lag phase after the fructose bolus at 54 hours. A rapid increase in cell dry weight is seen just after the fructose bolus during the lag phase of PHB production. However, the residual cell mass (RCM) is shown to be essentially constant during the actual linear PHB production. This linear production of PHB is seen to coincide with linear consumption of fructose, as shown in Figure 5.2.1-3.

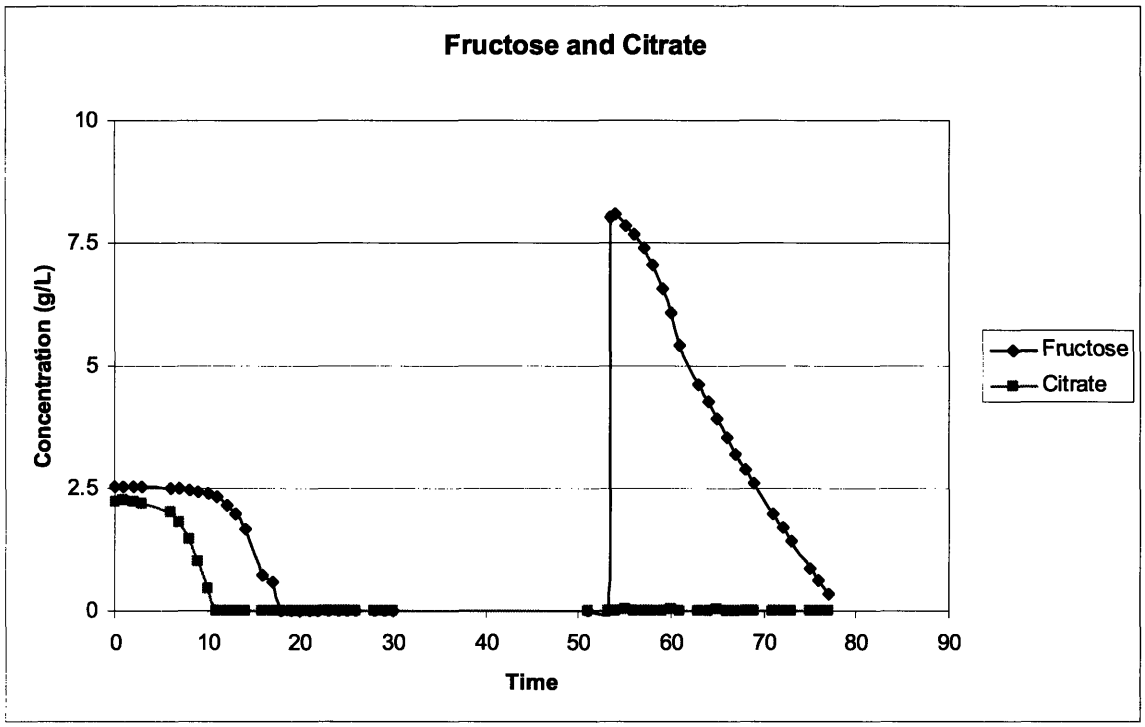

Figure 5.2.1-3: Fructose and Citrate vs Time

During the linear production phase, the carbon dioxide evolution (CER) rate is seen to decrease in a fairly linear fashion after increasing to a high value during the lag phase, as shown in Figure 5.2.1-4.

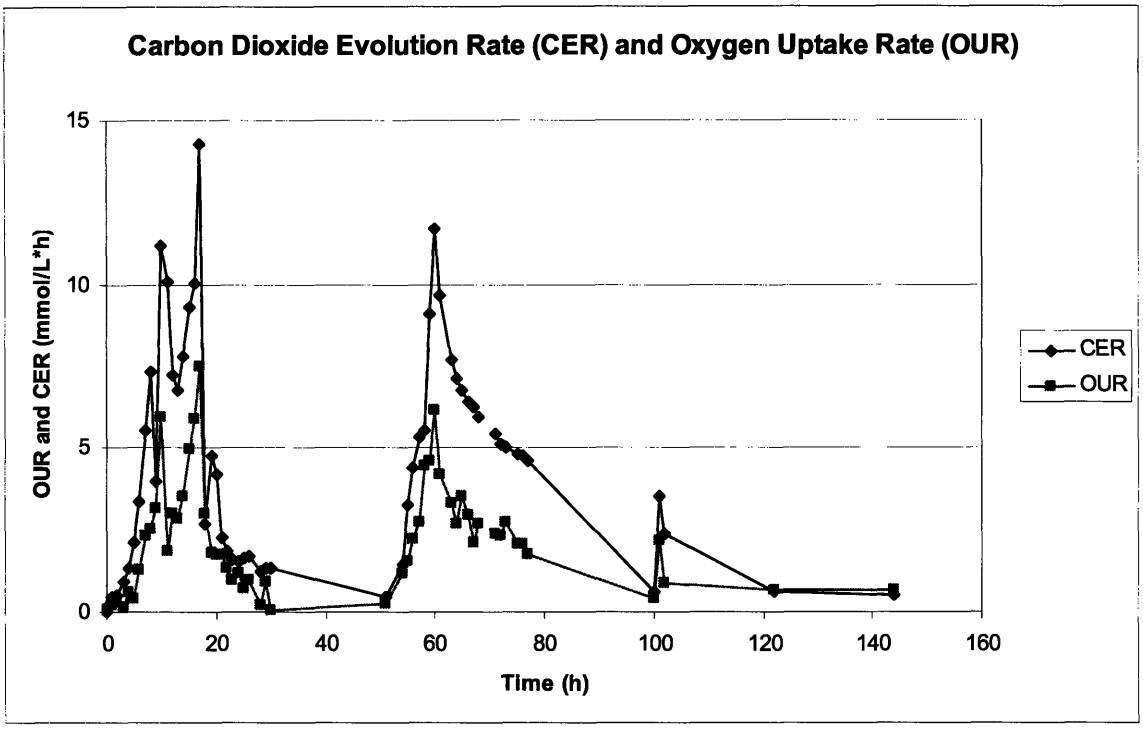

Figure 5.2.1-4: CER and OUR vs Time

The data from the linear PHB production phase for PHB concentration, RCM, fructose concentration, and CER were used to complete the carbon balance for the system and determine whether byproducts were produced.

5.2.2. Large Scale Carbon Balance

As described above, examination of the production phase showed two subphases: a lag phase and a linear production phase. A carbon balance was performed using data fits on the measurements during the linear production phase. It is notable that some of the experiments at the 500 mL scale under similar conditions did not show the lag phase before the linear production phase. Linear data fits of PHB, fructose, RCM, and CER during the production phase are shown in

Figures 5.2.2-1a, 5.2.2-1b, 5.2.2-1c, and 5.2.2-1d, respectively. The PHB, fructose, and CER are very linear; the RCM data show significant scatter, but remain fairly stable over time. Additionally, RCM only accounts for a small portion of the total carbon in the balance. The CER data is not as linear as the PHB and fructose concentrations; however, since CER is a rate, for the purposes of the carbon balance, only the average value is of interest. If the CER performance over time had shown significant nonlinear behavior, a weighted average would have been used.

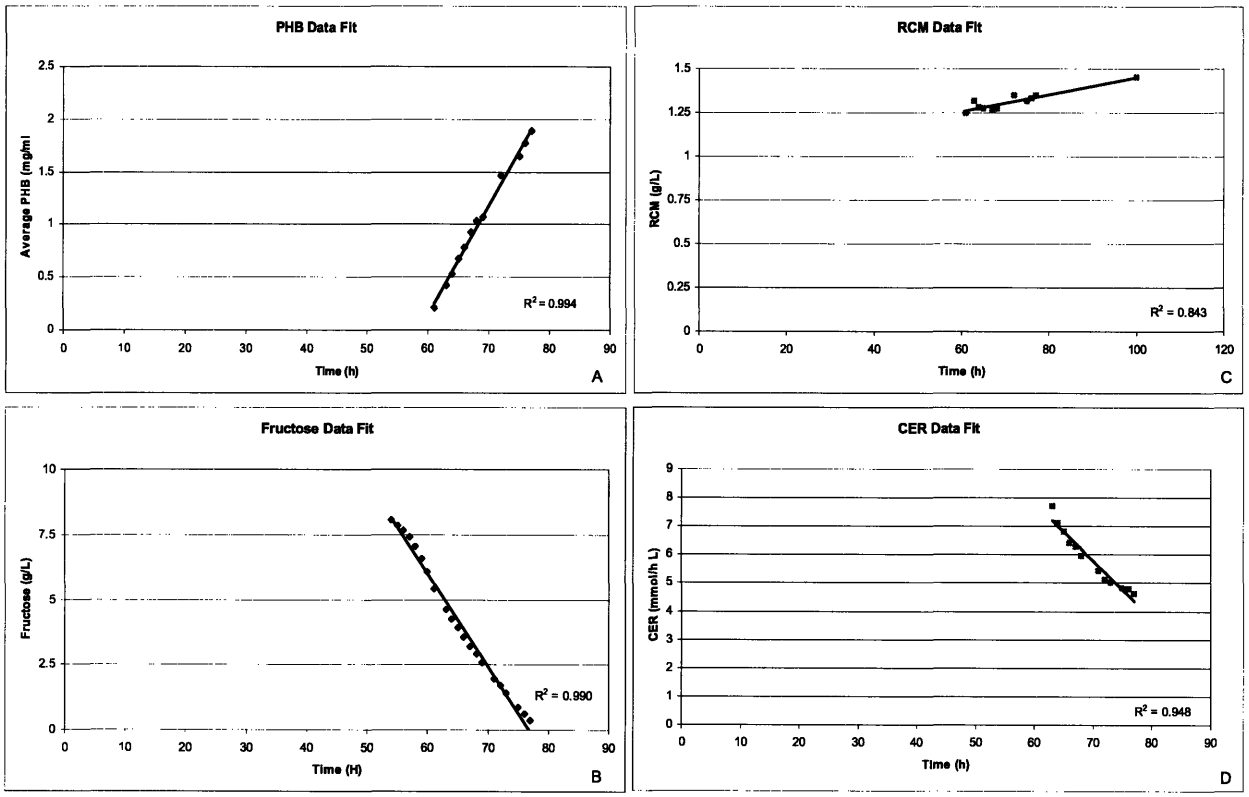

Figure 5.2.2-1: Carbon Balance Data Fits

In order to calculate the carbon balance, the slopes of the data fits were use to determine the rates of consumption or production of carbon for each variable. In the case of CER the average rate

was found by taking the average CER value during the linear PHB production phase. The rates were then used to compare the amount of carbon consumed from fructose against the amount of carbon produced in the forms of PHB, CO_2, and RCM. The carbon content of the RCM was estimated using the empirical elemental formula, $C_4H_8O_2N$. (Bormann, 2000) Without accounting for anything other than fructose, PHB, RCM, and CO_2, the carbon balance closes to within 7.5% as shown in Table 5.2.2-1. This suggests that no significant carbon-based byproducts are produced in the *R. eutropha* PHB fermentations. Additionally, the carbon balance showed that slightly more (48.7%) of the carbon consumed went into CO2 than went into PHB (42.2%).

Table 5.2.2-1: Carbon Balance

	RCM	CER	PHB	Sum	Fructose	% Closed
	g C/L h	g C/L h	g C/L h	g C/L h	g C/L h	%
Balance	0.0023	0.0694	0.0601	0.1321	0.1425	92.5%
Contribution	1.62%	48.7%	42.2%			

5.2.3. Molecular Weight

Molecular weight was also measured during the production phase. Previously, only end point molecular weights have been measured. This kinetic analysis of molecular weight may provide insight into how to control molecular weight to obtain desired physical properties. The molecular weight in this experiment increased very quickly after the fructose bolus and then remained stable for the rest of the fermentation, as shown in Figure 5.2.3-1. Though a small amount of PHB was present at the beginning of the PHB production phase (~2.5% CDW), the

molecular weight of this material has been subtracted out of the data in Figure 5.2.3-1. Additionally, the polydispersity was shown to decrease initially and then remain fairly low (~1.2) for most of the production phase.

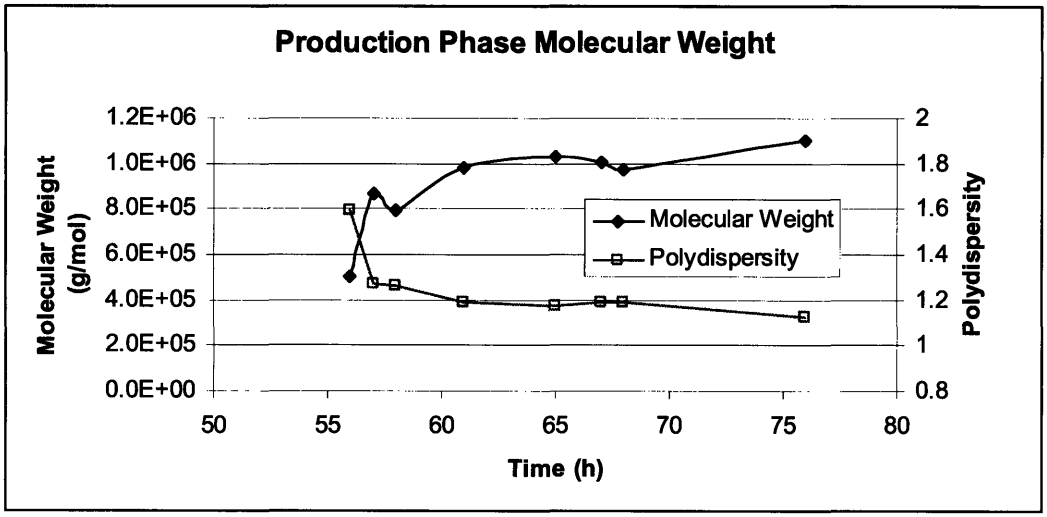

Figure 5.2.3-1: Production Phase Molecular Weight vs Time

The way the PHB molecular weight remains constant over a long period of time suggests that new PHB chains repeatedly reinitiate over the whole production phase. (Kawaguchi, 1992) Additionally, it appears that the time it takes to produce a single chain is very short compared to the sampling time as seen in the very rapid increase in PHB molecular weight. Data from other *R. eutropha in vivo* experiments suggest that a single chain is completed in approximately five minutes. (Tian, 2005) The molecular weight data seem to indicate that some control mechanism is in place to hold the molecular weight constant throughout most of the production phase.

5.2.4. Process Condition Experiments

Changes in process conditions were used to explore the kinetics of the PHB production phase. Higher temperature (37°C) and lower pH (pH 6) were used to attempt to perturb the PHB production rate and molecular weight kinetics. Only small changes were seen; both conditions slightly reduced the fructose consumption rate and the PHB production rate, as shown in Figures 5.2.4-1a and 5.2.4-1b, respectively.

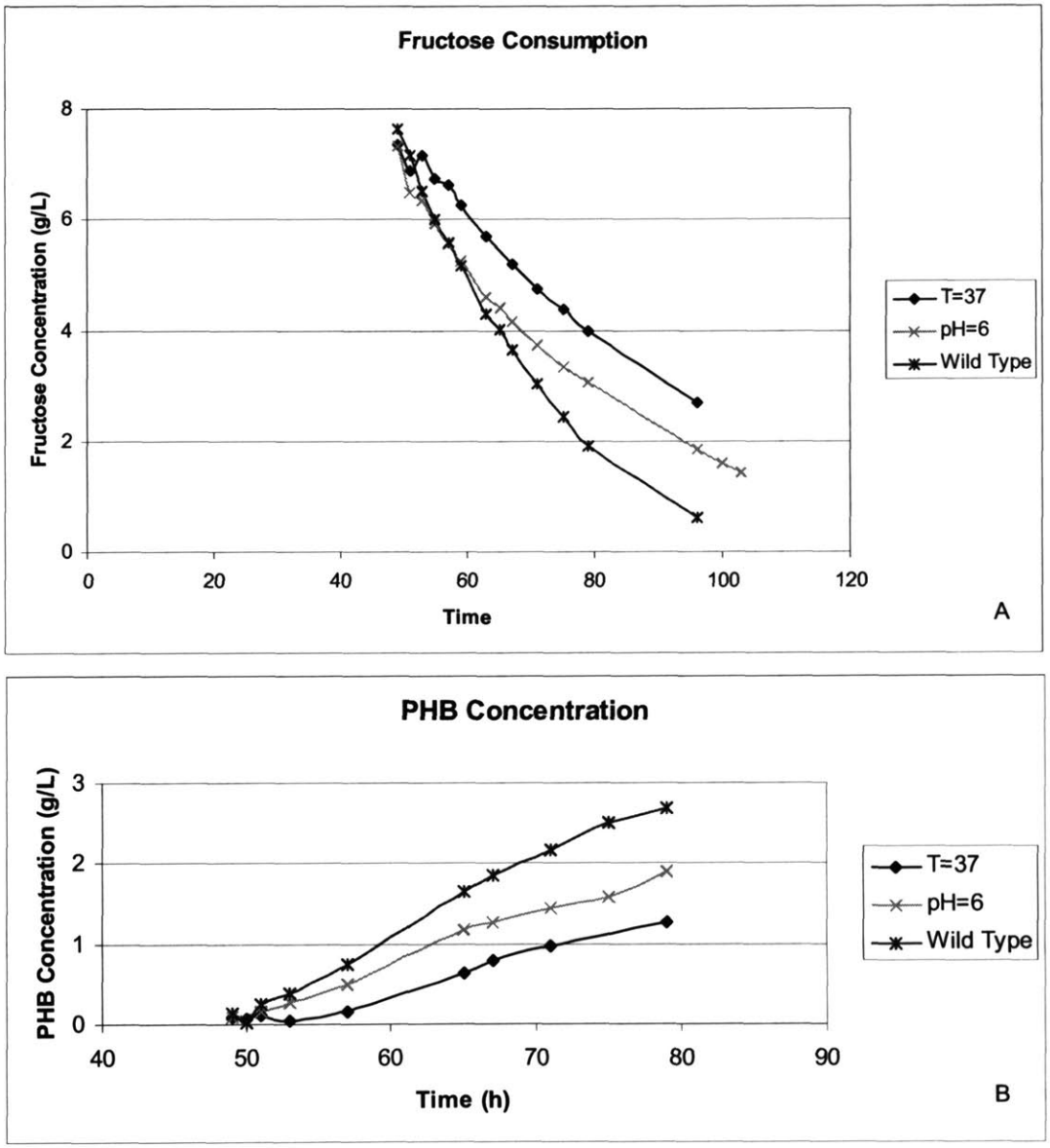

Figure 5.2.4-1: Fructose Consumption and PHB Production at Different Process Conditions

Table 5.2.4-1 compares the fructose consumption rates and the PHB production rates of the various conditions. Additionally, the rates from the 10 L fermentation used in the carbon balance described in section 5.2.1 are shown. Taking account of the amount of cells grown during the growth phase, specific PHB production rates were calculated. These rates reflected the absolute rates, where the reduction of the pH to 6 caused a reduction in the PHB production

rate and increasing the temperature to 37°C caused a slightly larger reduction in the PHB production rate.

Table 5.2.4-1: Process Condition PHB Production Rates

Condition	Fructose Consumption Rate (g/L hr)	PHB Production Rate (g/L hr)	Initial CDW (g/L)	Specific PHB Production Rate (g/L hr gCDW)
T=37	0.103	0.046	0.78	0.059
pH 7 500ml	0.258	0.091	1.27	0.073
pH 6	0.186	0.063	1.00	0.063
pH 7 10L	0.356	0.104	1.25	0.083

Kinetic molecular weight data were also collected for the perturbations in process conditions. The PHB molecular weight was slightly reduced due to the changes in process conditions, as shown in Figure 5.2.4-2. It is thought that this understanding of process condition effects on molecular weight will allow for the fine tuning of PHB molecular weight in commercial production.

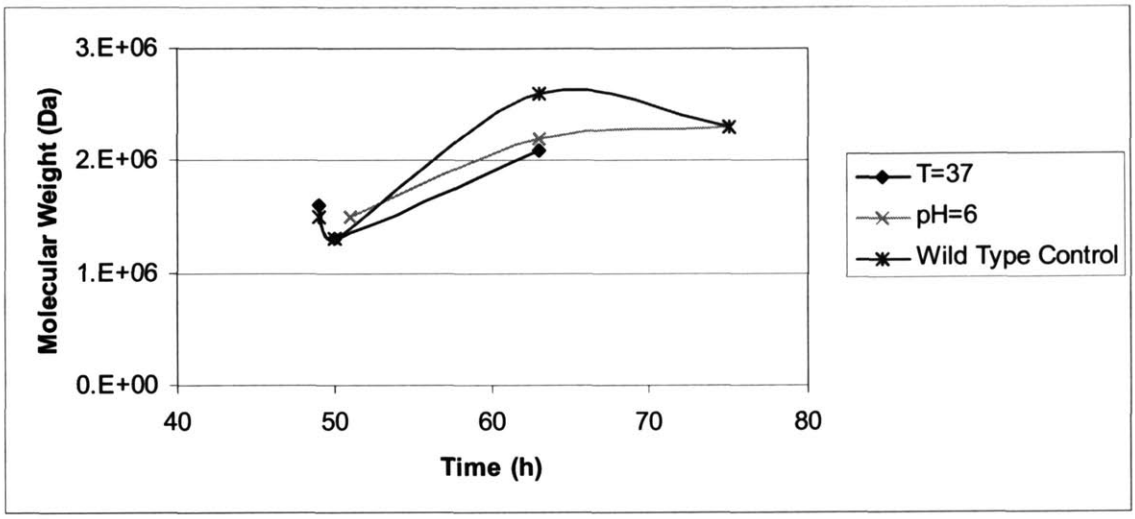

Figure 5.2.4-2: Process Condition Effects on Molecular Weight

5.2.5. Wild Type Fermentations Summary

Fermentations of wild type *R. eutropha* using the method described in section 4.7 that allows the growth and production phases to be separated showed three significant results. A carbon balance performed on the system, accounting for the carbon consumed from fructose and produced in PHB, biomass, and CO_2, was closed to within 7.5% and showed that no significant carbon-containing byproducts were produced in the *R. eutropha* PHB fermentations. Additionally, the kinetics of molecular weight formation were monitored, and it was shown that the molecular weight increased very quickly during the production phase and then remained fairly constant throughout the rest of the fermentation. It was also shown that a low production pH (pH=6) and a higher production phase temperature (T=37°C) both slightly reduced the PHB production rate and the PHB molecular weight.

6. SYNTHASE MUTANT EXPERIMENTS

6.1. Class I PHB Synthase Mutant Experiments

Multiple shake flask experiments and fermentations were performed to determine the effect of point mutations to the synthase enzyme. PHB produced from the mutant synthases was monitored for total PHB content, molecular weight, and PHB production rate. Additionally, it was thought that the data from the synthase mutants would provide insight into the mechanism for polymerization at the synthase enzyme.

6.1.1. Synthase Mutant Shake Flask Experiments

Nine synthase mutants were chosen for molecular weight determination. All of the mutants were precise point mutations to the enzyme. The nomenclature used to refer to the mutants is as follows. The first letter in the designation represents the amino acid originally present in the enzyme. The number after the first letter is the position at which that amino acid was present. The letter after the number represents the amino acid which was substituted for the original amino acid. Thus, S260A means the serine at position 260 was replaced with an alanine. Of the nine mutants selected, only the D480A did not produce any PHB. This is interesting because the analogous mutation in the class III synthase, D302A, did produce PHB and was used in multiple subsequent experiments. This indicates further differences between class I and class III synthases polymerization mechanisms. Each of the other mutants produced PHB with higher molecular weight and lower polydispersity than the wild type PHB, as shown in Figures 6.1.1-1a

and 6.1.1-1c, respectively. It is also interesting to note that each of the mutants produced lower total amounts of PHB than the wild type, as shown in Figures 6.1.1-1b and 6.1.1-1d.

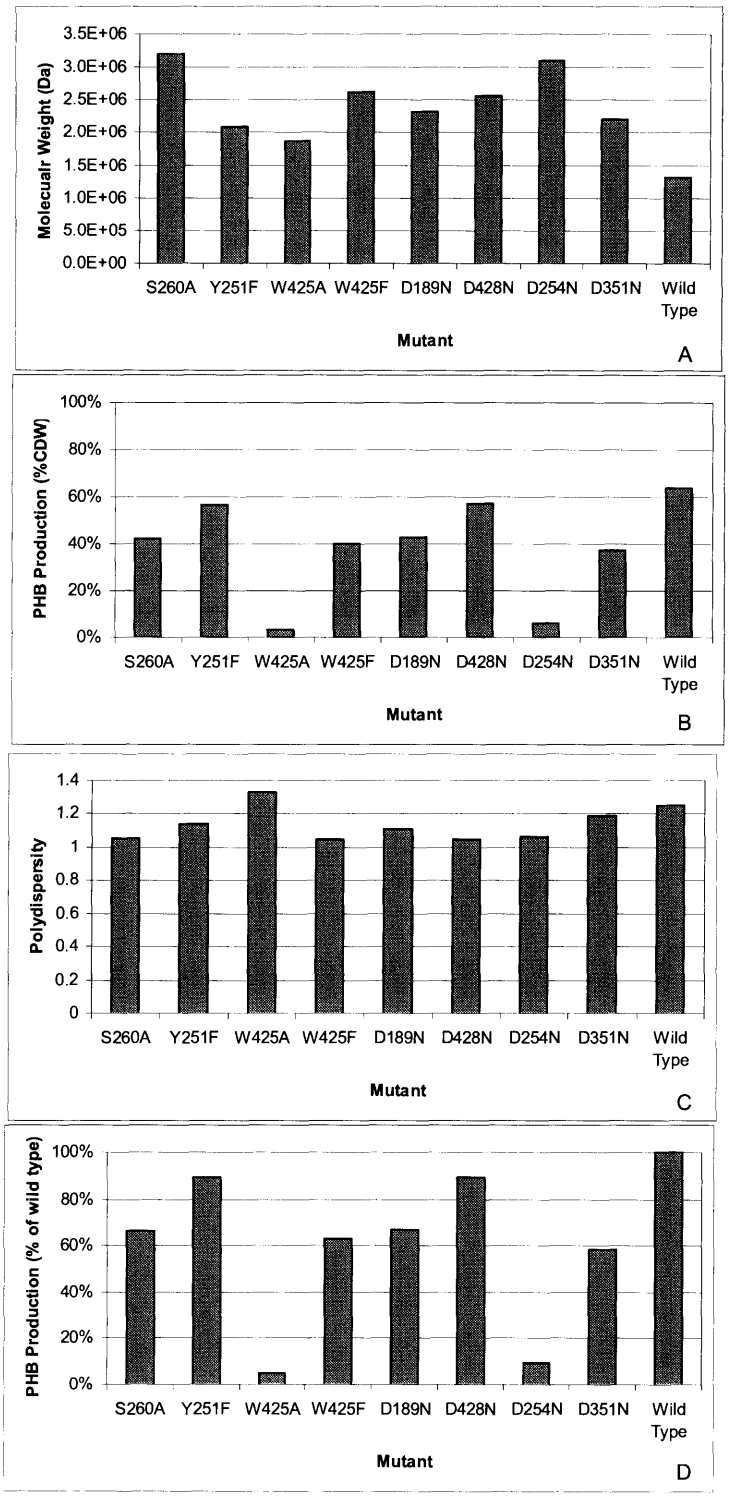

Figure 6.1.1-1: Synthase Mutant Shake Flask Experiments

6.1.2. Fermentor Experiments

The kinetics of PHB production and molecular weight formation were monitored in 500 mL fermentations. The S260A and D189N mutations were chosen because they produced different molecular weights of PHB but produced it in levels comparable to the wild type. PHB production in the fermentations mirrored the PHB production in the shake flasks, as shown in Figure 6.1.2-1.

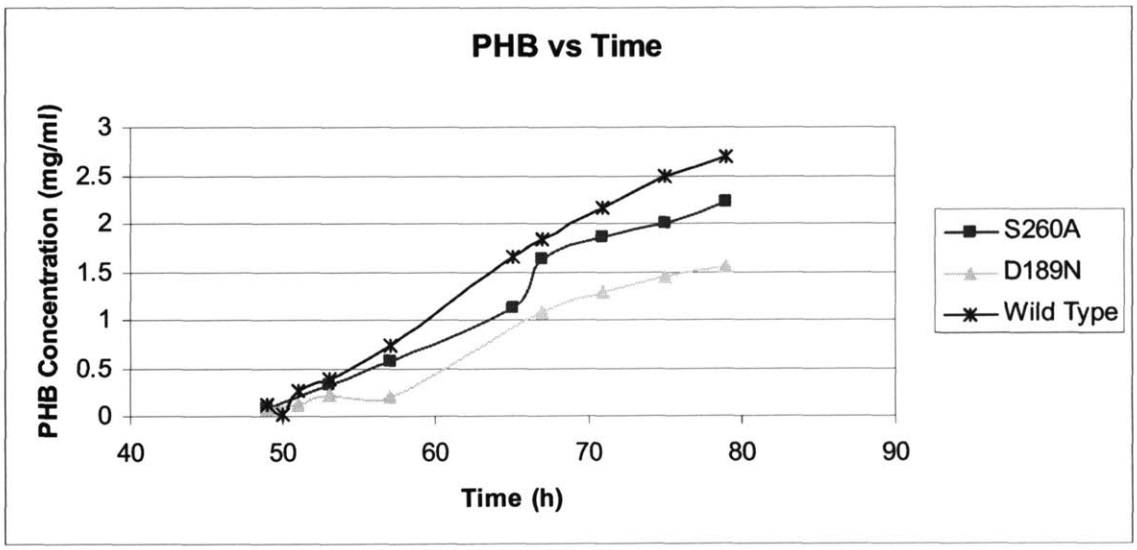

Figure 6.1.2-1: Synthase Mutant PHB Production

The synthase mutants produced PHB with higher molecular weight but at lower concentrations than the wild type, as shown in Figure 6.1.2-2a. Additionally, a small molecular weight peak that disappeared over time was seen, as shown in Figure 6.1.2-2b. The fructose bolus was added after the 49 hour sample, which accounts for the initial drop in molecular weights seen in the figure. This small molecular weight peak has not been seen in subsequent experiments. It is thought that small changes to the operation of the HPLC may cause the small peak to come off in

the void volume. While it is thought that the small molecular weight peak may have some significance to the PHB polymerization mechanism, a reliable method for reproducing the peak at early time points without pushing it into the void volume of the HPLC column has not been found. The peak masses (peaks on the HPLC trace), shown in Figure 6.1.2-2c, indicate how the PHB in the sample is distributed between the two peaks. The molecular weight seen in Figure 6.1.2-2a indicates that by using a class I synthase mutation the PHB molecular weight can be slightly increased; this, along with the reduction in PHB molecular weight seen from process conditions in Figure 5.2.4-2, demonstrates the ability to fine tune PHB molecular weight, which may prove important for bring PHB to market.

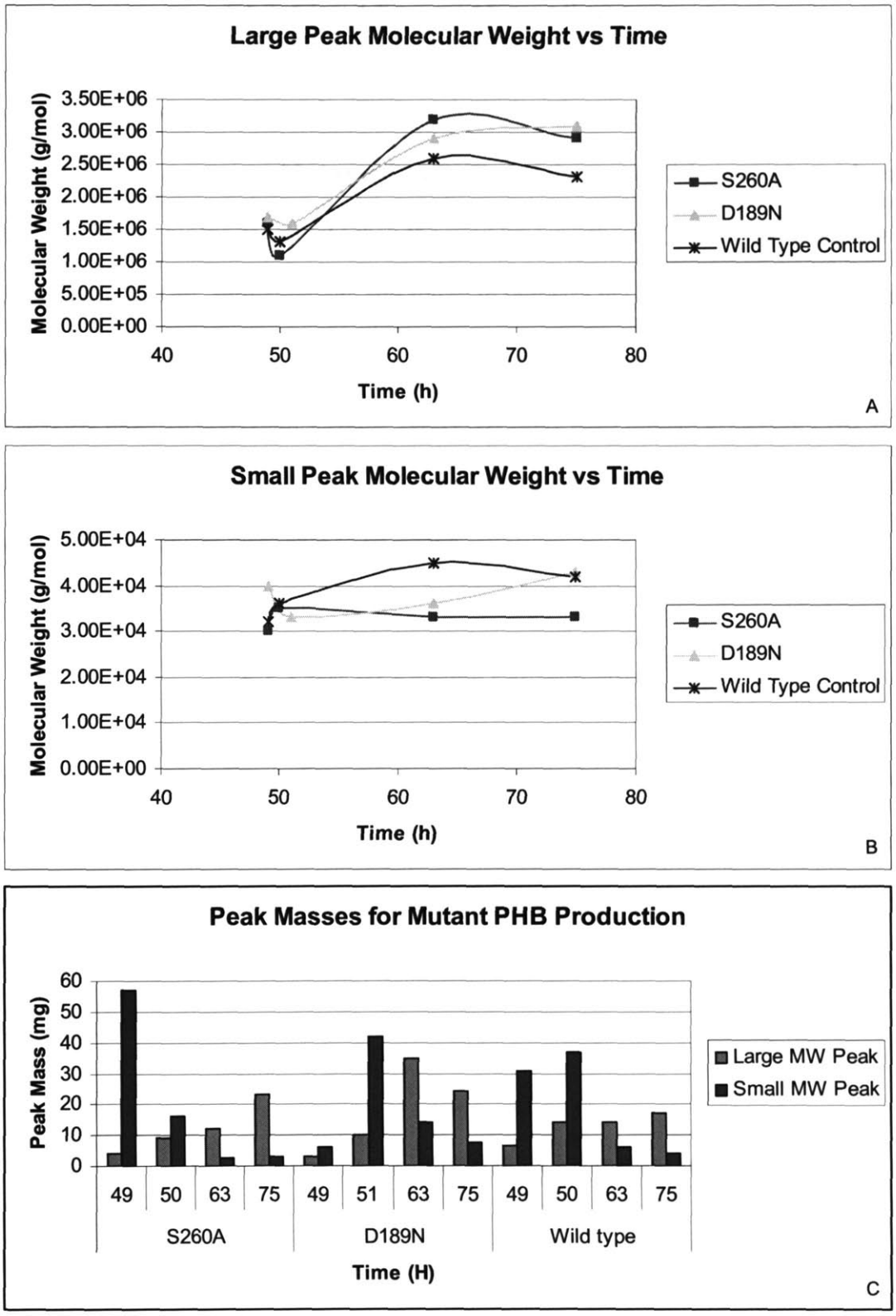

Figure 6.1.2-2: Synthase Mutant PHB Molecular Weights

6.1.3. Class I Enzyme Mutant Summary

Nine class I mutants were screened for PHB production and molecular weight. It was found that all but one of the mutants were able to produce PHB, and that most of the mutants produced less total PHB at a higher molecular weight than the wild type synthase. Two of the mutants were studied further in 500 mL fermentations and found to increase the PHB molecular weight at a lower PHB production rate. This provides a way to slightly increase the PHB molecular weight to hit a specific targeted molecular weight. However, since each mutant produced PHB with molecular weight higher than that of the wild type, no significant conclusions about the PHB polymerization mechanism were able to be drawn.

6.2. Class III Enzyme Experiments

Experiments with the class III synthase enzyme, also denoted as PhaEC, were performed to observe the differences in PHB production and molecular weight when compared to the class I synthase enzyme. Additionally, one class III synthase mutation was observed to have a very slow PHB production rate. The slow rate allowed for analysis of early time points that usually occur too quickly in the wild type synthase.

6.2.1. Initial PhaEC and D302A Fermentation

Fermentations were performed to determine whether the class III synthase enzyme exhibited different PHB production kinetics and molecular weight than the class I enzyme. Two strains of *R. eutropha* were used in parallel fermentations. In one strain the class III synthase enzyme

(PhaEC) was inserted to replace the class I synthase; in the other strain a mutant of the class III synthase (D302A) was inserted into the *R. eutropha* chromosome to replace the class I synthase. The fructose consumption and individual strain PHB production from the fermentations is shown in Figures 6.2.1-1a, 6.2.1-1b, and 6.2.1-1c, respectively. The interesting observation to note is that the D302A strain consumed all of the fructose bolus without producing very much PHB. This led to further fermentations to determine where the fructose went.

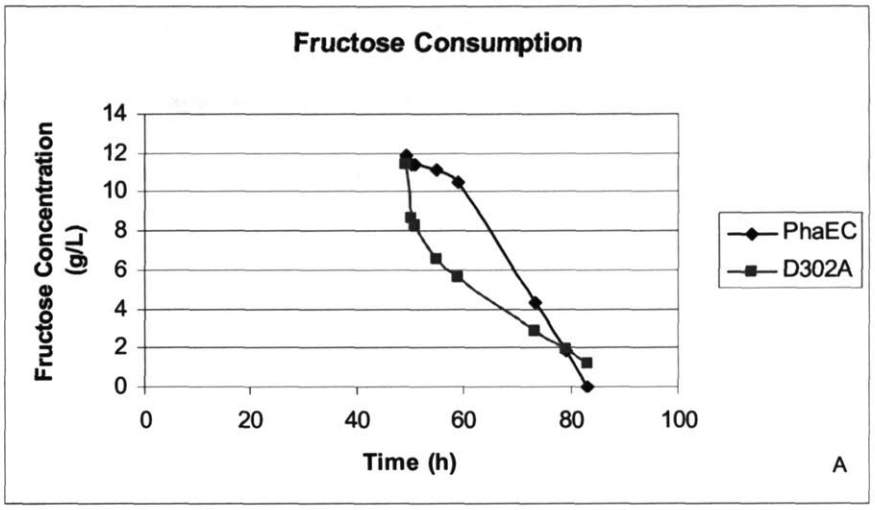

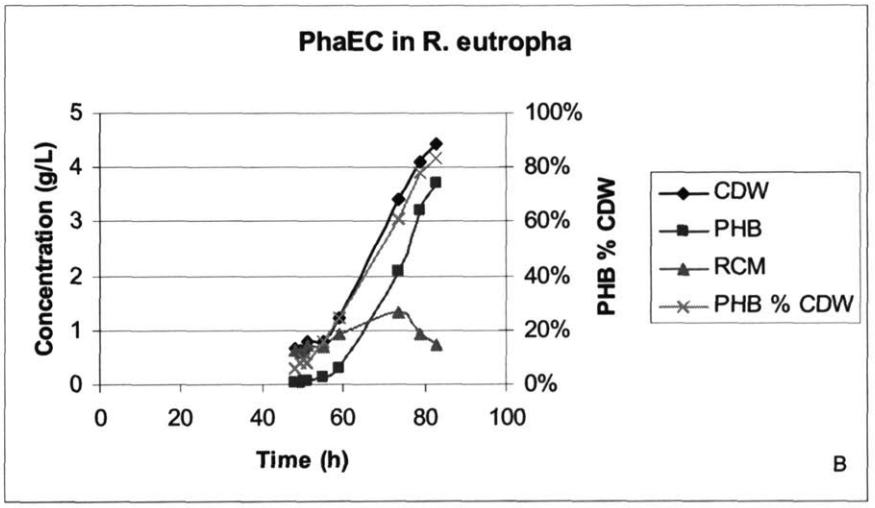

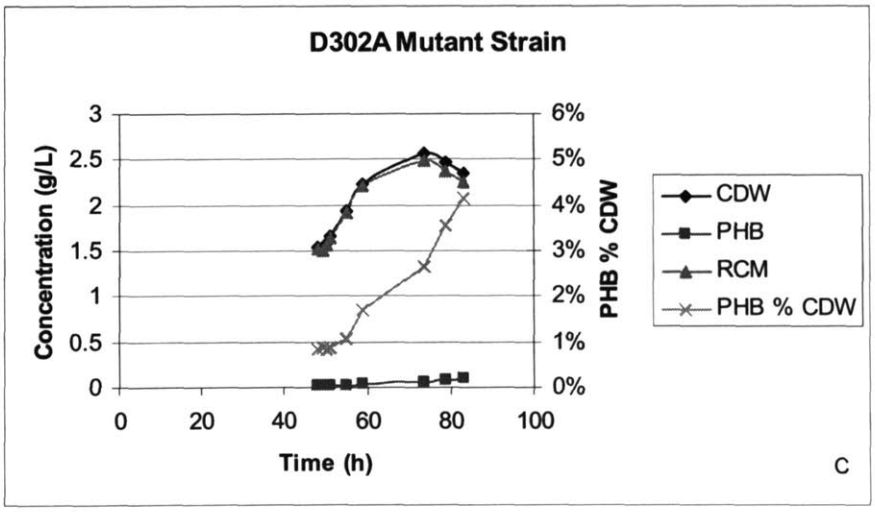

Figure 6.2.1-1: PhaEC and D302A Fructose Consumption

The molecular weight from both fermentations was also measured. The trend of the class III synthase molecular weight appears very similar to the trend of the class I synthase molecular weight, where the molecular weight increases very quickly and then remains constant throughout the rest of the production phase, as shown in Figure 6.2.1-2.

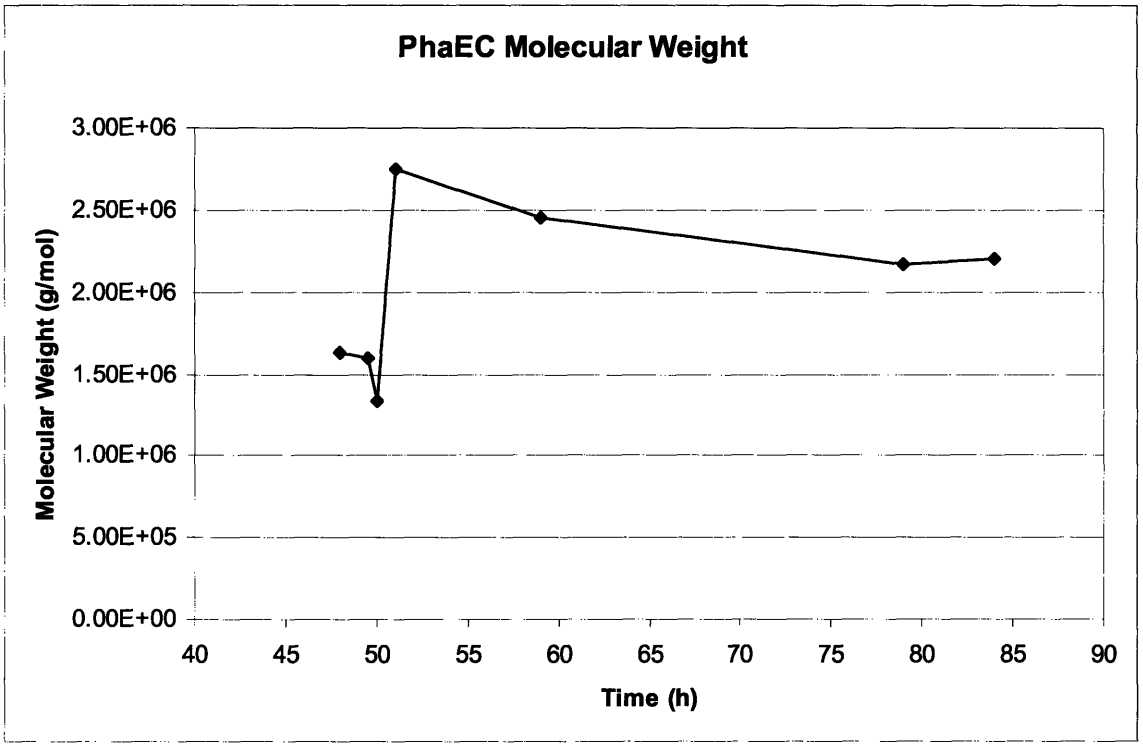

Figure 6.2.1-2: PhaEC Molecular Weight

The number of chains present was calculated from the PHB concentration data and the molecular weight data. Additionally, the number of new chains formed were also calculated and plotted in Figure 6.2.1-3. The trend is shown to be linear, indicating that the rate of initiation of new chains is constant throughout the production phase.

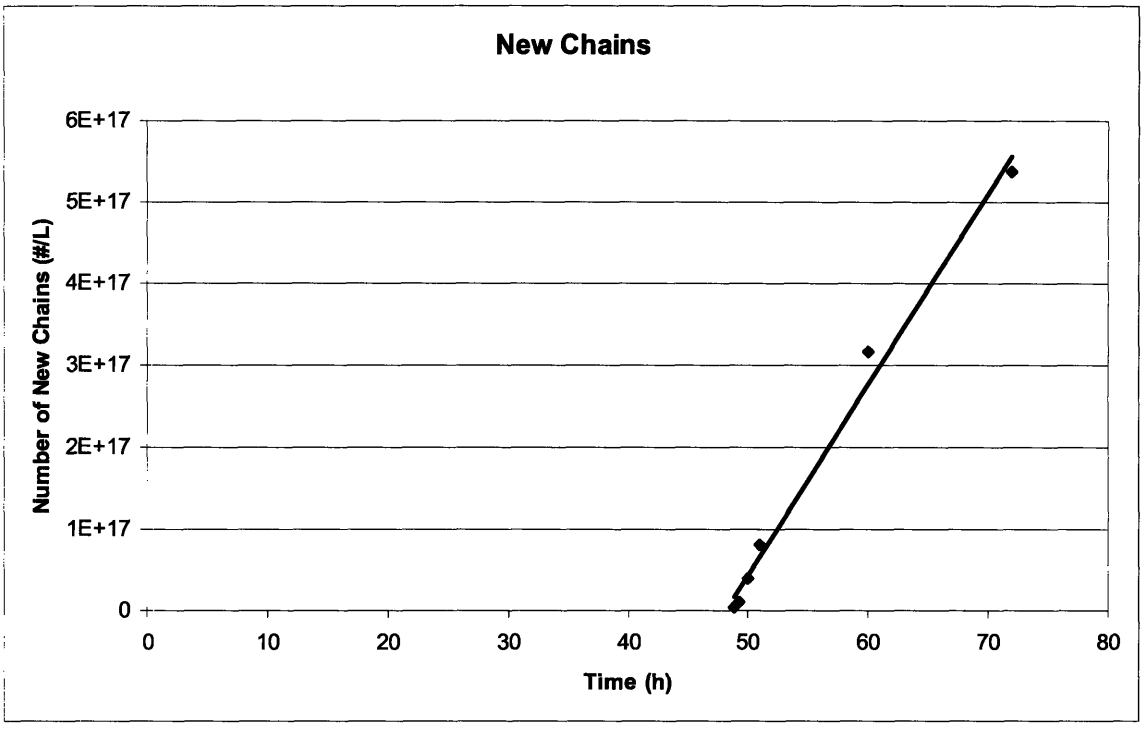

Figure 6.2.1-3: PhaEC New Chains per Unit Time

Only two samples of the D302A fermentation contained enough PHB for molecular weight analysis. However, these two samples showed a markedly different trend of increasing molecular weight over time, as shown in Figure 6.2.1-4. A small molecular weight peak was also seen in both samples, but the molecular weight did not change significantly between the samples. The observation that the D302A consumed all of the fructose while only producing a small amount of PHB led to further experiments with the class III synthase enzymes.

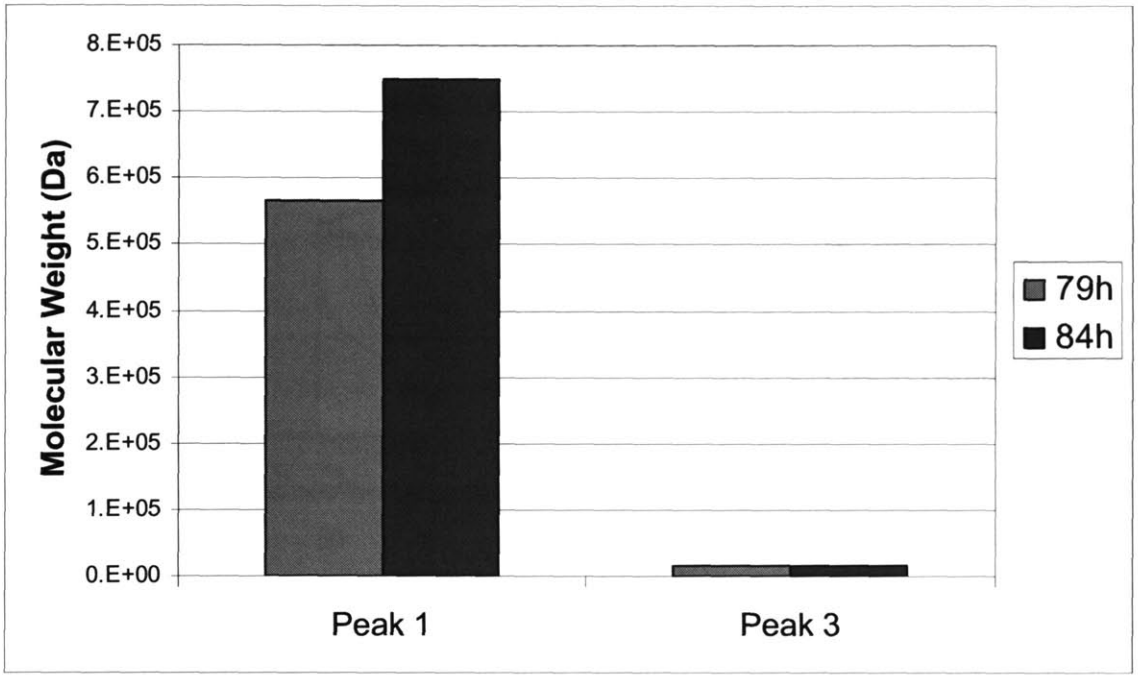

Figure 6.2.1-4: D302A Molecular Weight

6.2.2. PhaEC, ΔPhaC, and D302A Parallel Fermentations

Three parallel fermentations using the PhaEC, ΔPhaC, and D302A strains were performed to explore the D302A behavior of consuming all of the fructose without producing very much PHB. It was noted that the PhaEC and ΔPhaC did not use all of the fructose during the growth phase where the D302A strain did completely consume all of the fructose, as shown in Figure 6.2.2-1.

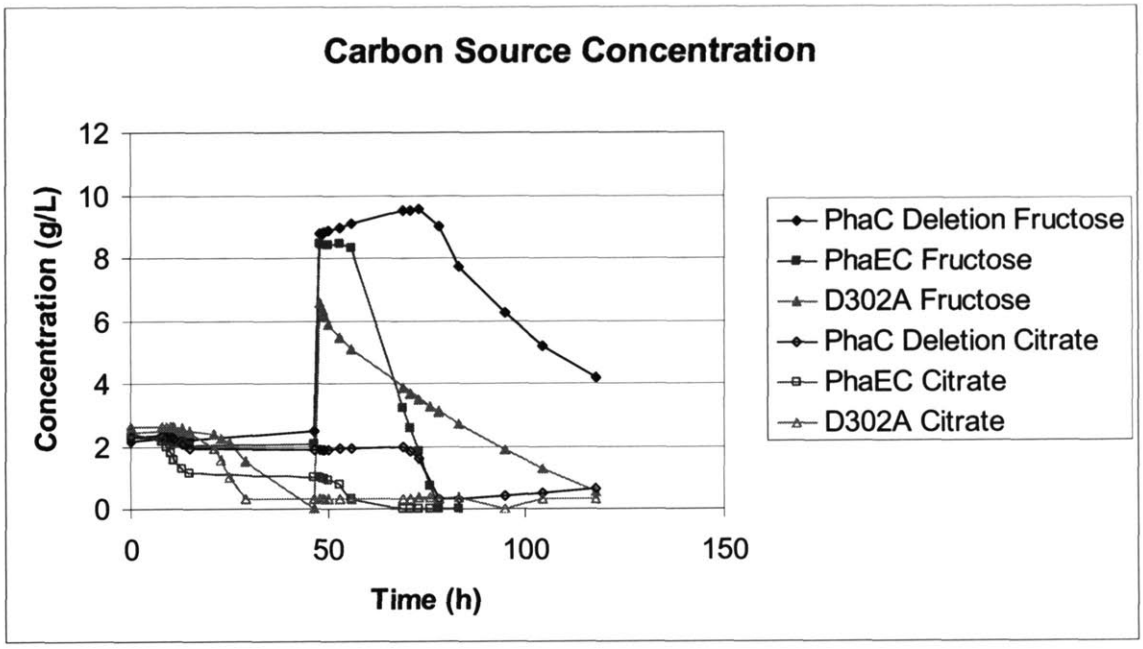

Figure 6.2.2-1: Parallel Fermentation Carbon Source Consumption

This appears to be related to the pH behavior, where if the pH gets too high too quickly, growth shuts down and further utilization of the fructose does not take place until the bolus. The process variable behavior of the three fermentations is shown in Figure 6.2.2-2. The PhaEC and ΔPhaC both showed the same pH behavior, where acid and then base were pumped soon after the fructose bolus, and then no activity was seen during the rest of the fermentation. In the D302A acid was pumped after the fructose bolus, but then base was pumped for the remainder of the production phase.

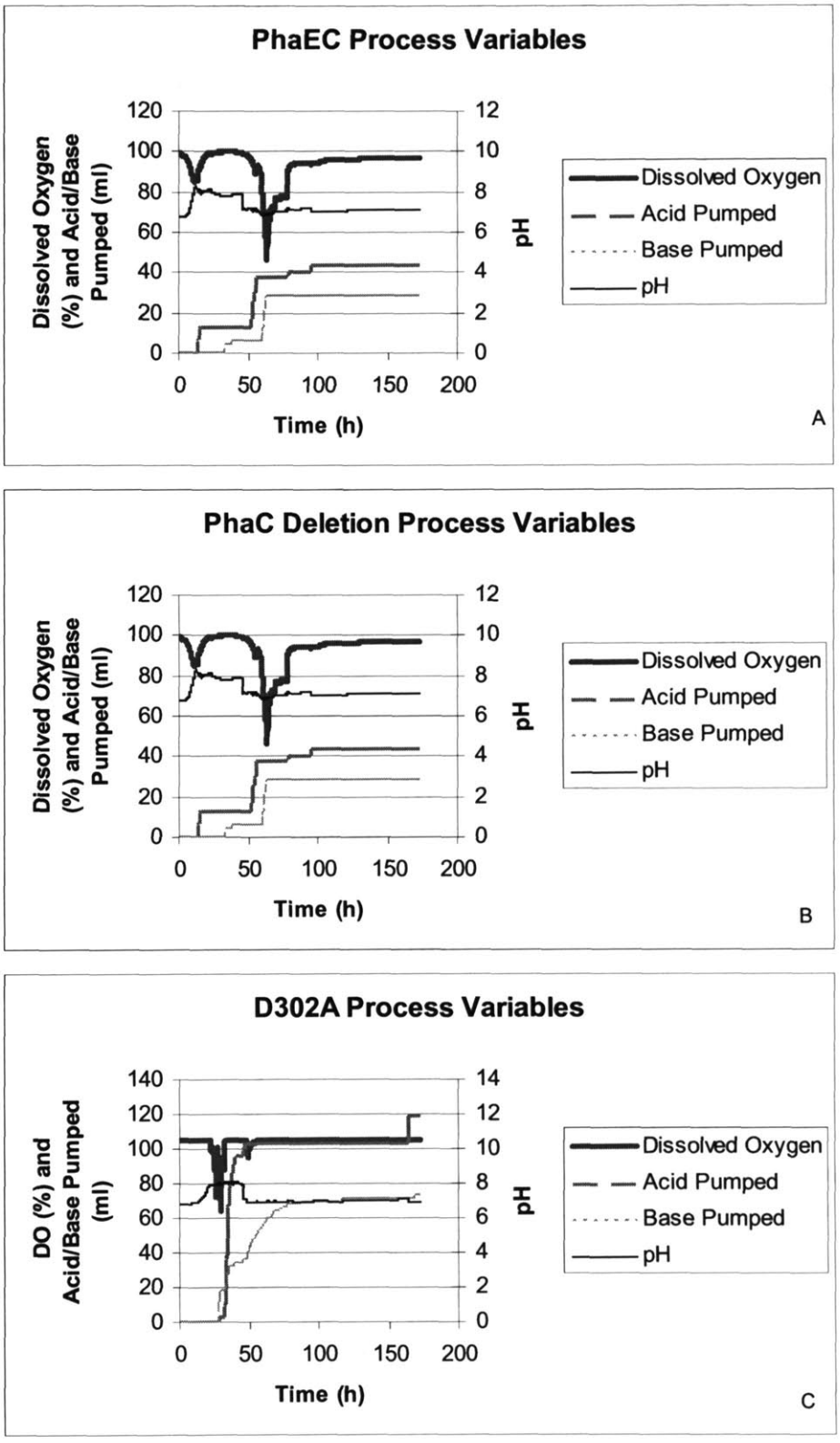

Figure 6.2.2-2: PhaEC, ΔPhaC, and D302A Fermentation Process Variables

The cell dry weight growth and PHB production are shown in Figures 6.2.2-3a and 6.2.2-3b, respectively. The PHB production in the PhaEC strain is much more rapid than in the D302A strain and reaches a much larger percent of cell dry weight. This is as expected from the low activity shown for the D302A enzyme.

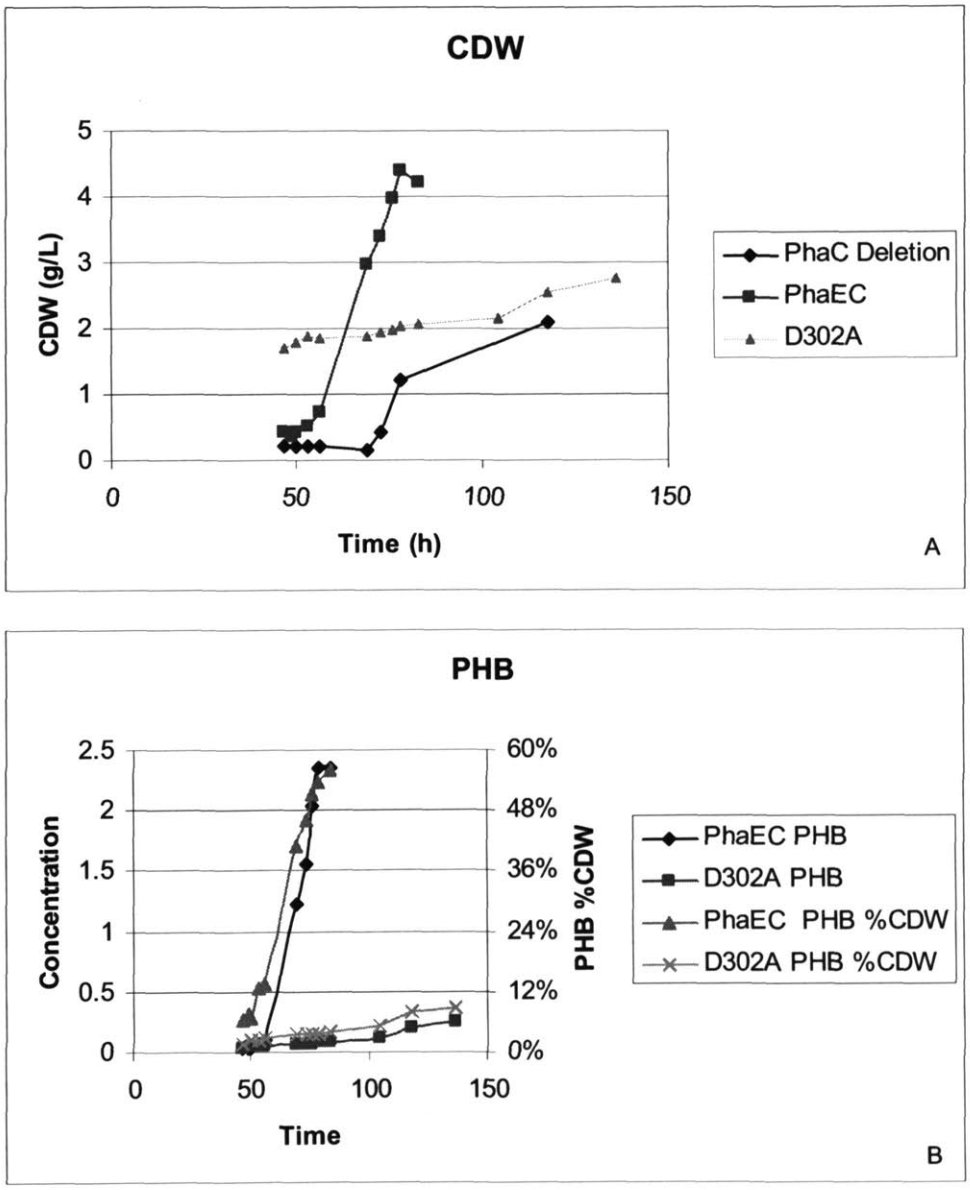

Figure 6.2.2-3: Parallel Fermentation Cell Dry Weight

Molecular weight for four D302A samples is shown in Figure 6.2.2-4. The molecular weight corroborates the measurements from the initial experiments where molecular weight increased with time. These data further suggest that the increase is linear, though it is difficult to confirm at the 500 mL scale because only a few data points can be taken.

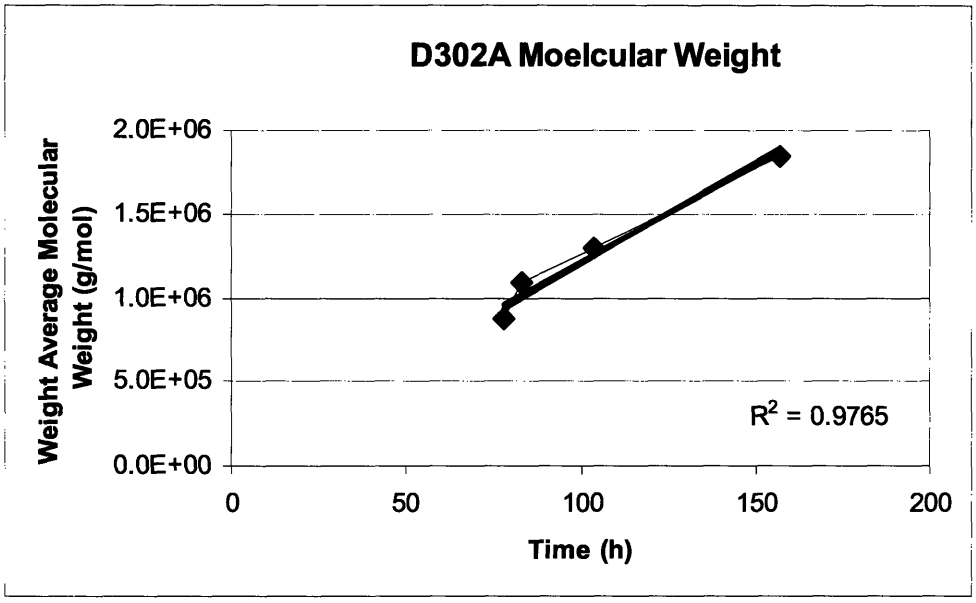

Figure 6.2.2-4: D302 Molecular Weight

Additionally, multiple late peaks were seen in the HPLC trace of the extracellular media. One of these peaks was identified as having the same retention time as 3-hydroxybutyrate. The area of these peaks was compared to a standard curve and the hypothetical concentration of 3-hydroxybutyrate was plotted in Figure 6.2.2-5. The concentration of 3-hydroxybutyrate in the media is seen to increase linearly and reach a concentration of approximately 0.8 g/L. The linear increase of PHB molecular weight and 3-hydroxybutyrate in the D302A fermentation suggest that the D302A mutant is significantly different that the wild type strain. Further study of the molecular weight may provide insight into the polymerization mechanism; additionally, the

D302A strain may provide a way to produce fairly large quantities of 3-hydroxybutyrate for synthetic polymerization.

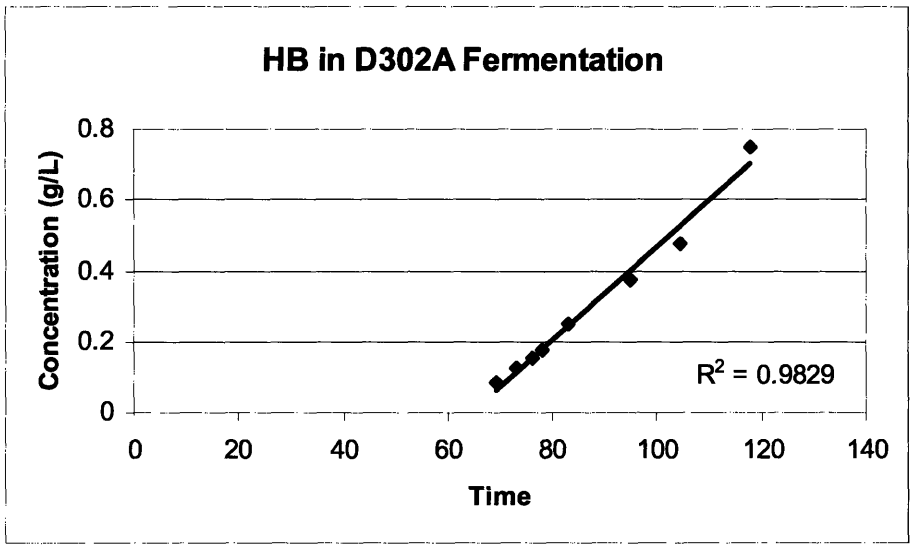

Figure 6.2.2-8: 3-hydroxybutyrate in D302A Fermentation

6.2.3. D302A Carbon Balance

A carbon balance was performed on a 10 L D302A fermentation to attempt to quantify where the carbon went in the D302A fermentation. Unfortunately, when switching from the 500 mL fermentation to the 10 L fermentation, some changes in the media were introduced that render the carbon balance data somewhat less useful. In the 10 L fermentation, the cells did not grow as well and reached a CDW of only about half that seen in the 500 mL fermentation. It is believed that this may be related to some precipitation that was seen in the fermentation media. However, the carbon balances well in the 10 L fermentation and may be useful when considering the situation in the 500 mL fermentations. The fructose consumption in the 10 L fermentation is shown in Figure 6.2.3-1a; the PHB production is shown in Figure 6.2.3-1b; the CDW is shown in

Figure 6.2.3-1c; and the CER data for the time over which the carbon balance was calculated is shown in Figure 6.2.3-1d.

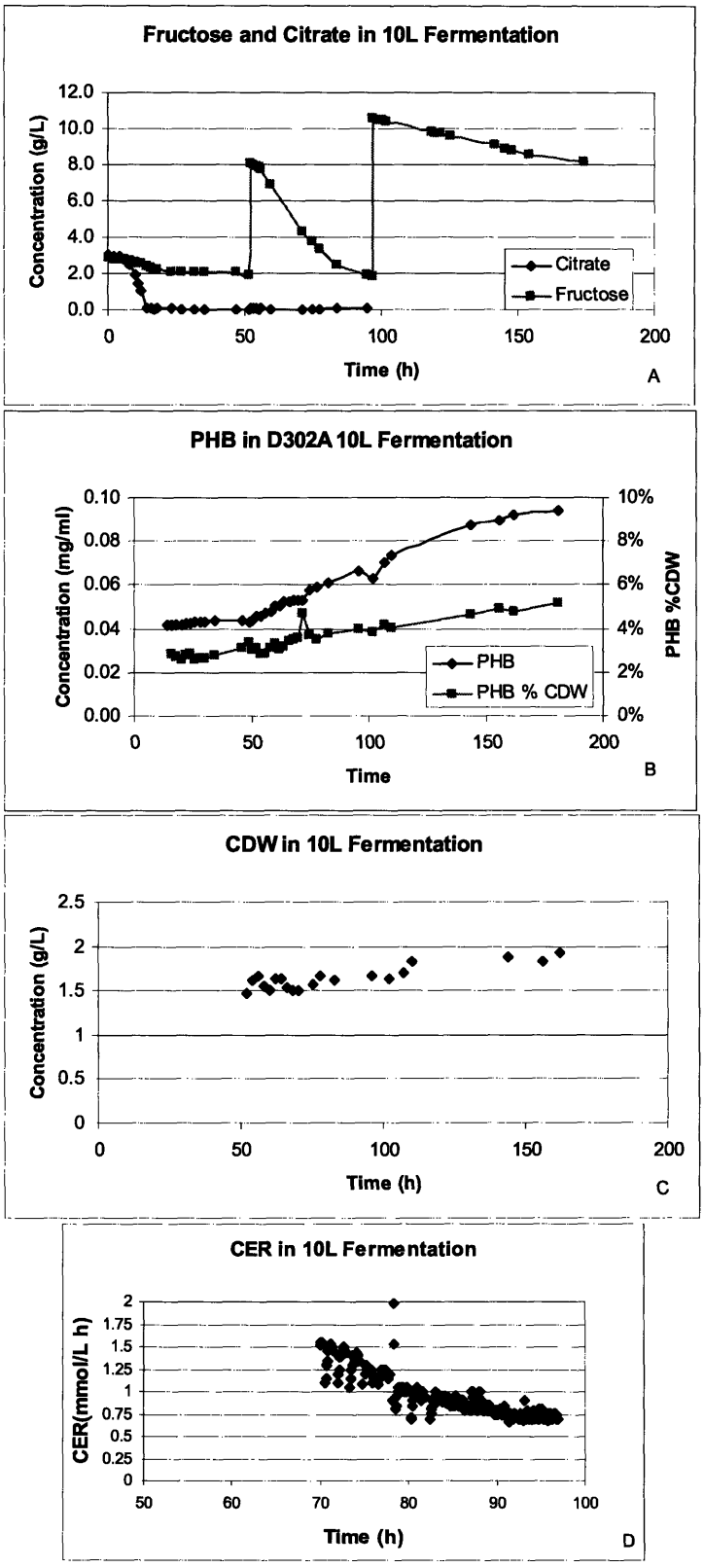

Figure 6.2.3-1: 10L D302A Fermentation Data for Carbon Balance

The carbon balance was performed over the time period from 75 hours to 95 hours to use the robust period of the production phase that was well out of the lag phase following the fructose bolus. As shown in Table 6.2.3-1, the carbon in the cell dry weight and PHB is multiple orders of magnitude below the carbon in the fructose consumed. Additionally, it is shown that the carbon in the fructose consumed closely matches the carbon in CO_2 produced. While this balance is less informative because no 3-hydroxybutyrate was produced and because the cell dry weight was approximately half of that seen produced from the same amount of fructose at the 500 mL scale, it does at least indicate that much of the fructose consumed ends up as CO_2.

Table 6.2.3-1: D302A 10L Carbon Balance

	Fructose Consumption	CO_2 Production	RCM Production	PHB Production	% Closed
Units	g C/L h	g C/L h	g C/L h	g C/L h	%
Balance	0.0365	0.0324	6.87E-05	1.22E-05	11.2%

Additionally, based on the data from Figure 6.2.2-8, the amount of carbon produced in 3-hydroxybutyrate would be approximately 0.008 g C/L h, which would represent approximately 20% of the carbon from the fructose consumed in that fermentation. Thus, the 3-hydroxybutyrate would be expected to play a significant role in the carbon balance, but it would appear that the CO_2 would still account for most of the carbon that was consumed from the fructose, unless some other byproduct was also produced in large amounts during the fermentation.

6.2.4. D302A Molecular Weight

Another set of D302A fermentations were performed to further explore the D302A molecular weight formation. Three parallel fermentations were performed. In one of the fermentations the starvation regime was used, and in the two other fermentations, a constant pH regime was used. The constant pH regime also had a shorter time between when the original fructose ran out and when the fructose bolus was applied. The fructose consumption for the three fermentations is shown in Figure 6.2.4-1. Multiple fructose boluses were used in the constant pH regime; a much larger fructose bolus was used for the starvation regime. Each of these fructose bolus patterns were used to attempt to reach high PHB levels in the D302A strain so molecular weight could be accurately measured.

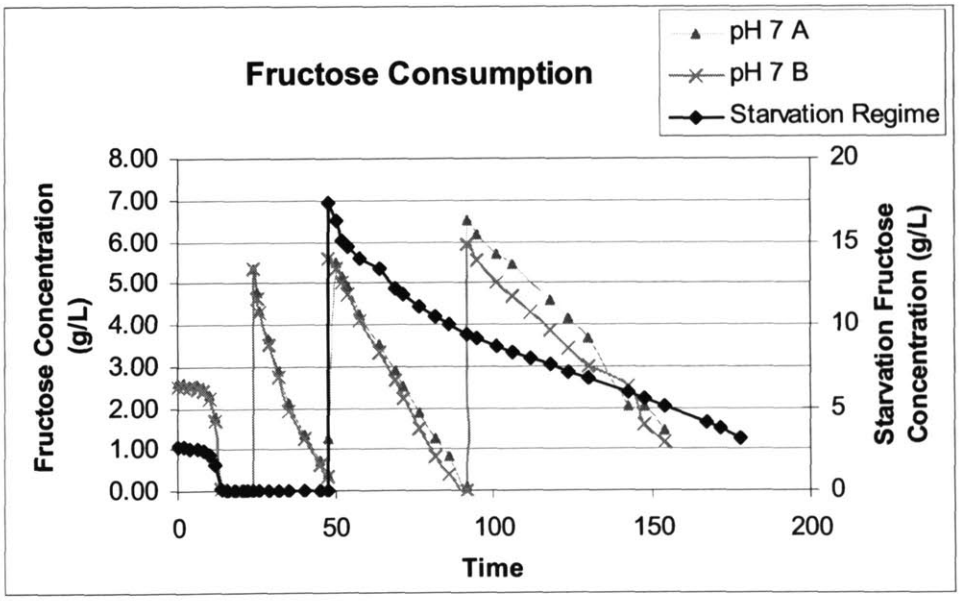

Figure 6.2.4-1: D302A Molecular Weight Experiment Fructose Consumption

The duplicate constant pH regime fermentations matched quite well for the fructose consumption data. The average cell dry weight data and PHB production data for these two fermentations are shown in Figure 6.2.4-2.

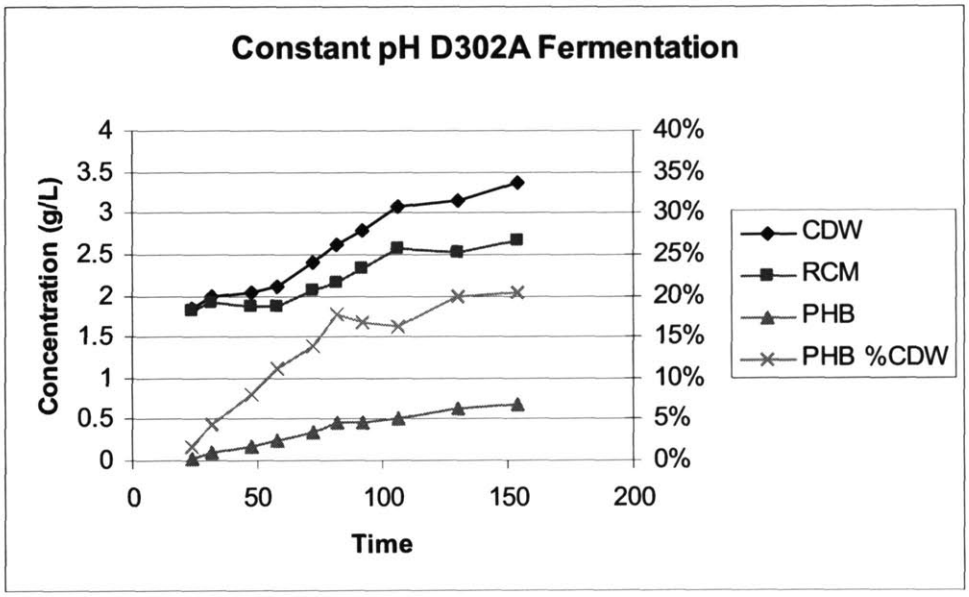

Figure 6.2.4-2: CDW and PHB for Constant pH D302A Fermentations

The PHB content of these fermentations is much higher than that seen in earlier D302A fermentations. It is believed that this is due to the removal of the starvation phase. The higher amount of PHB in the cells made it easier to recover sufficient PHB to perform molecular weight measurements. The molecular weight time course is shown in Figure 6.2.4-3, and as with the data in Figure 6.2.2-4, the molecular weight increases linearly over time.

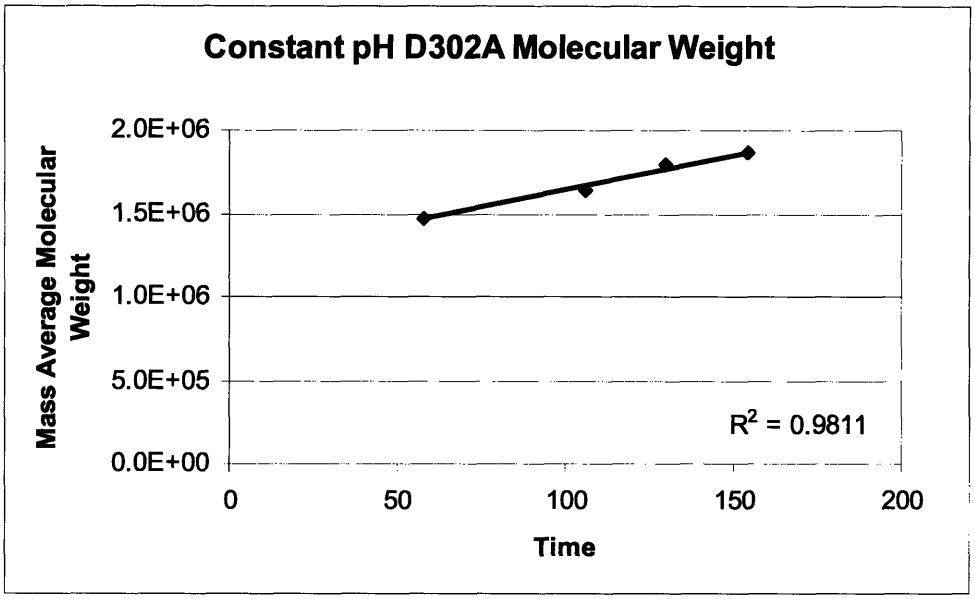

Figure 6.2.4-3: Constant pH D302A Molecular Weight

Additionally, the 3-hydroxybutyrate concentration was monitored throughout the fermentation, as shown in Figure 6.2.4-4. Since these fermentations were carried out for much longer periods of time than the previous fermentations, different behavior in the 3-hydroxybutyrate production was noted. The 3-hydroxybutyrate was shown to be produced in a fairly linear fashion, as in the previous experiments, however after a period of time, the concentration dropped until it completely disappeared from the medium.

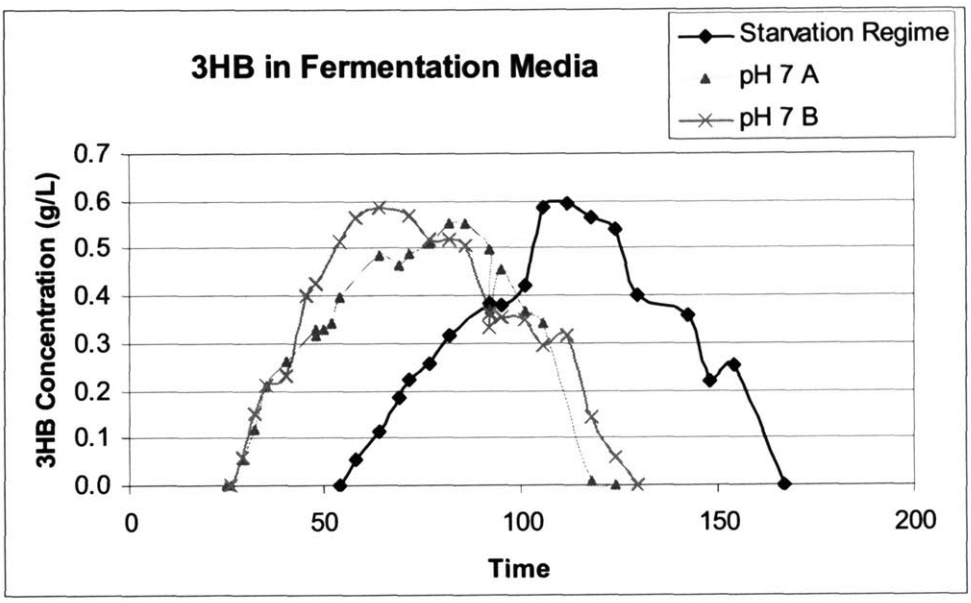

Figure 6.2.4-4: D302A 3-hydroxybutyrate in the Fermentation Media

These data confirm the results of the previous experiment. Additionally, the peak from the HPLC trace that was suspected to be 3-hydroxybutyrate was positively identified through GCMS. Figures 6.2.4-5a and 6.2.4-5b show the GC trace and molecular weight fracture pattern at a retention time of 10.45 minutes from a 3-hydroxybutyrate standard, respectively. Figures 6.2.4-5c and 6.2.4-5d show the GC trace and molecular weight fracture pattern from the 10.45 minute retention time peak from a 72 hour fermentation media sample, respectively. Both of the fracture patterns are the same, and were identified as the derivatized form of 3-hydroxybutyrate by the NIST database that accompanies the GCMS software.

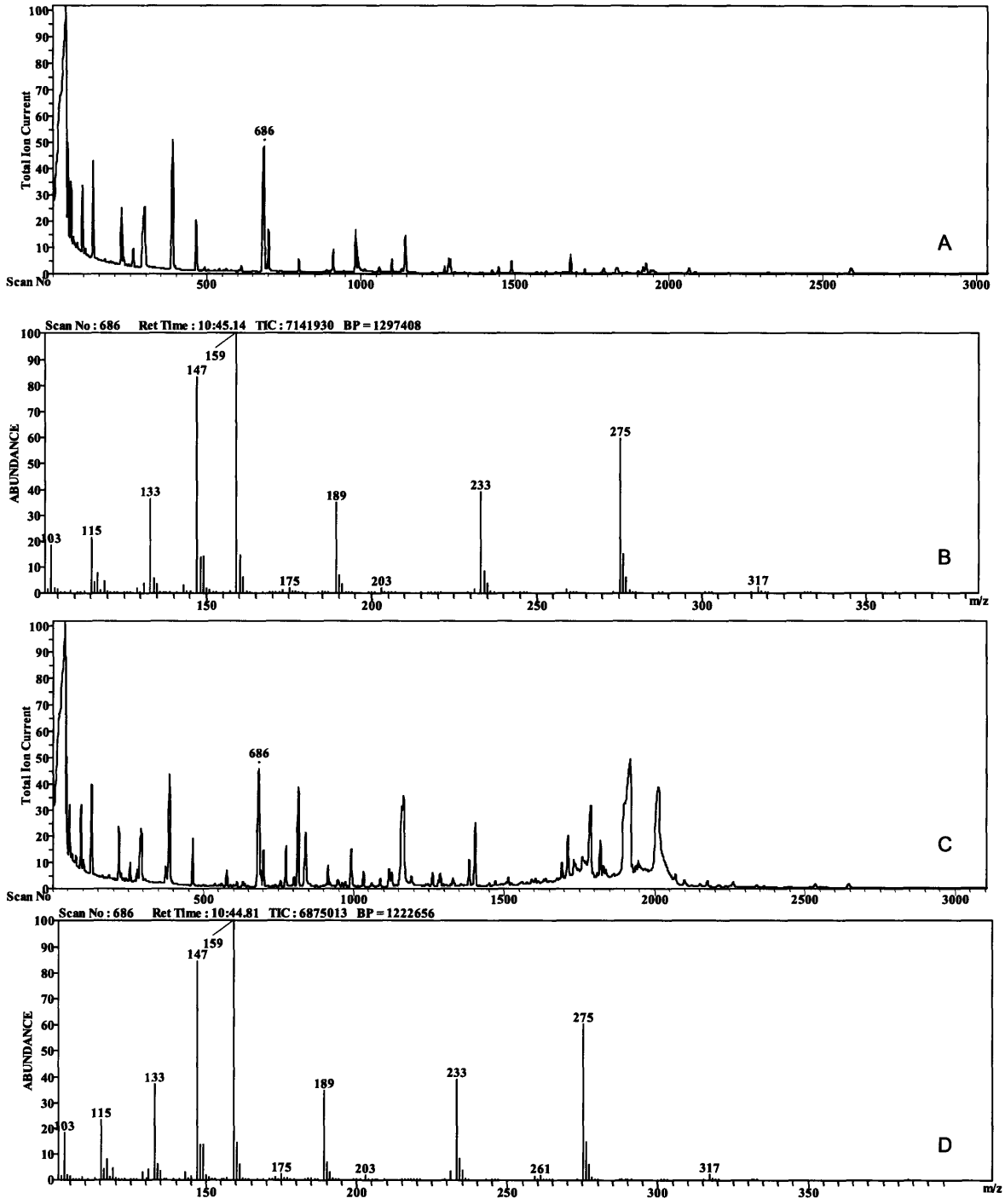

Figure 6.2.4-5: GCMS Traces and 3-hydroxybutyrate Molecular Weight Fracture Patterns

6.2.5. Class III Enzyme Summary

The wild type class III synthase enzyme from *A. vinosum* was shown to have similar activity to the wild type class I synthase enzyme from *R. eutropha*. As with the class I enzyme, the class III enzyme produced PHB that showed a rapid increase in molecular weight at the beginning of the production phase and then remained constant for the majority of the rest of the production phase. A single class III mutant, D302A, was studied and found to have a low activity. However, it consumed all of its fructose bolus. Further studies showed that the D302A mutant excreted fairly large amount of 3-hydroxybutyrate into the fermentation media and showed linearly increasing molecular weight.

7. MODELING CONSIDERATIONS

7.1. Synthesis Pathway Kinetic Model

Two details of the wild type fermentations stood out from the other data: linear production rate and constant molecular weight. Considering the entire PHB synthesis pathway for rate limiting steps may provide some insight into the PHB production process. Figure 7.1-1 shows the PHB synthesis pathway and considers what would have to be limiting for each step to be the rate determining step.

Fructose Mass Transfer	Rate Laws	Linear If:
$F_M \xrightarrow{k_L} F_S$	$r=k_L[F_M]$	$[F_M]$=constant
Fructose Membrane Transport		
$F_S + E_T \underset{k_{-1}}{\overset{k_1}{\leftrightarrow}} EF_S \xrightarrow{k_{cat}} E + F_C$	$r = \frac{k_{cat}[E_T][F_S]}{K_M + [F_S]}$	$[F_S] >> K_M$
Metabolism		
$F_C \xrightarrow{k_{cat}} S_B$	$r=k_{cat}[F_C][E_x]$	$[F_C],[E_x]$=constant
Monomer Mass Transfer		
$S_B \xrightarrow{k_L} S_S$	$r = k_L[S_B]$	$[S_B]$=constant
Initiation		
$S_S + E \xrightarrow{k_I} E_S$	$r = k_I[S_S][E]$	$[S_S],[E]$=constant
Elongation		
$S_S + ES \xrightarrow{k_{El}} ES_2$		
$S_S + ES_n \xrightarrow{k_{El}} ES_{n+1}$	$r = k_{El}[S_S][ES_n]$	$k_{El} \neq f(n)$; $[S_S],[ES_n]$=constant
or		
$S_S + ES_n \underset{k_{-1}}{\overset{k_1}{\leftrightarrow}} ES_nS_S \xrightarrow{k_{cat}} ES_{n+1}$	$r = \frac{k_{cat}[ES_n][S_S]}{K_M + [S_S]}$	$k_{cat} \neq f(n)$ $[S_S] >> K_M$ $[ES_n]$=constant
Termination		
$ES_n \xrightarrow{k_T} E + S_n$	$r = k_T[ES_n]$	$k_T \neq f(n)$
$ES_n + CT \xrightarrow{k_T} E + S_n$	$r = k_T[ES_n][CT]$	$[ES_n],[CT]$ = constant

F_M=Fructose in media
F_S=Fructose at cell surface
F_C=Fructose in cytoplasm
S_B=3HBCoA in bulk
S_S=3HBCoA at surface of the granule
E=Synthase
E_x=Unknown slow step enzyme
E_T=Fructose transporter enzyme
S_n=PHB with n monomer units
CT=Chain terminating agent

Other important factors:
V_c=Cytoplasm volume
decreases over time
A_g=Granule surface area
increases over time
Enzyme concentrations
increase over time due
to V_c decrease

Figure 7.1-1: Limiting Steps in PHB Synthesis Pathway

7.2. Fructose Mass Transfer

Fructose mass transfer is a possible limiting step that could explain the linear PHB production behavior. The equation governing fructose mass transfer to the cell is shown in equation 7.2-1.

$$F_M \xrightarrow{k_L} F_S \qquad (7.2\text{-}1)$$

F_M=Fructose in media

F_S=Fructose at cell surface

k_L=mass transfer coefficient

The rate law for equation 7.2-1 is shown in 7.2-2. This rate law is linear if the fructose concentration in the media is constant.

$$r=k_L[F_M] \qquad (7.2\text{-}2)$$

r=rate of mass transfer

k_L=mass transfer coefficient

F_M=Fructose in media

However, if fructose is transferred into the cell based on a concentration gradient, then as the fructose concentration in the media decreases the mass transfer rate should decrease; this would result in a non-linear portion of the production rate. It is possible that if the concentration of fructose is suitably high, the mass transfer rate could be saturated during most of the production phase, which would result in the linear PHB production, and the non-linear production rate

would occur over such a small amount of time that it would not be seen in the data. But this is less likely that some of the other candidates for explaining the linear PHB production behavior.

7.3. Fructose Membrane Transport

Another likely slow step if fructose membrane transport. Though little is known about the fructose transporter enzyme, it is probably similar to the glucose transporter enzyme in *E. coli* and may operate according to the Michaelis-Menten mechanism shown in equation 7.3-1.

$$F_S + E_T \underset{k_{-1}}{\overset{k_1}{\leftrightarrow}} EF_S \xrightarrow{k_{cat}} E_T + F_C \qquad (7.3\text{-}1)$$

F_S=Fructose at cell surface

F_C=Fructose in cytoplasm

E_T=Fructose transporter enzyme

EF_S=Fructose transporter enzyme-fructose complex

k_1, k_{-1}, k_{cat}=kinetic rate constants

The rate law that governs equation 7.3-1 is shown in equation 7.3-2.

$$r = \frac{k_{cat}[E_T][F_S]}{K_M + [F_S]} \qquad (7.3\text{-}2)$$

r=rate of fructose transport

F_S=Fructose at cell surface

E_T=Fructose transporter enzyme

k_{cat}=Maximum rate of catalysis

K_M=Michaelis-Menten Constant, $\frac{k_{cat} + k_{-1}}{k_1}$

This rate will result in a linear production rate for most of the production phase if the fructose concentration is very large compared to the Michaelis-Menten constant. This is a very likely situation, and it provides a simple and convenient explanation for the linear production rate.

7.4. Metabolism

Metabolism of fructose to 3-hydroxybutyrate could have a slow reaction step that would result in a linear production rate. Tracking down the actual slow step would likely prove very difficult. However, it would be reasonable to assume that all reactions upstream of the slow step would be at equilibrium. In this case the rate would ultimately depend on the fructose concentration in the cytoplasm; the net reaction is shown in equation 7.4-1.

$$F_C \xrightarrow{k_{cat}} S_B \qquad (7.4\text{-}1)$$

F_C=Fructose in cytoplasm

S_B=3HBCoA in bulk

k_{cat}=Maximum rate of catalysis

The rate law for equation 7.4-1 is shown in equation 7.4-2.

$$r=k_{cat}[F_C][E_x] \qquad (7.4\text{-}2)$$

r=rate of metabolism

F_C=Fructose in cytoplasm

k_{cat}=Maximum rate of catalysis

E_x=Unknown rate limiting enzyme

It is reasonable that the fructose concentration in the cytoplasm is constant if it is assumed that the amount of fructose transported into the cell is regulated. However, this mechanism also requires that the concentration of the unknown rate limiting enzyme remains constant throughout the PHB production phase. This is unlikely given that as PHB accumulates the free volume inside the cell decreases. Though some of the enzyme may become deactivated over time, it is very unlikely that the rate of deactivation exactly balances the rate of increase in enzyme concentration inside the cell due to the loss of volume to the PHB granule.

7.5. Monomer Mass Transfer

Mass transfer is often a limiting culprit for linear behavior. In the case of PHB production, it is possible that mass transfer of the monomer, 3HBCoA, to the surface of the synthase enzyme could be the rate limiting step. This makes more sense if it is assumed that the synthase is immobilized on the granule surface and that the monomer has to diffuse through a thin film around the enzyme/granule. The phenomenon is described by equation 7.5-1.

$$S_B \xrightarrow{k_L} S_S \qquad (7.5\text{-}1)$$

S_B=3HBCoA in bulk

S_S=3HBCoA at surface of the granule

k_L=mass transfer coefficient

This mechanism is governed by the rate law shown in equation 7.5-2.

$$r = k_L [S_B] \qquad (7.5\text{-}2)$$

r=rate of mass transfer

S_B=3HBCoA in bulk

k_L=mass transfer coefficient

In order give an overall linear PHB production rate, the concentration of 3HBCoA in the cytoplasm must be constant. This is reasonable if the thiolase and reductase enzymes operate at equilibrium; i.e. if the 3HBCoA concentration rises, the enzymes catalyze the reaction in the reverse direction to hold the concentration constant, which could happen as the free volume in the cell is reduced due to PHB granule growth.

7.6. Initiation

Another possibility for the rate determining step is initiation of the polymer chain. The exact initiation mechanism is unknown. However, conceptually, initiation would occur when a monomer molecule and an enzyme combine, which is described in equation 7.6-1.

$$S_S + E \xrightarrow{k_I} ES \qquad (7.6\text{-}1)$$

S_S=3HBCoA at surface of the granule

E=Synthase enzyme

ES=Synthase with one 3HB unit primed for further elongation

k_I=initiation rate constant

The simple initiation mechanism shown in equation 9.6-1 is governed by the rate law shown in equation 7.6-1.

$$r = k_I [S_S] [E] \qquad (7.6\text{-}2)$$

r=rate of initiation

S_S=3HBCoA at surface of the granule

E=Synthase enzyme

k_I=initiation rate constant

If initiation is the rate determining step, then to have linear PHB production behavior the concentration of active synthase enzyme as well as the concentration of substrate at the surface of the synthase enzyme must be constant. This is not really reasonable because it is known that the free volume inside the cell decreases over time due to granule growth. This makes initiation a less likely candidate for the rate determining step. However, if a more complicated initiation mechanism were used, it is possible that the synthase enzyme concentration might not play such a prominent role and preclude the step from being the rate determining step.

7.7. Elongation

Elongation is another step which is likely as the rate determining step. As with the initiation step, the exact mechanism for elongation is not known. Two different simple mechanisms, addition elongation and Michaelis-Menten elongation, are shown in sections 7.7.1 and 7.7.2, respectively.

7.7.1. Addition Elongation

In the addition elongation mechanism, substrate at the surface of the enzyme is added directly to the growing polymer chain, as shown in equation 7.7-1.

$$S_S + ES_n \xrightarrow{k_{El}} ES_{n+1} \qquad (7.7\text{-}1)$$

S_S=3HBCoA at surface of the granule

ES_n=Synthase enzyme with growing polymer chain of n units

ES_{n+1}=Synthase enzyme with growing polymer chain of n+1 units

k_{El}=elongation rate constant

This mechanism is governed by the rate law shown in equation 7.7-2.

$$r = k_{El}\,[S_S]\,[ES_n] \qquad (7.7\text{-}2)$$

r=elongation rate

S_S=3HBCoA at surface of the granule

ES_n=Synthase enzyme with growing polymer chain of n units

k_{El}=elongation rate constant

In order for this mechanism to produce linear PHB production behavior, the concentration of synthase enzymes with growing polymer chains and the concentration of 3HBCoA at the surface of the enzyme must be constant. The implications for the constant substrate concentration are discussed in section 7.5. The concentration of enzyme with growing chains would probably not be constant due to the reduction of free volume in the cell. However, in this case the important value is not the volume concentration of enzyme; it is the area concentration of enzyme. Therefore, for this mechanism it is assumed that each enzyme remains on the surface of the PHB granule and essentially acts as a catalytic site, as seen in heterogeneous catalysis. Thus, it is possible to get a linear production rate from this mechanism, even though the free volume in the cell is decreasing over time. Another important assumption is that the elongation rate constant is not affected by the length of the growing chain. If the polymerization rate decreases as the polymer chain increases in length, a non-linear production rate would be expected.

7.7.2. Michaelis-Menten Elongation

Another likely mechanism for the elongation step of PHB synthesis is a Michaelis-Menten mechanism. The Michaelis-Menten mechanism is a common method for many enzymes and is shown in equation 7.7-3.

$$S_S + ES_n \underset{k_{-1}}{\overset{k_1}{\leftrightarrow}} ES_nS_S \xrightarrow{k_{cat}} ES_{n+1} \qquad (7.7\text{-}3)$$

S_S=3HBCoA at surface of the granule

ES_n=Synthase enzyme with growing polymer chain of n units

ES_nS_S=Synthase enzyme complex with growing chain and an additional monomer unit

ES_{n+1}=Synthase enzyme with growing polymer chain of n+1 units

k_1, k_{-1}, k_{cat}=kinetic rate constants

The rate law that governs the Michaelis-Menten mechanism is shown in equation 7.7-4.

$$r = \frac{k_{cat}[ES_n][S_S]}{K_M + [S_S]} \tag{7.7-4}$$

r=elongation rate

S_S=3HBCoA at surface of the granule

ES_n=Synthase enzyme with growing polymer chain of n units

K_M, k_{cat}=kinetic rate constants

In order for this mechanism to produce a linear production rate, the concentration of substrate at the surface of the enzyme needs to be very large in comparison to the Michaelis-Menten constant, K_M. A linear production rate could also occur if the substrate concentration at the surface of the enzyme was constant and very small compared to the Michaelis-Menten constant. However, due to the rapid production rate, this seems like a much less likely scenario. If the substrate concentration is high, a linear production rate would occur if each of the enzymes was saturated. In this case, it must be assumed that all of the synthase enzymes remain active for the entire production phase and that they are all operating at the maximum rate. As with the addition

elongation mechanism, it must also be assumed that the catalytic rate constant does not change due to the length of the growing polymer chain.

7.8. Chain Termination

As with many of the other mechanisms in the PHB synthesis pathway, the chain termination mechanism is not known. However, it is clear that chain termination would have a significant effect on molecular weight. Therefore, in order for chain termination to be the rate determining step that produces a linear PHB production rate, the mechanism must also account for the constant molecular weight seen in the fermentation data. Two simple chain termination mechanisms, spontaneous chain termination and assisted chain termination, are shown in sections 7.8.1 and 7.8.1, respectively.

7.8.1. Spontaneous Chain Termination

Spontaneous chain termination would likely be based on molecular weight. Thus, when a growing polymer chain reaches a certain molecular weight, it would spontaneously terminate the elongation process and then remain that the fixed cutoff molecular weight. The cutoff molecular weight would probably not be a fixed value, but would occur over a range of molecular weights. However, due to the low polydispersity seen in PHB fermentations, it appears that this range would be quite tight. The cause behind the spontaneous termination would likely be that at some chain length the polymer can no longer be tightly held by the synthase active site, leading to termination and reinitiation. A simple mechanism for spontaneous chain termination is shown in equation 7.8-1.

$$ES_n \xrightarrow{k_T} E + S_n \qquad (7.8\text{-}1)$$

ES_n=Synthase enzyme with growing polymer chain of n units

E=Synthase enzyme

S_n=PHB with n monomer units

k_T=Chain termination rate constant

This mechanism is governed by the rate law shown in equation 7.8-2.

$$r = k_T [ES_n] \qquad (7.8\text{-}2)$$

r=chain termination rate

ES_n=Synthase enzyme with growing polymer chain of n units

k_T=Chain termination rate constant

This mechanism only accounts for the linear PHB production rate and the essentially constant PHB molecular weight if the chain termination rate constant is dependent on the degree of polymerization. If the rate constant does not tightly control the molecular weight, then a larger range of molecular weights would be expected.

7.8.2. Assisted Chain Termination

In the assisted chain termination mechanism, PHB chain termination would occur through the action of some chain terminating agent, as shown in equation 7.8-3.

$$ES_n + CT \xrightarrow{k_T} E + S_n \qquad (7.8\text{-}3)$$

ES_n=Synthase enzyme with growing polymer chain of n units

CT=chain terminating agent

E=Synthase enzyme

S_n=PHB with n monomer units

k_T=Chain termination rate constant

This mechanism is governed by the rate law shown in equation 7.8-4.

$$r = k_T [ES_n] [CT] \qquad (7.8\text{-}4)$$

r=chain termination rate

ES_n=Synthase enzyme with growing polymer chain of n units

CT=chain terminating agent

k_T=Chain termination rate constant

In order for this mechanism to account for the linear PHB production rate and the constant molecular weight, the concentration of the chain terminating agent would have to remain constant throughout the PHB production phase. However, due to the decreasing free volume in the cell, it is unlikely that a soluble chain terminating agent would have a constant concentration. Additionally, as with the spontaneous chain termination mechanism, the chain termination rate constant would have to be dependent on the degree of polymerization of the PHB chain.

However, both mechanisms still remain as good possibilities for the actual chain termination mechanism; they just do not appear to be the rate determining step in PHB polymerization.

7.9. Modeling Conclusions

Monomer mass transfer or fructose membrane transport look like the best candidates for being the slow step for the following reasons. These steps do not depend on constant enzyme concentrations inside the cell or having a kinetic constant that is independent from molecular weight. Initiation as the slow step, without some complicated priming step that has not yet been identified, does not really make sense because basically the same thing (monomer going to the enzyme and adding) happens many many times during elongation. Elongation is a good second choice, but it basically requires a constant active enzyme concentration which seems less likely because some of the enzyme is probably lost within the PHB granule. It would also require the elongation rate constant (k_{El}) to not be dependent on the degree of polymerization (n). Additionally, chain termination does not appear to be the rate determining step because of the molecular weight implications.

8. CONTRIBUTIONS AND CONCLUSIONS

Experimental methods and data generated from the presented research provide insight into PHB production in *R. eutropha*. Additionally, some new phenomena were seen when dealing with synthase mutants, and the implications of the data were considered within the full framework of the PHB synthesis pathway. The contributions are listed in detail below.

1. A method for separating the growth and PHB production phases in wild type *R. eutropha* was developed.
2. Kinetic data points for wild type *R. eutropha* PHB molecular weight were taken and shown to be fairly constant over the entire production phase.
3. Temperature and pH were shown to have a small effect on PHB production and to cause a slight reduction in PHB molecular weight.
4. Multiple class I synthase mutants were shown to in increase the PHB molecular weight.
5. Molecular weight was measured for the class III synthase inserted into *R. eutropha*.
6. The D302A mutant of the class III synthase was examined in *R. eutropha* and found to produce linearly increasing molecular weight and to produce monomer in the fermentation media.
7. Mass transfer and elongation steps in the PHB synthesis pathway were identified potential rate determining steps based on the implications of the production and molecular weight data.

9. RECOMMENDATIONS FOR FUTURE WORK

A number of future experiments would significantly improve the knowledge surrounding molecular weight formation in PHB production. The following list indicates some of the first steps to determining how to control PHB molecular weight.

1. Develop a fed batch procedure for D302A fermentations in order to achieve large 3-hydroxybutyrate concentrations
2. Determine the final limit of PHB molecular weight produced from the D302A enzyme
3. Pursue further experiments with D480A, the class I analog of D302A
4. Develop a procedure to obtain very early production phase time point data from wild type fermentations
5. Compare PHB production kinetics with the PHB production kinetics in the presence of a chain terminating agent

10. ACKNOWLEDGEMENTS

I would like to thank the following people, without whom this research could not have been completed.

Julie Waters

Charles Cooney

Anthony Sinskey

Bill Perry

Adam Lawrence

Gregory Stephanopoulos

Paul Barton

Other members of the Sinskey, Cooney, and Stephanopoulos Laboratories

11. WORKS CITED

E. Bormann. Stoichiometrically calculated yields of the growth-associated production of polyhydroxybutyrate in bacteria. Biotechnology Letters 22(18) 1437-42 Sep 2000

J. Choi, Lee, SY. Process analysis and economic evaluation for poly(3-hydroxybutyrate) production by fermentation. Bioprocess Engineering 17(6) 335-42 Nov 1997

W. Cleland. The kinetics of enzyme-catalyzed reactions with two or more substrates or products I. Nomenclature and rate equations. Biochimica et biophysica acta. International journal of biochemistry and biophysics 67(104-37

J. Davis, Moore, RN, Imperaili, B, Pratt, AJ, Kobayashi, K, Masamune, S, Sinskey, AJ, Walsh, CT, Fukui, T, Tomita, K. Biosynthetic thiolase from zoogloea-ramigera 1. Preliminary characterization and analysis of proton-transfer reaction. Journal of Biological Chemistry 262(1) 82-9 Jan 5 1987

Y. Doi. Microbial polyesters. New York: VCH Publishers, 1990

Goodfellow. Polypropylene (PP) - Material Information. http://www.goodfellow.com/csp/active/STATIC/E/Polypropylene.HTML 2005

L. Jurasek, Marchessault, RH. Polyhydroxyalkanoate (PHA) granule formation in Ralstonia eutropha cells: a computer simulation. Applied Microbiology and Biotechnology 64(5) 611-7 Jun 2004

Y. Kawaguchi, Doi, Y. Kinetics and Mechanism of Synthesis and Degradation of Poly(3-hydroxybutyrate) in Alcaligenes-eutrophus. Macromolecules 25(9) 2324-9 Apr 1992

S. Kusaka, Iwata, T, Doi, Y. Microbial synthesis and physical properties of ultra-high-molecular-weight poly[(R)-3-hydroxybutyrate]. Journal of Macromolecular Science-Pure and Applied Chemistry A35(2) 319-35 1998

K. Laidler, Bunting, PS. The chemical kinetics of enzyme action. Oxford: Clarendon, 1973

A. Lawrence, Choi, JH, Rha, CK, Stubbe, JA, Sinskey, AJ. In vitro analysis of the chain termination reaction in the synthesis of poly-(R)-beta-hydroxybutyrate by the class III synthase from Allochromatium vinosum. Biomacromolecules 6(4) 2113-9 Jul-Aug 2005

A. Lawrence, Schoenheit, J, He, A, Tian, J, Liu, P, Stubbe, J, Sinskey, AJ. Transcriptional analysis of Ralstonia eutropha genes related to poly-(R)-3-hydroxybutyrate homeostasis during batch fermentation. http://www.springerlink.com/media/ACECBDAQVK5YWHBUGT33/Contributions/N/5/4/G/N54G126261445600_html/fulltext.html

T. Leaf, Srienc, F. Metabolic modeling of polyhydroxybutyrate biosynthesis. Biotechnology and Bioengineering 57(5) 557-70 Mar 5 1998

N. Mantzaris, Kelley, AS, Daoutidis, P, Srienc, F. A population balance model describing the dynamics of molecular weight distributions and the structure of PHA copolymer chains. Chemical Engineering Science 57(21) 4643-63 Nov 2002

T. Maskow, Babel, W. Calorimetrically recognized maximum yield of poly-3-hydroxybutyrate (PHB) continuously synthesized from toxic substrates. Journal of Biotechnology 77(2-3) 247-53 Feb 17 2000

O. Peoples, Sinskey, AJ. Poly-beta-hydroxybutyrate(PHB) biosynthesis in alcaligenes-eutrophus H16 - identification and characterization of the PHB polymerase gene (PHBC). Journal of Biological Chemistry 264(26) 15298-303 Sep 15 1989

B. Rehm, Steinbuchel, A. Biochemical and genetic analysis of PHA synthases and other proteins required for PHA synthesis. International Journal of Biological Macromolecules 25(1-3) 3-19 Jun-Jul 1999

Y. Saito, Nakamura, S, Hiramitsu, M, Doi, Y. Microbial synthesis and properties of poly(3-hydroxybutyrate-co-4-hydroxybutyrate). Polymer International 39(3) 169-74 Mar 1996

J. Stubbe, Tian, J, He, A, Sinskey, AJ, Lawrence, AG, Liu, P. Nontemplate-dependent Polymerization Processes: Polyhydroxyalkanoate Synthases as a Paradigm (1). Annu Rev Biochem 74(433-80 Jul 7 2005

K. Sudesh, Abe, H, Doi, Y. Synthesis, structure and properties of polyhydroxyalkanoates: biological polyesters. Progress in Polymer Science 25(10) 1503-55 Dec 2000

A. Sugiyama, Kobayashi, T, Shiraki, M, Saito, T. Roles of poly (3-hydroxybutyrate) depolymerase and 3HB-oligomer hydrolase in bacterial PHB metabolism. Current Microbiology 48(6) 424-7 Jun 2004

J. Tian, He, AM, Lawrence, AG, Liu, PH, Watson, N, Sinskey, AJ, Stubbe, J. Analysis of transient polyhydroxybutyrate production in Wautersia eutropha H16 by quantitative western analysis and transmission electron microscopy. Journal of Bacteriology 187(11) 3825-32 Jun 2005

R. van Wegen, Lee, SY, Middelberg, APJ. Metabolic and kinetic analysis of poly(3-hydroxybutyrate) production by recombinant Escherichia coli. Biotechnology and Bioengineering 74(1) 70-80 Jul 5 2001

R. van Wegen, Ling, Y, Middelberg, APJ. Industrial production of polyhydroxyalkanoates using Escherichia coli: An economic analysis. Chemical Engineering Research & Design 76(A3) 417-26 Mar 1998

S. Villas-Boas, Moxley, JF, Akesson, M, Stephanopoulos, G, Nielsen, J. High-throughput metabolic state analysis: the missing link in integrated functional genomics of yeasts. Biochemical Journal 388(669-77 Part 2 Jun 1 2005

L. Wallen, Rohwedder, WK. Poly-b-hydroxyalkanoate from activated sludge. Environmental Science Technology 8(576-9 1974

H. Wong, Lee, SY. Poly-(3-hydroxybutyrate) production from whey by high-density cultivation of recombinant Escherichia coli. Applied Microbiology and Biotechnology 50(1) 30-3 Jul 1998

G. York, Junker, BH, Stubbe, J, Sinskey, AJ. Accumulation of the PhaP phasin of Ralstonia eutropha is dependent on production of polyhydroxybutyrate in cells. Journal of Bacteriology 183(14) 4217-26 Jul 2001

G. York, Lupberger, J, Tian, JM, Lawrence, AG, Stubbe, J, Sinskey, AJ. Ralstonia eutropha H16 encodes two and possibly three intracellular poly[D-(-)-3-hydroxybutyrate] depolymerase genes. Journal of Bacteriology 185(13) 3788-94 Jul 2003

G. York, Stubbe, J, Sinskey, AJ. The Ralstonia eutropha PhaR protein couples synthesis of the PhaP phasin to the presence of polyhydroxybutyrate in cells and promotes polyhydroxybutyrate production. Journal of Bacteriology 184(1) 59-66 Jan 2002

12. APPENDIX A: DYNAMICS OF LOCAL START-UP INNOVATION

Introduction

Innovation is challenging. Continuous, sustained innovation, without an incredible supporting culture, seems overwhelmingly daunting for many large organizations and locales. However, the benefits of capitalizing upon innovation appear even greater[1]. Given this situation, many organizations have questioned what it takes to create this culture of sustained innovation. While some details seem obvious, the connections between the various moving parts create a complexity that makes the complete system very intractable for simple generalizations.

However, the benefits of understanding the nature of innovation and the ecosystem required to support it compel further study. The following model seeks to address the requirements for major pieces of the supporting innovation ecosystem and construct informative scenarios around how such a system could behave over time. This model particularly focuses on the plight of small countries and regions and how mobile components, such as technically trained workers and available funding, can influence the overall innovative performance. Additionally, the model offers recommendations on how policy decisions can facilitate the development of the holistic innovation culture.

This study was motivated by the MIT Portugal Program (MPP). The MPP is a long-term collaboration between MIT and institutions of higher learning in Portugal that focuses on

basic research and is supported by the Portuguese government through the Ministry of Science, Technology, and Higher Education[2]. One of the objectives of the Bio-Engineering Systems sub-program of the MPP is to train future leaders in bio-engineering technical innovation[3]. In pursuit of this goal, one of MIT's signature programs, Innovation Teams, is being transported to Portuguese universities. Innovation Teams focuses on assessment of the commercialization potential of university research[4]. When conducted in Cambridge, Innovation Teams benefits significantly from the local start-up environment. In order to consider conducting Innovation Teams in Portugal, these advantageous relationships must be recreated in some form. This study attempts to identify the critical pieces of a generic start-up ecosystem so that the connections between the Portuguese version of Innovation Teams and the local start-up environment can be made.

This study utilizes the tools of System Dynamics[5]. System Dynamics is a methodology for developing and analyzing computer simulation models of complex problems, which was developed by Jay Forrester at MIT in the 1950s[6]. System Dynamics has its roots in engineering feedback control systems analysis[7]. System Dynamics models generally have a high-level, strategic perspective on problems and attempt to utilize rich, realistic theories of how elements of a complex system interact. The models also have the capability to account for behavioral factors and integrate a wide range of relevant information.

The major components of a Systems Dynamics model are stocks, flows, feedback loops, and delays, which are typically combined in a complex network. Stocks represent quantities that accumulate within the system over time. Flows describe the movement of the quantities within the stocks. Feedback loops allow other quantities in the system to affect the flows in a positive or negative way. Delays control how quickly feedback loops can respond to changes in the system.

Background

Innovation has proven difficult for large, established firms[8]. Even firms that begin as innovative firms generally face difficulty in retaining the innovative spirit over a long period[9]. In the context of technologically novel products, many established firms do not survive when a disruptive technology hits the market[10].

Over time, companies that begin in innovative markets must shift their sources of competitive advantage as the market changes[11]. For example, in the early phase of technology development, companies depend on R&D capabilities[12]. Once a standard design captures the market, companies must develop process innovation skills and focus on reducing costs and achieving economies of scale[13]. Typically, chronic overcapacity in a market drives the product to become a commodity[14]. At this point, existing firms must shift to a market driven perspective and be prepared to innovate again as disruptive technologies emerge[15]. Each of these shifts typically prove very challenging and can

result in a new market leader at each stage and cause the failure of existing market leaders.

However, it has been noted that a number of strategies can allow a company to thrive in the tumultuous, innovative marketplace[16]. In particular, the reliance on market pull can prove less risky and attempting to push a new technology[17]. Fighting active inertia can also help companies retain innovative skills[18]. Companies also have some control over how a novel market environment forms and can significantly influence their own survival[19]. Finally, a firm's local environment can be a source of competitive advantage[20]. This model attempts to identify what factors in a generic local environment can be fostered in order to develop a competitive advantage for innovative companies.

Model Description

At a very high level, this model considers the productive application of technical capability in order to develop novel products, which in turn lead to new ventures and companies. This objective modularizes the model nicely between the formation of technical capability and new venture creation. The model depends on a variety of feedback loops and delays, some of which cross between the two modules.

In this context, technical capability represents all of the resources of a region that can be applied toward new product development. The interrelationship between these resources is quite complex and has been simplified for the purposes of the model. Thus, technical

capability has been defined as technically trained people employed productively to develop novel technologies, which have to potential to become marketable products. However, in order to be productive, technically trained people require a variety of resources. The most important of these have been identified as technical experience, management effectiveness, and technical infrastructure, as shown in Figure A1.

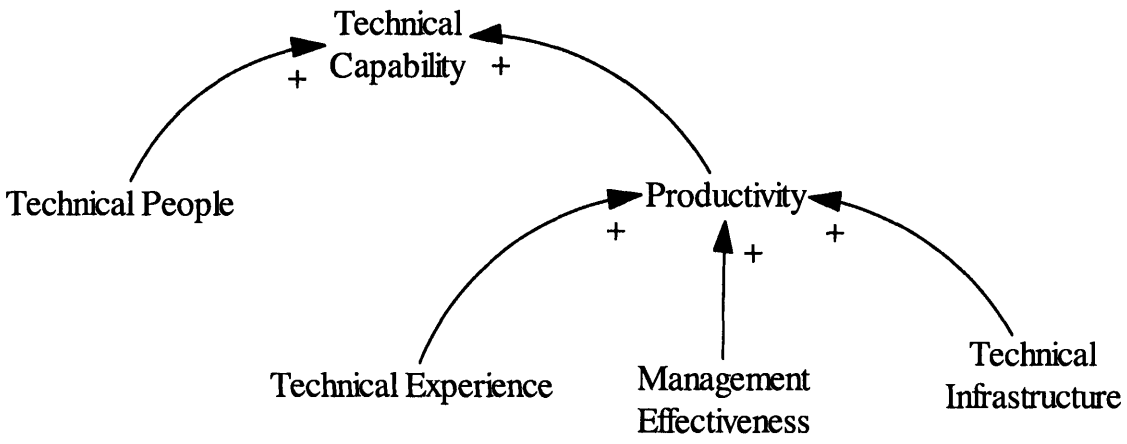

Figure A1: Components of Technical Capability

Technical experience is defined in the model as years that a technically trained person has spent applying their skills in a technical field. New graduates are treated as having zero years of experience, and all technical people are credited an additional year of experience for each year that passes. At a higher level, professional development could improve this situation, where new graduates would start with technical experience and technical people would receive more than one year of effective experience for each year worked. However, for the results presented in this article, this effect was not activated.

Management effectiveness represents the requirement for proficient supervising managers in a technical venture. Without effective management, technically trained people face large challenges in identifying market opportunities for novel technologies. Additionally, effective management helps focus research along productive lines. Therefore, management effectiveness has been treated as a critical factor in the productive application of technical capability.

Technical infrastructure is another critical aspect for the productive application of technical capability. Without any supporting infrastructure, technical people will not be productive. Experience and creative management can achieve superior results from inferior infrastructure, but the absence of any technical infrastructure will halt all progress. By the same argument, a lack of experience and poor management can impair the productivity of superb technical infrastructure. Thus, all three components are considered in the productivity calculations.

However, it is important to note that technical capability only represents the potential of a region to create novel products. The market also plays a role in determining whether technical capability is productively employed. Thus, the amount of technical capability actually demanded by the market represents the utilization rate. A simple representation is shown in Figure A2; in the complete model, market demand and direct demand for technical people are used as shown in the next section.

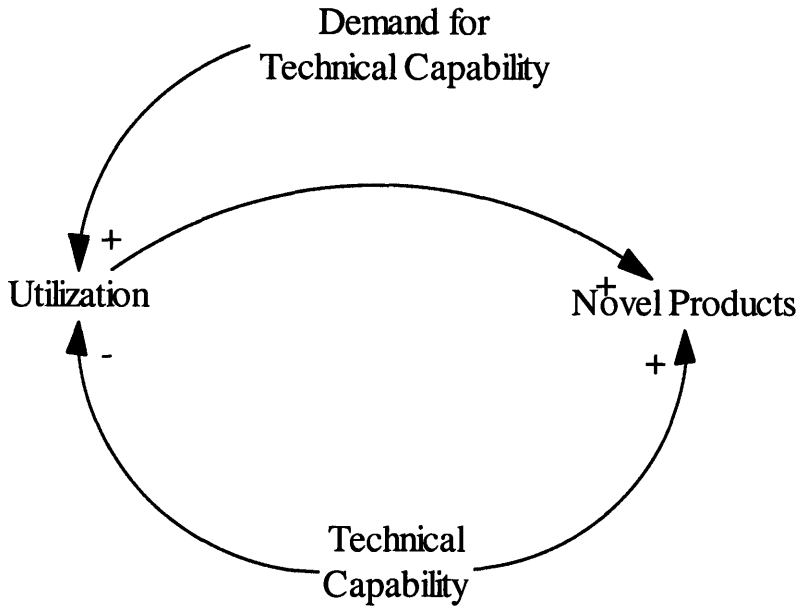

Figure A2: Utilization of Technical Capability

Technical people, for the purposes of the model, are assumed to be advanced degree holders in science and engineering. In a closed country, the only way to gain new technical people would only be to educate new graduates, and the only way to lose technical people would be through retirement or transfers to non-technical positions. However, the scenarios in this model consider a small country with open borders. In this case, immigration and emigration play a very important role. When new technical capability is required, and the prospective payoff is high, it can essentially be imported through the immigration of foreign technical talent from abroad, as shown in Figure A3.

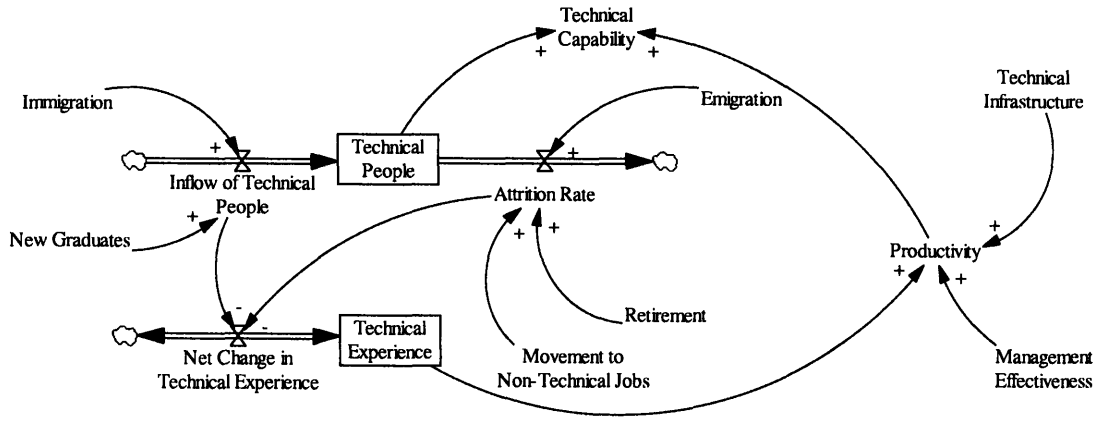

Figure A3: Detailed Components of Technical Capability

The feedback loops that drive immigration, emigration, and the attraction of new technical students beyond the base level depend on utilization. As the market demands more technical capability, utilization rises and more immigrants and new students are attracted to the region. However, there is a significant delay, especially for the new students who must pass through the education system, before these groups can join the local pool of technical people. Emigration feedback works in a similar way, where low utilization drives skilled technical people to seek employment elsewhere. These dynamics are detailed in Figure A4.

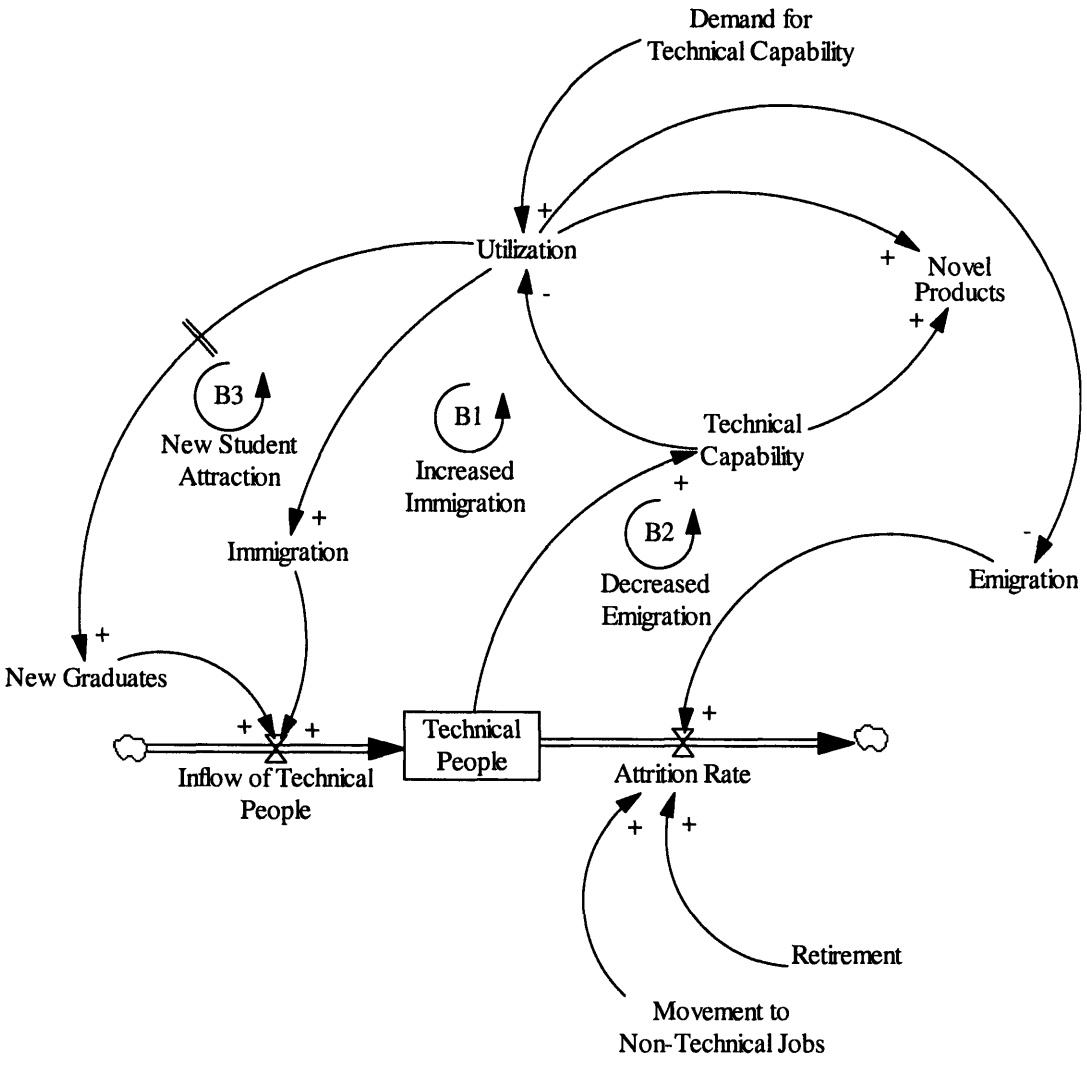

Figure A4: Feedback Loops for Technical People

The technical capability model links to the new venture ecosystem through a positive feedback loop. The positive feedback loop represents the new demand that is generated from the start-up community as the new venture ecosystem develops. Figure A5 shows a simplified version of this feedback loop as well as the effect of learning by the region about how to develop new products. This learning is represented as a gain in productivity.

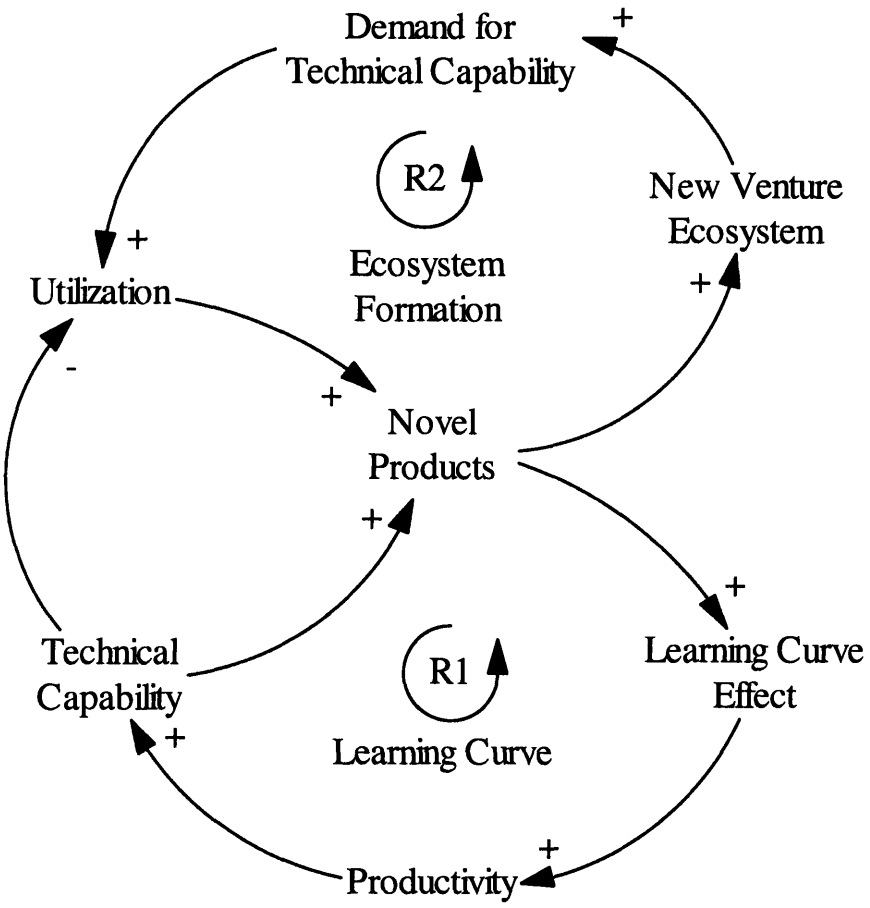

Figure A5: Connection from Technical Capability to the New Venture Ecosystem

The new venture ecosystem, which is modified from the contextual model described by Weil, focuses on new ventures and new companies[14]. In the model technical capability is applied to market signals to produce novel products. However, many novel products never make it to the market because the entrepreneurs do not believe they have strong potential. When the technologies do appear promising, the entrepreneurs proceed with a new venture. The new venture stage represents the time period where the founders of a company choose to develop a business plan and begin to seek funding. Many new

ventures never develop into actual companies that receive funding and begin hiring employees. Additionally, it is important to note that there is a significant delay before new ventures become new companies.

Some of the most basic feedback loops of the new venture ecosystem are around role models and spin-offs. The impact of role models is one of the most important in new company creation. Role models inspire potential entrepreneurs to initiate their own new ventures. The widespread existence of role models has a profound effect on the development of the ecosystem and draws many new ventures. Additionally, as new companies are created, they develop technology that diverges from their core competencies. These technologies are often spun off as new ventures. The role model and spin-off feedback loops are shown in Figure A6.

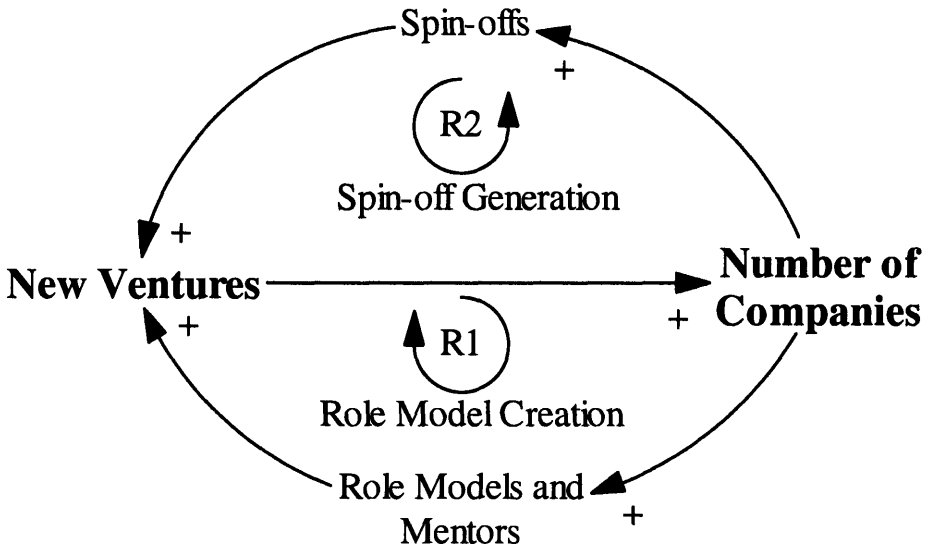

Figure A6: Role Model and Spin-off Feedback Loops

Additionally, as more new companies form, network effects begin to benefit the start-up ecology. One of the first places network effects show up is in cluster creation. As more new companies form, additional start-up jobs are created. These additional jobs provide places employees of failing start-ups to find alternative positions. Universities, which provide positions for start-up entrepreneurs, also enhance the cluster effect. Thus, the cluster effect reduces the consequences of failure, which lead more entrepreneurs to start new ventures. The cluster formation loop is shown in Figure A7.

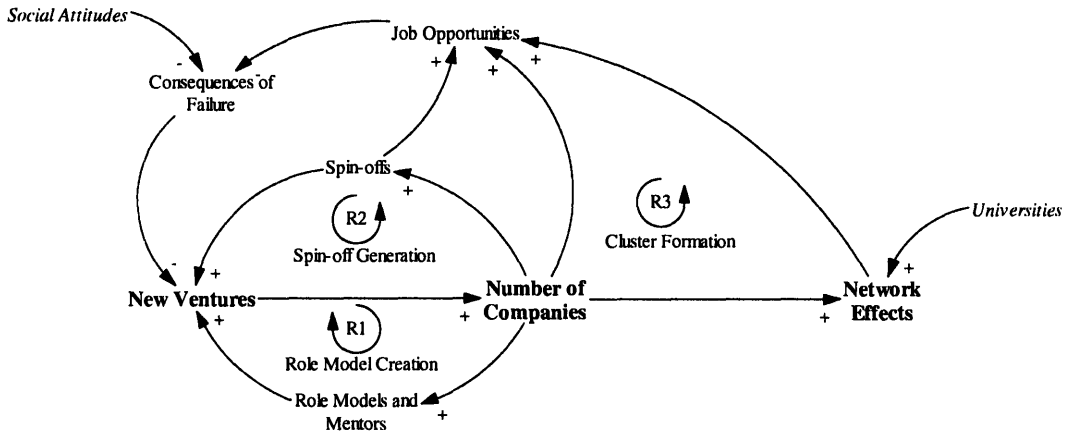

Figure A7: Cluster Formation Feedback Loops

Additional network effects attract better entrepreneurs and funding. As the start-up ecosystem forms, the local region is viewed as a more attractive place for funding new ventures. This phenomenon attracts funding from more diverse sources and allows more new ventures to form. Furthermore, as better entrepreneurs are attracted, more new

ventures succeed in converting into new companies. These network effects are shown in Figure A8.

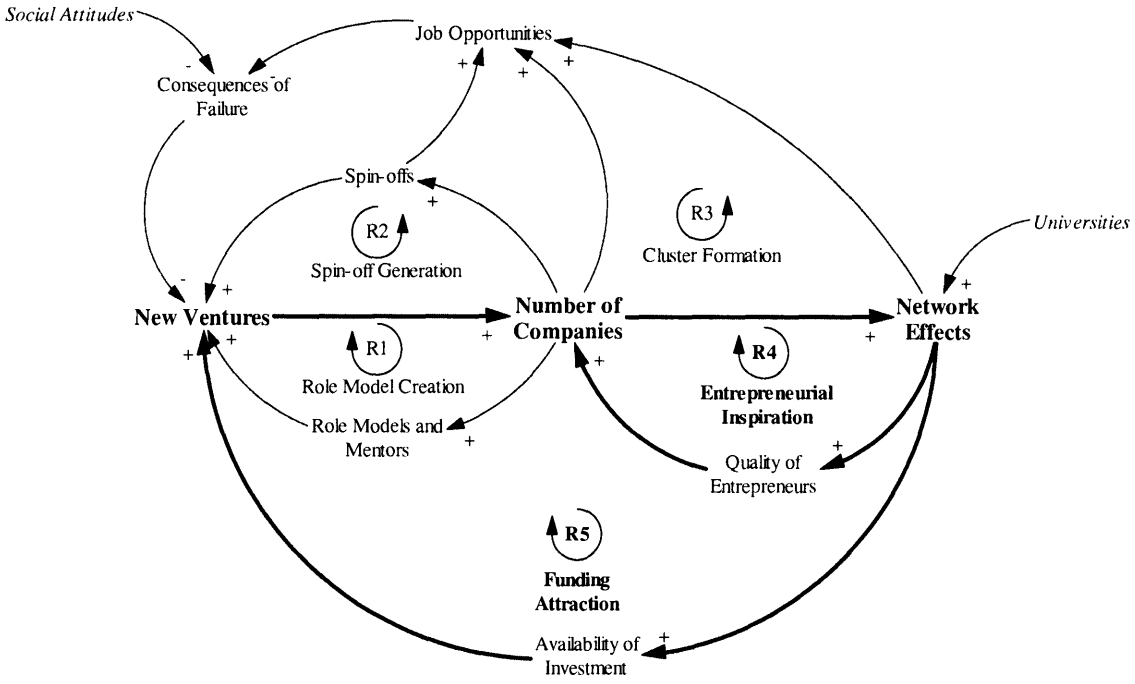

Figure A8: Entrepreneurial and Funding Attraction Network Effects

Furthermore, as more companies are formed, market opportunities serving the new companies are created. These opportunities can strongly influence potential entrepreneurs to start new ventures. The government can also serve as an important role in market opportunity creation by acting as a lead user and serving as a guaranteed market for successful technologies. The feedback loop created by this network effect is shown in Figure A9.

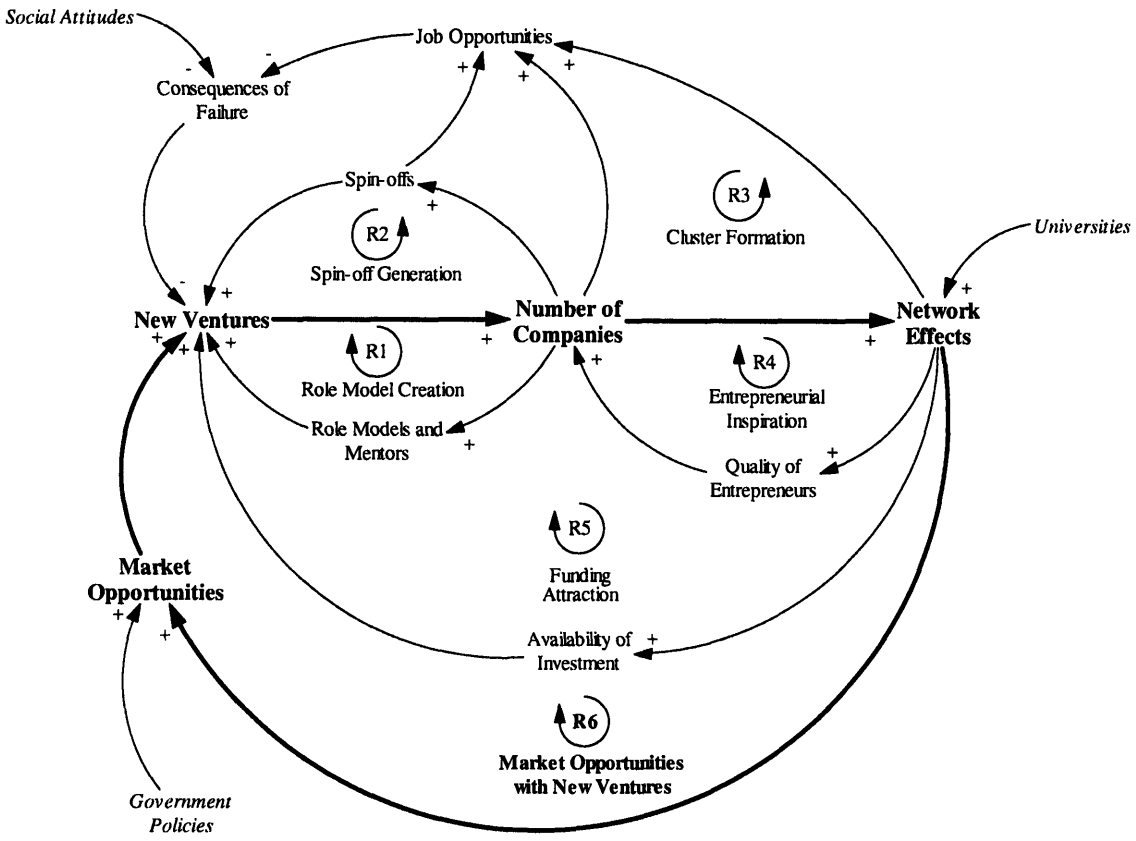

Figure A9: Market Opportunities Network Effect

To this point, all of the feedback loops discussed in the new venture ecosystem have been reinforcing loops. Some balancing loops exist in the new venture ecosystem, and these can short-circuit its formation. One of the most damaging loops to the ecosystem is the failure loop. Too many failures can discourage further new venture creation. Though role models can help reduce the failure rate by mentoring young companies, if the failure loop is too strong, it can prevent any new ventures from forming. Additionally, as more new companies form, the amount of funding must be spread among more companies, and if the funding attracted by network effects does not keep pace, a funding shortage will occur. These loops are shown in Figure A10.

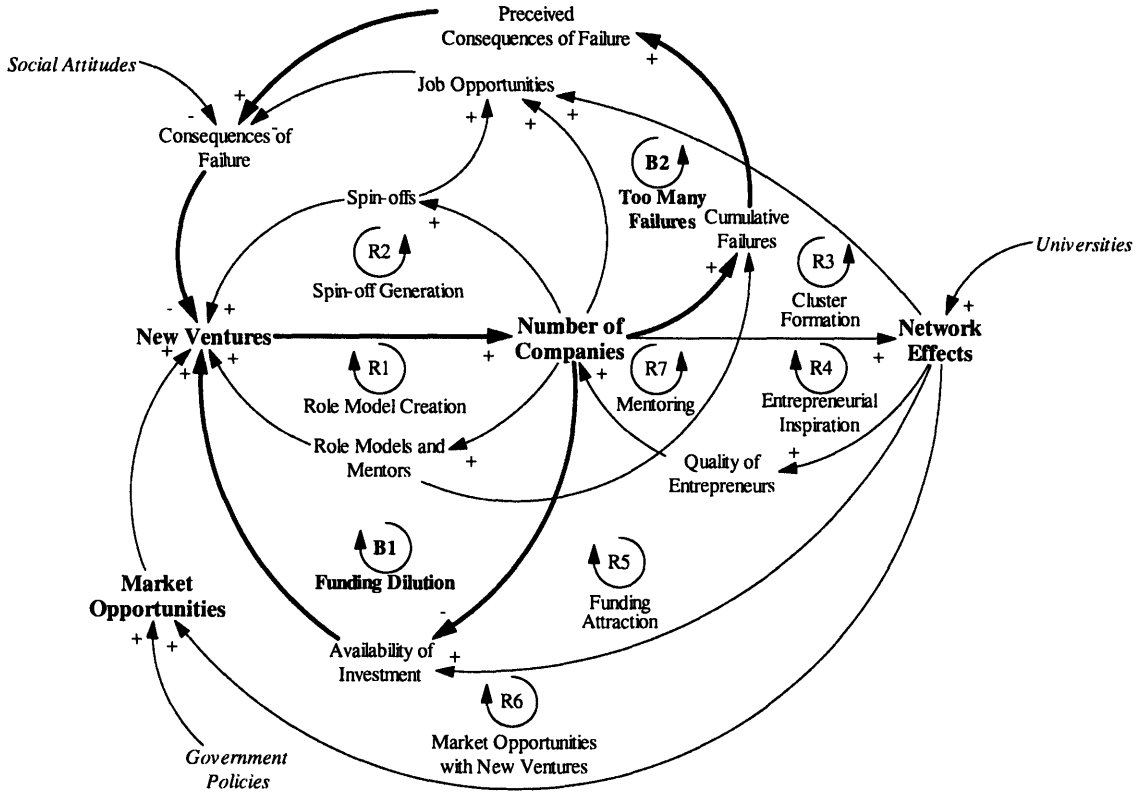

Figure A10: New Venture Ecosystem Balancing Loops

While the model has been simplified for descriptive purposes, a complete model with all the associated parameters is shown in Figure A11.

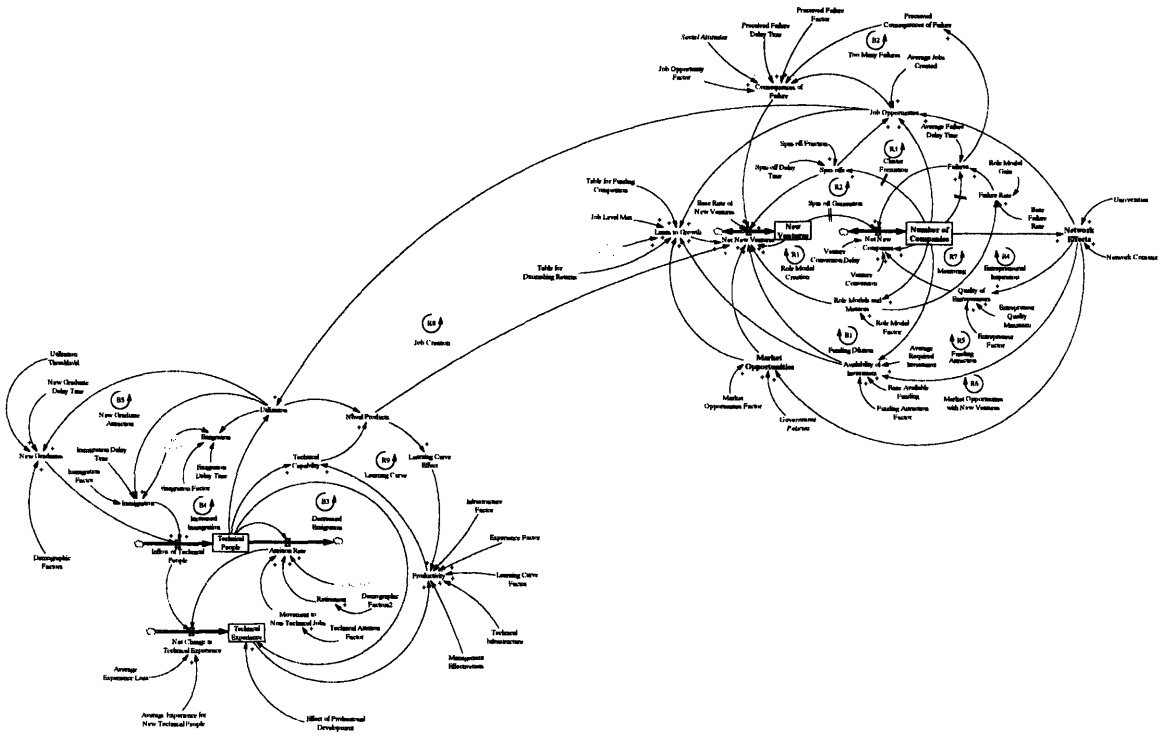

Figure A11: Complete Model

Policies

External factors can drastically alter the behavior of the model. Changes in certain aspects of the external environment can make different feedback loops become dominant, which may completely reverse the dynamics of the system. Some of these factors, such as the economic growth of the region, cannot be manipulated directly. However, other external factors may be significantly shifted by changes in policy. Crafting an integrated, coherent policy program can have a profound impact on the success of a start-up ecosystem. The most applicable policy factors are: education spending, immigration, business regulatory, and intellectual property.

Education spending policies play an important role in commercialization. Education spending can focus on technical education, management education, or technical infrastructure. Each of these factors play an important role in commercialization, thus neglecting one over the others will cripple the system. While the value of technical education is obvious, the value of management education and current infrastructure cannot be overstated. In addition to traditional programs, management education can: introduce role models, improve professional development of technically trained people, and focus technically trained people on market based endeavors. Up-to-date technical infrastructure is also critical. Many types of ventures cannot be started without access to technical infrastructure. Additionally, technical infrastructure serves as a multiplier of technical experience and can improve productivity without increasing the number of technical people. Universities also serve an important role by introducing potential entrepreneurs to the state of the art technical methods that may form the foundation of the new ventures.

Policies surrounding the business environment can also facilitate new venture creation. For example, attracting technical immigrants and retaining technical nationals is a key factor in creating market-driven technical capability. Therefore, facilitating the movement of technical people will enhance new venture development. Under this policy enhancement, technically trained immigrants will be able to relocate easily as the start-up ecosystem becomes attractive. They will also feel more secure because they will be able to leave easily if the company they work for begins to fail. This situation also protects technically trained nationals because when jobs become scarce, it is likely that the

immigrants will be the first to leave and the system will self-regulate to a high utilization level.

Another important policy is business regulations. Difficulties encountered in starting and failing new companies can discourage the commercialization of promising technologies. Creating a business-friendly environment is critical to attracting new ventures. If starting a company is too difficult, entrepreneurs will take prospective technologies to competing ecosystems. Additionally, if failing a company is too difficult, the resident laggards in the start-up ecosystem will make it appear less-desirable to potential entrepreneurs and funding sources. Therefore, creating a business environment that is supportive of start-up ventures is very important. Another business regulation issue is anti-competitive policies. Anti-competitive policies can prevent university research from ever reaching the market. Since some of these technologies are the most promising for new ventures, regulations that prevent university professors from participating in start-ups should be avoided.

Intellectual property protection can also deter start-up businesses. If it is costly or difficult to obtain intellectual property protection, entrepreneurs may be deterred from starting new ventures. Additionally, if the strength of the intellectual property protection is suspect or the costs of enforcing the protection appear prohibitive, entrepreneurs may seek other venues. However, if intellectual property protection is especially strong or easy to obtain, technologies for new ventures may be attracted from other regions.

Results

While the model has not been calibrated to actual data, a number of different scenarios can be considered within a reasonable range of parameter values. These scenarios can describe possible outcomes that occur under specific conditions. By viewing these results, reasonable expectations for actual results can be achieved. Additionally, it can be shown that certain parameter combinations give results that correspond to situations that would actually be expected to arise in the start-up environment. However, it is important to note that many parameters used in the model cannot be measured or quantified. Therefore, in a sense, the model can only indicate possible outcomes and it is important to remember the famous quote from George Box, "All models are wrong..."

Complete Ecosystem Failure

In the complete ecosystem failure scenario, the number of new companies quickly falls to zero and does not recover, as shown in Figure A12. This occurs because the consequences of failure are very high, and none of the positive venture-forming feedback loops become relevant. This result is modeled by significantly increasing the values in the ventures deterred by failure table. This matches the scenario in reality where a few initial companies fail and no new companies replace them as entrepreneurs are discouraged by past failures and the negative consequences of failing. Clearly this is not a desirable situation for the start-up community. A number of steps can be taken to avoid this outcome. The most obvious step is to attempt to reduce the consequences of failure. This can be done in a variety of ways, including educating the public about innovation,

strengthening the social safety net, or assisting entrepreneurs with job placement after start-up failures. Alternatively, the positive loops could be strengthened through funding assistance, facilitation of mentoring and interaction with role models, or identifying more market opportunities.

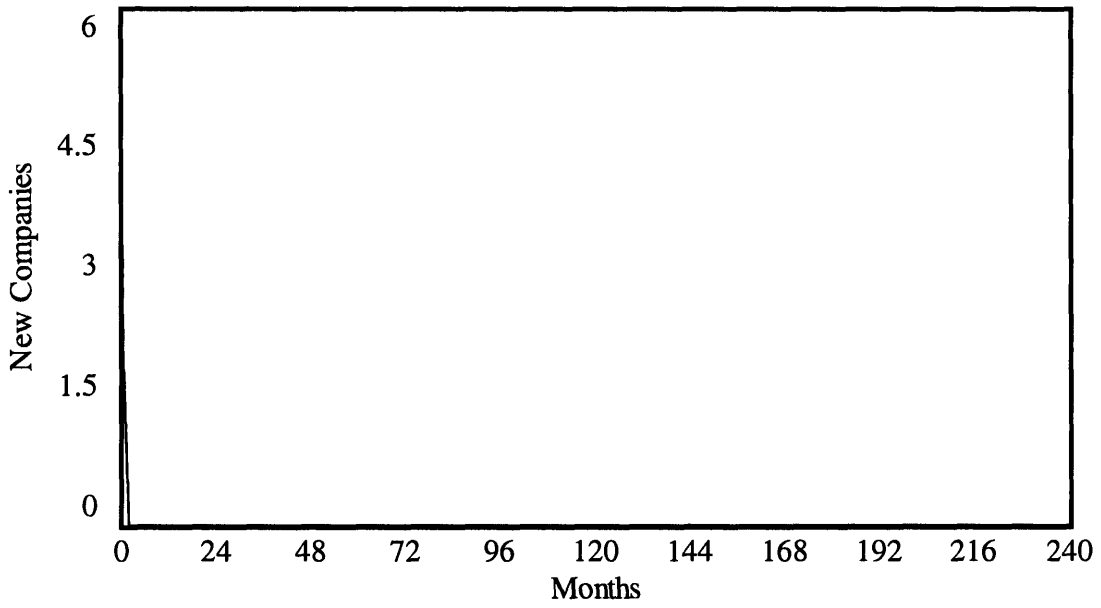

Figure A12: Complete Ecosystem Failure

Periodic Ecosystem Failure

The periodic ecosystem failure scenario reflects a bandwagon effect where the number of new companies swings up and down through a boom-and-bust cycle, as shown in Figure A13. This outcome is largely driven by the average failure delay time. A longer average failure delay time increases the amplitude of the peaks in the number of new companies. This scenario is particularly troubling because the number of new companies falls to zero, which has the potential to halt all growth of the start-up ecosystem. This scenario is seen in reality when a small initial number of companies experience success, and many new

ventures and sources of funding are attracted. However, the rapid inflow results in massive failures, which trigger the failure loop and halt new venture creation. Building a sustainable system that does not experience this extreme form of the boom-and-bust cycle requires companies to be able to fail quickly. Otherwise, the longer delay can result in many companies failing at the same time and impeding growth of the positive loops, such as funding attraction and role model inspiration, which sustain the ecosystem. Therefore, facilitating the inspiration of potential entrepreneurs by role models and ensuring the availability of sufficient funding can protect the ecosystem against this type of situation. Alternatively, improving the ability of role models to mentor new companies and reduce the failure rate will also help avoid these cycles.

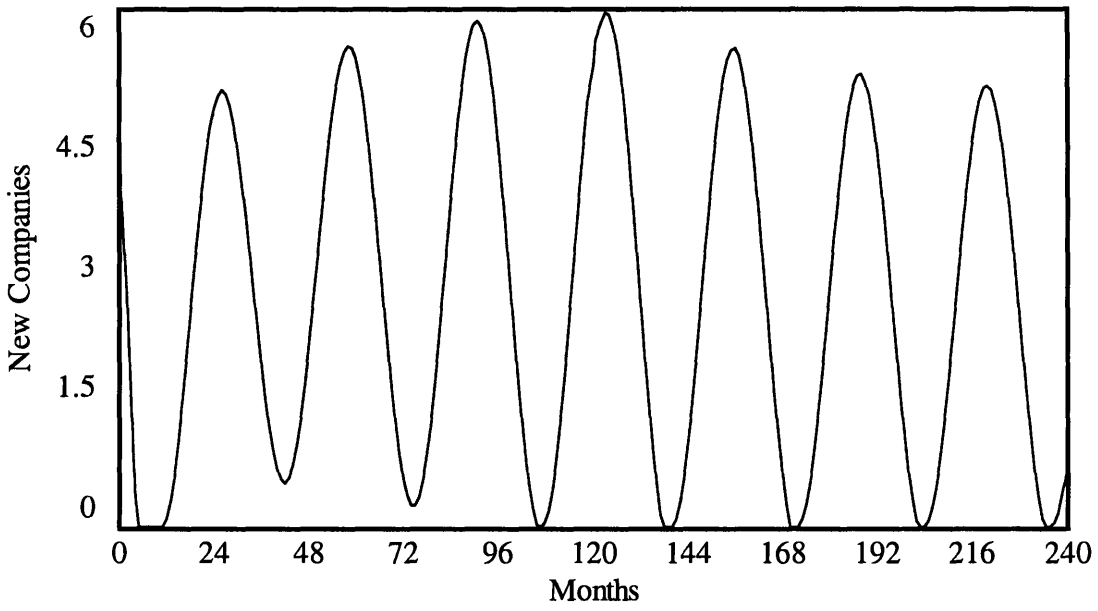

Figure A13: Periodic Ecosystem Failure

Bad News/Good News

In the bad news/good news scenario, the number of new companies falls after a short amount of time. However, as the simulation continues, the number of new companies rises and, during the peaks of the growth, grows higher and higher, as shown in Figure A14. This phenomenon occurs because of mismatched delays on the network effects and the consequences of failure loop. Bringing these values to a more equitable level smoothes out the oscillations. In reality this scenario occurs when a small number of companies are started and fail. However, the longer delays on network effects have drawn in funding and begun changing the public's perception of failure. Then, when more companies begin forming again, growth takes off. Unfortunately, this scenario does not take external efforts into account. It is easy to see how policy interventions in this scenario could be put in place to spur the creation of the new venture ecosystem. When the first group of companies fail, this assistance could be terminated as a failed effort just before the desired growth takes off. In addition to matching the delays of the failure and network effects loops, supporting the small number of initial companies so that failure is prevented can allow the ecosystem to begin to grow until it becomes self-sustaining.

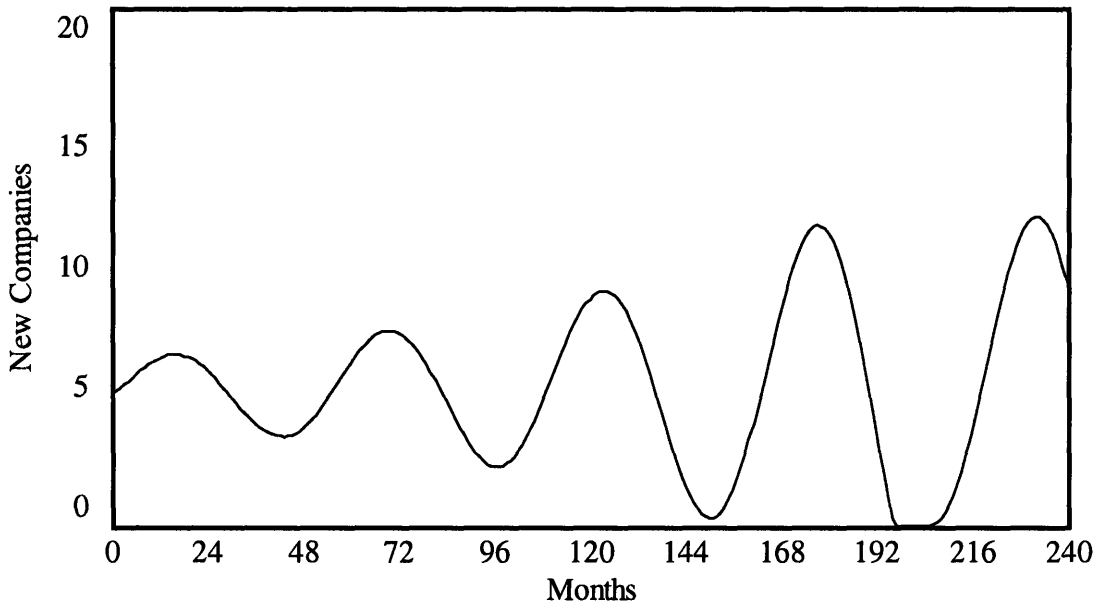

Figure A14: Bad News/Good News

Good News/Bad News

The good news/bad news scenario represents a reversal of the bad news/good news case, as shown in Figure A15, where the number of new companies initially grows before falling rapidly and failing to recover. This effect is modeled by significantly increasing the failure delay as well as the number of companies deterred by failure parameter on the consequences of failure loop. Thus, the situation is similar to the complete ecosystem failure scenario; however, in this case the ecosystem grows slightly before the failure loop dominates and halts the growth of new ventures. In reality, this situation can occur when there is a lot of initial emotional support for start-up ventures. However, after some time passes the support fades and many companies begin failing at the same time. This rush of failures deters potential entrepreneurs, and no new ventures are formed to take the place of the failed companies. This situation can be moderated by strengthening the

mentoring loop, which reduces the failure rate, as well as taking steps to allow companies to fail quickly rather than having many companies all fail at the same time in the future.

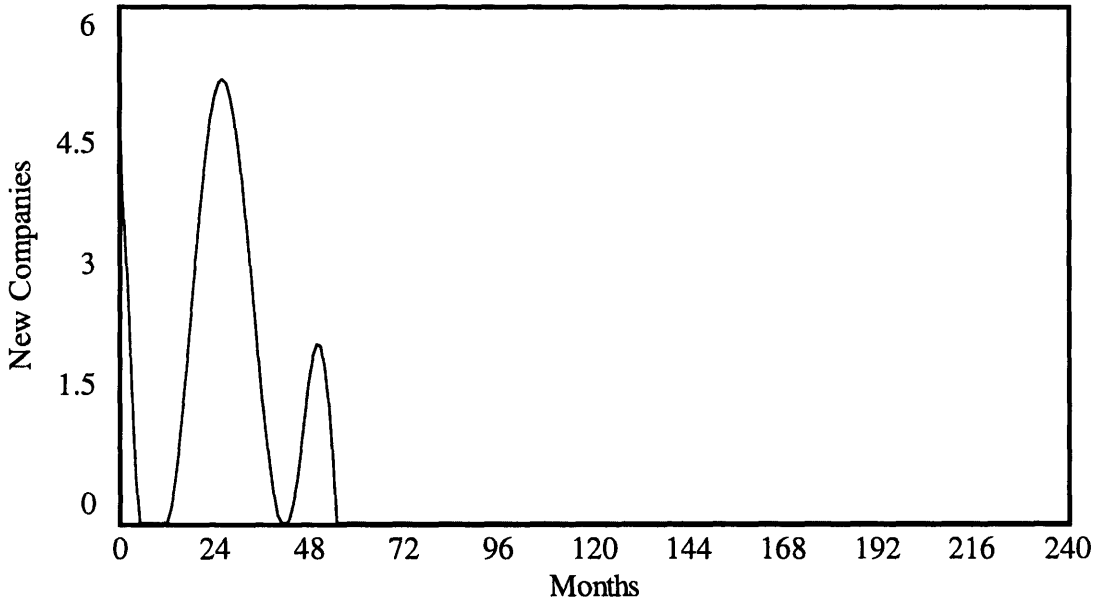

Figure A15: Good News/Bad News

Saturation

In the saturation scenario, the number of new companies grows rapidly to a saturation level and then remains constant for the remainder of the simulation, as shown in Figure A16. This situation occurs when two or more of the dominating feedback loops balance each other at some level of new companies that is different than the initial level. An example of this is when the failure loop deters the same number of companies as the role model loop creates. The level where this balance occurs can be altered by adjusting the number of companies created by role models and the number of companies deterred by failure factors. This situation often occurs in reality for a variety of reasons, such as the law of diminishing returns, competition from other ecosystems for funding and technical

talent, and the depletion of low-hanging fruit types of ventures. Even ecosystems that show fantastic growth will eventually saturate. However, the level of saturation can be improved through enhancement of the positive ecosystem-forming feedback loops, such as role model inspiration, funding attraction, and increased market opportunities.

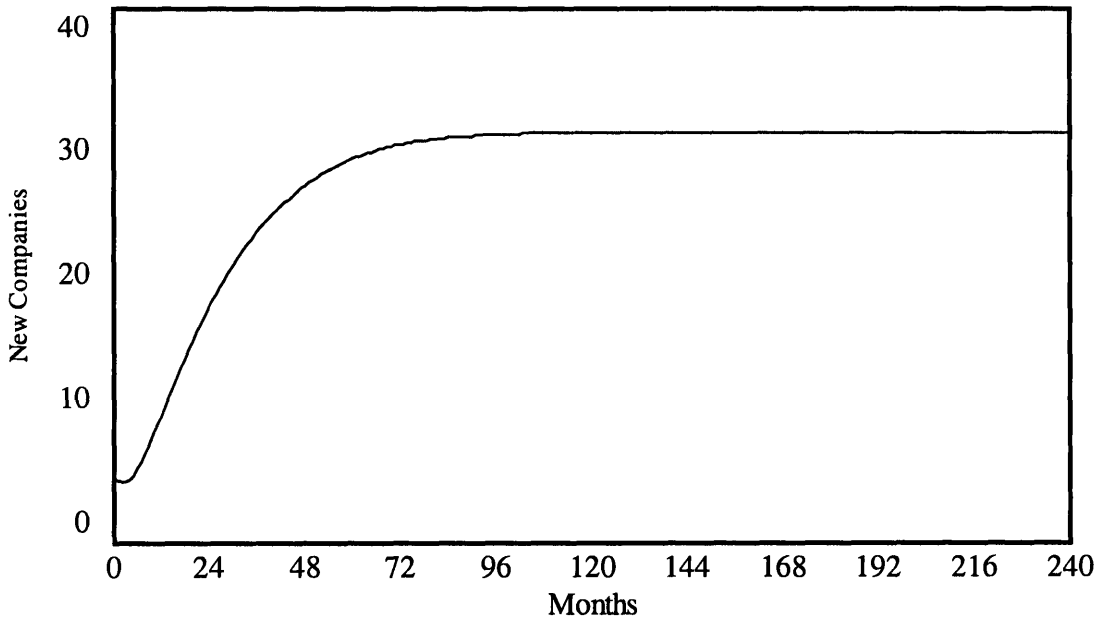

Figure A16: Growth to Saturation

Worse-Before-Better Saturation

In some cases, worse-before-better behavior is seen for saturation scenarios where the number of new companies initially falls before recovering to grow to a saturation level, as shown in Figure A17. In these situations, the failure loop initially dominates as the role model and funding attraction loops grow in strength. In general the driving factors of these dynamics are the same as those in the basic saturation scenario. However, the implications for this type of behavior are more important to understand. In a worse-before-better situation, it would be easy for policy makers to get discouraged and stop

supporting ecosystem formation. However, this withdrawal of support could actually prevent the number of new companies from recovering. This could lead to the ecosystem actually failing, as in the complete ecosystem failure scenario. Therefore, it is important to distinguish between the two cases early in the cycle.

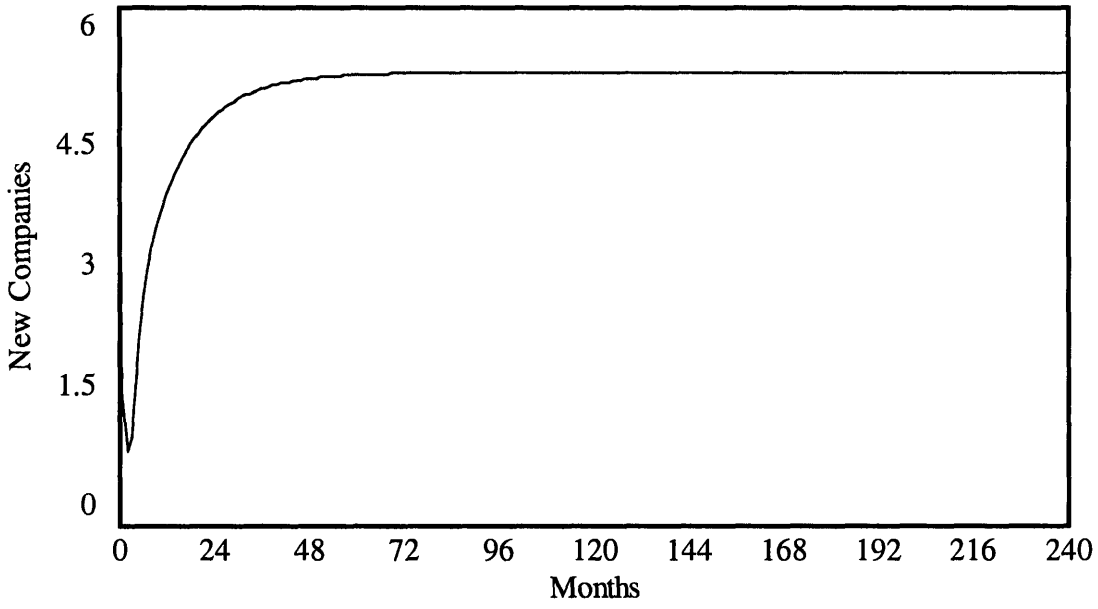

Figure A17: Worse-Before-Better Growth to Saturation

Exponential Growth

When the positive loops in the system dominate, exponential growth in the number of new companies occurs, as shown in Figure A18. This type of growth is the most desirable; however, it takes a significant imbalance between the failure and growth-supporting feedback loops to occur. In the model, this type of growth occurs by decreasing the base failure rate and increasing the strength of the role model inspiration, funding attraction, mentoring, and market opportunity loops. Additionally, exponential growth can only occur over a fixed time period. Eventually, the growth must level off, as

in the saturation scenario, or the ecosystem would become larger than the world economy. The easiest way to achieve this type of growth is to eliminate the failure of new companies. However, in reality, this is quite difficult to do. In order to compensate for actual failures, the ecosystem-supporting feedback loops must be strengthened, as described above. Unfortunately, at some point the resources it takes to further strengthen the loops will have diminishing returns and will not be able to continue to support the growth.

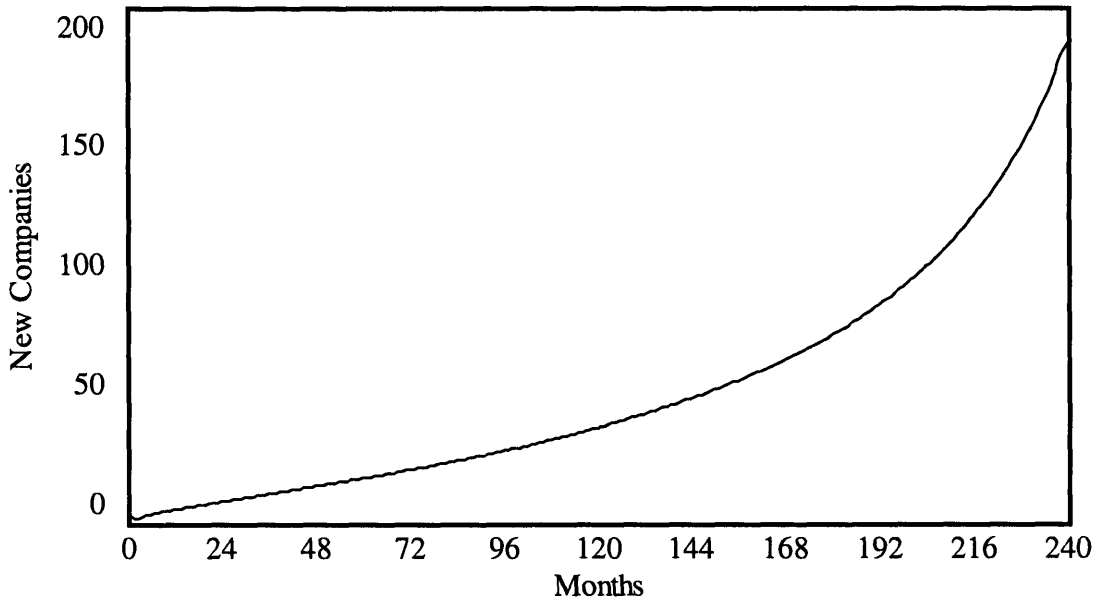

Figure A18: Exponential Growth

Conclusions

This model has sought to identify the key components required to support an innovative business environment. These factors fall into two broad groups: attributes that enhance or deter the formation of new ventures and resource limitations. Policies that could alter

these factors were also described. Strengthening the new venture enhancement properties of the region, while eliminating deterrence and resource limitations, can greatly improve the chances of building a successful, self-sustaining culture of business innovation and help develop a competitive advantage for a region.

The results of the modeling indicate that network effects, such as the development of new markets within the ecosystem, play a crucial role in supporting ecosystem growth. Furthermore, the critical impact of role models through inspiration and mentoring was shown. Thus, a number of policies that can promote these effects, such as facilitating interactions between entrepreneurs and potential entrepreneurs as well as having a government that can serve as a lead user of technology, were identified.

The modeling also highlighted the importance of deterrence in the system. It was shown that if deterrence became too high, no new companies could be formed at all. Therefore, policies, such as educating the public about innovation to reduce the cultural stigma associated with entrepreneurial failure, were described.

Finally, resource limitation, through funding or technical capability, was addressed. While a superficial consideration of the situation would indicate that a lack of technically trained people in a region would inhibit ecosystem growth, it was shown that technical talent resources could be supplemented from outside the region. Furthermore, this phenomenon underscores the need for special policy interventions to aid growth in an infant innovation ecosystem.

Exploiting all of these factors will result in a region that strongly favors innovation. While the ecosystem will still have to compete with other start-up regions across the globe and face many challenges, these steps will greatly increase the likelihood of the program's success. The final benefits of a strong supporting ecosystem are clear from the MIT example, and with enough effort and a little luck, these should be transferable to other areas.

Recommendations

In addition to the general dynamics of the start-up ecosystem, this exercise has identified a variety of concrete steps that can be taken to improve the chances of success of the start-up ecosystem. These steps include education and social measures as well as changes in policies that would require significant funding.

- Role Models: Increase the access to and communication between current and potential entrepreneurs.

- Social Attitudes: Begin promoting entrepreneurship at an early age and reduce the stigma of entrepreneurial failure.

- Universities: Increase familiarity with funding sources and markets while serving to connect role models with potential entrepreneurs.

- Job Creation: Improve employment regulations, job-opportunity communications, and worker mobility.

- Funding Attraction: Advertise successes aggressively and recruit international sources.

- Education Spending Policy: Attract new students and improve infrastructure and management effectiveness.

- Immigration Policy: Ease the movement of immigrants to attract technical talent and increase technical capabilities.

- Business Regulatory Policy: Simplify company creation, failure, and spin-off.

- Intellectual Property Protection Policy: Enhance intellectual property protection to attract new ventures from other, less protected regions.

Works Cited

[1] BankBoston. MIT: The Impact of Innovation. http://web.mit.edu/newsoffice/founders/Founders2.pdf.
[2] http://www.mitportugal.org/About.aspx
[3] http://www.mitportugal.org/bioengineering/
[4] http://web.mit.edu/deshpandecenter/iteams/about.html
[5] Sterman, John. Business Dynamics: Systems Thinking and Modeling for a Complex World. McGraw-Hill: Boston, 2000.
[6] Weil, H., Stoughton, M., Commoditization of Technology-based Products and Services: The Base Case Scenarios for Three Industries. MIT International Center of Research on the Management of Technology, 1998.
[7] Ngai, S., Weild, H., Cooney, C., Business Dynamics of the Pharmaceutical Industry: A Case Study of the US Statin Market. Unpublished Presentation. May, 2006.
[8] Christensen, C., Overdorf, M., Meeting the Challenge of Disruptive Change. Harvard Business Review. Mar-Apr 2000. 66-76.
[9] Gavetti, G., Henderson, R., Giorgi, S., Kodak. Harvard Business School Case N9-703-503, April 24, 2003.
[10] Christensen, C., Suarez, F., Utterback, J., Strategies for survival in Fast-Changing Industries. Management Science. 44(12) Part 2 of 2, S207-S220, December 1998.
[11] Klepper, S., Graddy, E., the evolution of New Industries and the Determinants of market Structure. RAND Journal of Economics. 21(1). 27-44. Spring, 1990.
[12] Roberts, E., The problem of Aging Organizations: A study of R&D Units. Business Horizons. 51-8. Winter, 1967.
[13] Utterback, J., Suarez, F., Innovation, Competition, and Industry Structure. Research Policy. Vol 22, 1-21. 1993.
[14] Weil, H., Turning Innovation into Value Phase 1 Report. Centre of Competitiveness and Innovation. April 6, 2006.
[15] Munir, K., Phillips, N., The concept of industry and the case of radical technological changes. Journal of High Technology managemet Research. Vol 13. 279-97. 2002.
[16] Afuah, A., Utterback. J., Responding to Structural Changes: A Technological Evolution Perspective. Industrial and Corporate change. 6(1). 183-202. 1997
[17] Lyneis, J., A Dynamic Model of Technology Diffusion. Proceedings of the 1993 International Systems Dynamics Conference.
[18] Sull, D., Why Good Companies Go Bad. Harvard Business Review. July-August 1999. 42-52.
[19] Milling, P., Modeling innovation processes for decision support and management simulation. System Dynamics Review. 12(3). 211-234. Fall 1996.
[20] Utterback, J., Afuah., The Dynamic Diamond: A Technoligical Innovation Perspective. Econ Innov new Techn. Vol 6. 183-99. 1998.